Tumor imaging and treatment monitoring in patients with neuroendocrine tumors

Helle-Brit Fiebrich

Tumor imaging and treatment monitoring in patients with neuroendocrine tumors

Helle-Brit Fiebrich

Stellingen

1. ^{18}F-DOPA PET/CT is de eerste keus voor beeldvorming om catecholamine-producerende tumoren op te sporen.

2. Endoscopische echografie is de meest gevoelige techniek om een eilandjesceltumor in de pancreas te lokaliseren.

3. Bij patiënten die langdurig somatostatine-analoog krijgen moeten regelmatig de bloedspiegels van de vetoplosbare vitamines gecontroleerd worden.

4. Het glucose-verhogende effect van everolimus bij gemetastaseerde insulinomen wordt veroorzaakt door een direct anti-tumoreffect en een effect op de perifere insulinegevoeligheid.

5. Patiënten met uitgezaaide eilandjesceltumoren kunnen ook cardiale metastasen hebben.

6. Betere behandeling van het gemetastaseerde carcinoïd heeft geleid tot een lagere incidentie van de carcinoïde hartziekte.

7. Een rookverbod in de openbare ruimte reduceert de incidentie van het acuut coronair syndroom in niet-rokers en rokers.

8. De frequente toepassing van medische beeldvorming leidt voor patiënten tot een substantiële blootstelling aan straling met als gevolg een verhoogd risico op het ontwikkelen van kanker.

9. Aspectparen van het Russische werkwoord moeten eerder als 2 verschillende woorden dan als 2 vormen van 1 woord beschouwd worden.

10. Overal bereikbaar zijn is gelijk aan altijd gestoord kunnen worden.

11. Nederlanders zouden beter met Duitsers overweg kunnen als ze niet tegen hen hoefden te voetballen.

12. De echte kunst van het promoveren is het om de meningen van alle medeonderzoekers tot een geheel te combineren.

13. Op hoge hakken overzie je de wereld beter.

Financial support was kindly provided by:
Stichting Werkgroep Interne Oncologie, Rijksuniversiteit Groningen, Ipsen Farmaceutica B.V.

NOVARTIS
ONCOLOGY

ISBN: 978-90-367-4408-9
Cover design: Thomas Pijper
Printed by: Ipskamp drukkers, Enschede

cmb.

Rijksuniversiteit Groningen

Tumor imaging and treatment monitoring in patients with neuroendocrine tumors

Proefschrift

ter verkrijging van het doctoraat in de
Medische Wetenschappen
aan de Rijksuniversiteit Groningen
op gezag van de
Rector Magnificus, dr. F. Zwarts,
in het openbaar te verdedigen op
woensdag 23 juni 2010
om 13.15 uur

door

Helle-Brit Fiebrich
geboren op 28 april 1982
te Hendstedt-Ulzburg, Duitsland

Promotores:	Prof. dr. E.G.E. de Vries
	Prof. dr. T.P. Links
	Prof. dr. I.P. Kema
Copromotor:	Dr. A.H. Brouwers
Beoordelingscommissie:	Prof. dr. W.T.A. van der Graaf
	Prof. dr. C.J. Lips
	Prof. dr. T. Wiggers

Contents

Chapter 1

Introduction

INTRODUCTION

Neuroendocrine tumors are a heterogeneous group of rare tumors, which arise from cells of the (neuro)endocrine system. These cells are located throughout the body and are capable of secreting biologically active amines, peptides and hormones. They can be divided into cell types that form localized glands (for example the adrenal medulla and the paraganglia) and cells that are dispersed throughout the entire body in other organs: the diffuse neuroendocrine system.[1] Tumors originating from the chromaffin cells of the adrenal medulla are classified as pheochromocytoma, while tumors of the sympathetic and parasympathetic paraganglia are called paraganglioma.[2] Neuroendocrine tumors that arise from the diffuse neuroendocrine system are mainly localized in the intestine, pancreas and lung, although they can originate in other organs as well.[3] Intestinal neuroendocrine tumors are most commonly found in the small intestine, followed by the rectum and appendix. Neuroendocrine tumors that arise from the pancreas are called islet cell tumors.

The World Health Organisation (WHO) categorizes neuroendocrine tumors based on histological features.[2] The main categories defined by this classification system are well differentiated (neuro)endocrine tumor, well-differentiated neuroendocrine tumors of uncertain behavior, well-differentiated neuroendocrine carcinomas and poorly differentiated neuroendocrine carcinomas. In this thesis the term carcinoid tumor is used to describe the well-differentiated neuroendocrine tumor of the gastrointestinal tract.

For tumor localization anatomical imaging, including computer tomography (CT), magnetic resonance imaging (MRI) or endoscopic ultrasound, in combination with nuclear functional imaging is performed, such as somatostatin receptor scintigraphy (SRS) using ^{111}In-octreotide (for carcinoids and islet cell tumors) or scintigraphy with ^{123}I-labeled meta-

iodobenzylguanidine (for pheochromocytomas). Positron emission tomography (PET) using 6-[F-18]fluoro-L-dihydroxyphenylalanine (^{18}F-DOPA) or ^{11}C-5-hydroxytryptophan (^{11}C-5-HTP) exploit the intrinsic property of neuroendocrine tumors to take up, decarboxylate, and store amine precursors.

Surgical excision is the curative treatment option, but it can also be used in a palliative setting to prevent local problems and decrease hormone production. Also in case of metastatic disease median survival for well-differentiated neuroendocrine tumors is relatively long.[3]

Not only new imaging modalities but also new therapeutic options are currently being developed. New targeted drugs have shown promising results in patients with neuroendocrine tumors.[4-7]

Aim of this thesis

The aim of this thesis is to address the diagnosis and management of patients with neuroendocrine tumors, focusing on carcinoid tumors, islet cell tumors and pheochromocytomas.

Outline of this thesis

Chapter 2 gives an extensive literature overview of the imaging methods used to visualize neuroendocrine tumors of the pancreas. A search was performed in the PubMed Medline and Embase databases of all English publications on imaging of islet cell tumors between 1995 and December 2009. When more than 5 studies were available for an imaging technique, only studies with more than 10 patients for that imaging technique were considered. Three indications can be distinguished for imaging of these tumors namely 1) tumor localization and staging of a patient with symptomatic pancreatic hormone hypersecretion, 2) a chance finding of a neuroendocrine tumor or its metastases and the subsequent search for a

primary (pancreatic) tumor, and 3) screening in asymptomatic VHL and MEN1-mutation carriers. The number of patients in the studies was used as a weight factor in summarizing results for different imaging techniques per imaging indication and results are presented in Forest plots. For the applicability of each imaging technique a level of evidence is assigned, based on the system of the Oxford Centre of Evidence Based Medicine.

Currently, no criteria exist to unequivocally predict malignancy of pheochromocytomas. Only the presence of chromaffin tissue at sites, where it is normally absent, establishes a definite diagnosis of malignancy.[8] Therefore, adequate staging is essential since the detection of metastases affects treatment. ^{18}F-DOPA PET has shown the potential to improve pheochromocytoma localization in initial small studies.[9-11] **Chapter 3** describes the study designed to compare the sensitivity of ^{18}F-DOPA PET imaging with the results of morphological imaging using CT and MRI, and functional whole body imaging with ^{123}I-MIBG scintigraphy in patients with proven catecholamine excess. A total of 48 patients were studied. Analysis was performed on a patient and lesion-based level. Results of cytological, histological findings, all imaging tests, follow-up and biochemical data served as a composite reference standard. Metanephrines and 3-methoxytyramine were determined in plasma and urine. In addition, uptake of ^{18}F-DOPA was measured with PET to determine the whole-body metabolic burden and correlated with biochemical tumor markers.

Chapter 4 describes the study which was performed to investigate the value of ^{11}C-5-HTP PET to detect cardiac metastases in patients with a metastasized islet cell tumor. Thus far only in one patient a cardiac metastasis from an islet cell tumour has been reported. The frequency of cardiac metastases may be underestimated as MRI, CT and [^{18}F]fluoro-2-deoxy-d-glucose (^{18}F-FDG) PET do have trouble detection these due to their technical properties. A renewed analysis was performed of all 26 patients with metastasized islet cell tumors who underwent an ^{11}C-5-HTP PET scan

earlier. An ^{11}C-5-HTP PET scan was found to be the best method to visualize islet cell tumors. When lesions suspect for cardiac metastases were identified with ^{11}C-5-HTP PET scan, chest-CT scans were reviewed and fused with the ^{11}C-5-HTP PET.

Chapter 4a addresses the value of ^{18}F-DOPA PET to detect also cardiac metastases in a patient with a metastasized carcinoid. This patient underwent ^{18}F-DOPA PET, SRS, echocardiography, elektrocardiography and cardiac MRI as a part of his oncological work-up.

Second primary malignancies occur more frequently in carcinoid patients than in the general population. Given the relative long survival, even in case of metastatic carcinoid disease, a second primary malignancy can deserve full treatment. Distinguishing a second primary malignancy from a carcinoid metastasis is therefore important, and may have therapeutic consequences. The aim of the study described in **chapter 5** was to analyze whether differentiation between carcinoid metastases and the second primary malignancy scan be achieved using the difference in uptake between different PET tracers. ^{18}F-DOPA PET, which uses the ability of neuroendocrine tumors to take up and decarboxylate amine precursors, was performed to localize the carcinoid tumor. Staging of the second primary malignancy was performed using ^{18}F-FDG as radiotracer for the glucose metabolism, which is ideal to detect fast-growing tumors, but inadequate to detect the slow-growing carcinoid tumors. We checked the charts of 109 carcinoid patients to identify patients who presented with a new second primary malignancy and in whom differentiation between carcinoid lesions and the second primary malignancy was guided by PET imaging with the two aforementioned tracers.

Biochemical tumor markers in plasma or urine are when produced by metastatic carcinoids, used in the diagnosis and follow-up. PET imaging opens ways to analyze whole-body metabolic tumor burden as new quantitative measure of the overall tumor load. ^{18}F-DOPA-tumor uptake

and the levels of secreted biochemical tumor markers are mediated by its endocrine metabolic activity. The aim of the study described in **Chapter 6** was to evaluate whether total ^{18}F-DOPA-tumor uptake on PET, defined as the whole-body metabolic tumor burden reflects tumor load per patient, as measured with tumor markers.

Data of 76 patients with a carcinoid tumor who underwent ^{18}F-DOPA PET as well as a careful collection of relevant biochemical tumor markers in two previously published ^{18}F-DOPA PET studies of our institute were analyzed. The inclusion criteria for these studies were patients with a strong suspicion of a carcinoid tumor, based on clinical and biochemical findings, and patients with histopathologically proven carcinoid tumor, with a clinical indication for (re)staging. All patients had to have at least one abnormal lesion on conventional imaging. As tumor markers served 24-hour urinary serotonin, urine and plasma 5-hydroxindole acetic acid (5HIAA); catecholamines (nor)epinephrine, dopamine and their metabolites, measured in urine and plasma, and serum chromogranin A. For all tumor lesions mean standardized uptake values (SUVmean) at 40% of the maximal SUV and tumor volume at this SUVmean on ^{18}F-DOPA PET were determined using a computer-generated volume of interest. SUVmean and tumor volume were multiplied to calculate a metabolic burden per lesion. Whole-body metabolic burden was the sum of the metabolic burden of all individual tumor lesions per patient. Whole-body metabolic tumor burden was correlated with the tumor markers.

Recently the mTOR inhibitor everolimus administered to four insulinoma patients showed rapid effect on glucose normalization.[12] The precise explanation for these findings is however not yet unraveled. In **Chapter 7** we describe the analyses which we performed to identify the kinetics of everolimus-effects on control of hypoglycemias and to understand underlying mechanisms. Three patients with metastatic insulinoma received everolimus orally daily. We measured serial serum

glucose and plasma insulin and proinsulin levels in three patients with a metastasized symptomatic insulinoma. CT scans were performed before and after 2 and 5 months treatment. ^{18}F-FDG-PET to visualize whole body glucose metabolism were done before and after 2 weeks, 5 weeks and 5 months of treatment. Standardized uptake values of tumor lesions on PET were calculated to quantify tracer uptake.

Somatostatin analogues negatively influence fat uptake in the bowel, frequently resulting in steatorrhea. Together with fecal fat loss, potentially fat-soluble vitamins can be lost. The effect of long-term somatostatin analogue treatment on fat-soluble vitamin levels is unknown. In **Chapter 8** we investigated the frequency and severity of fat-soluble vitamin deficiencies in 19 acromegaly and 35 carcinoid patients, which were treated with a somatostatin analogue for more than 18 months. In these patients we determined the levels of the fat-soluble vitamins and checked for signs and symptoms of vitamin deficiencies. Possible influencing factors were also recorded.

Chapter 9 summarizes our observations and addresses future perspectives.

Chapter 10 gives a summary of this thesis in Dutch.

REFERENCES

1. Kloppel G: Tumour biology and histopathology of neuroendocrine tumours. Best Practice & Research Clinical Endocrinology & Metabolism 2007;21:15-31
2. Solcia E, Kloppel G, Sobin L.H Histological typing of endocrine tumors. 2nd ed. Berlin: Springer, 2000
3. Yao J, Hassan M, Phan A, et al. One hundred years after "carcinoid": Epidemiology of and prognostic factors for neuroendocrine tumors in 35,825 cases in the United States. J Clin Oncol 2008;26:3063-3072
4. Yao J, Phan A, Chang D, et al. Efficacy of RAD001 (everolimus) and octreotide LAR in advanced low- to intermediate-grade neuroendocrine tumors: Results of a phase II study. J Clin Oncol 2008;26:4311-4318
5. Kulke M, Lenz H, Meropol N, et al. Activity of sunitinib in patients with advanced neuroendocrine tumors. J Clin Oncol 2008;26:3403-3410
6. Yao J, Phan A, Hoff P, et al. Targeting vascular endothelial growth factor in advanced carcinoid tumor: A random assignment phase II study of depot octreotide with bevacizumab and pegylated interferon alfa-2b. J Clin Oncol 2008;26:1316-1323
7. Yao J, Lombard-Bohas C, Baudin E, et al. Daily oral everolimus activity in patients with metastatic pancreatic neuroendocrine tumors after failure of cytotoxic chemotherapy: A phase II trial. J Clin Oncol 2010;28:69-76
8. Scholz T, Eisenhofer G, Pacak K, et al. Clinical review: Current treatment of malignant pheochromocytoma. J Clin Endocrinol Metab 2007;92:1217-1225
9. Hoegerle S, Nitzsche E, Altehoefer C, et al. Pheochromocytomas: detection with 18F DOPA whole body PET--initial results. Radiology 2002;222:507-512
10. Taieb D, Tessonnier L, Sebag F, et al. The role of 18F-FDOPA and 18F-FDG-PET in the management of malignant and multifocal pheochromocytomas. Clinical Endocrinology 2008;69:580-586
11. Timmers HJ, Hadi M, Carrasquillo JA, et al. The effects of carbidopa on uptake of 6-18F-fluoro-L-DOPA in PET of pheochromocytoma and extraadrenal abdominal paraganglioma. J Nucl Med 2007;48:1599-1606
12. Kulke MH, Bergsland EK, Yao JC Glycemic control in patients with insulinoma treated with everolimus. N Engl J Med 2009;360:195-197

Chapter 2

Tailored imaging of islet cell tumors of the pancreas amidst increasing options

Helle-Brit Fiebrich[1], Sophie J. van Asselt[2], Adrienne H. Brouwers[x], Milan E.J. Pijl[x], Hendrik M. van Dullemen[x], Philip H. Elsinga[x], Elisabeth G.E. de Vries[1], Thera P. Links[2]

Departments of [1]Medical Oncology, [2]Endocrinology, [x]Nuclear Medicine and Molecular Imaging, [x]Gastroenterology, University Medical Center Groningen, University of Groningen, Groningen, The Netherlands
[x]Department of Radiology, Martini Hospital, Groningen, The Netherlands

Submitted

ABSTRACT

Islet cell tumors of the pancreas are rare neuroendocrine tumors, which can produce hormones in 40% of the cases. They arise sporadically or as part of the hereditary cancer syndromes. The literature on the value of imaging of islet cell tumors presents an array of varying results for different imaging techniques. Currently, technical innovation improves conventional imaging techniques. In addition apart from anatomical imaging, specific molecular imaging, permitted by the neuroendocrine nature of these tumors, increasingly plays a role. To organize the heterogeneous results described for the imaging of these tumors, we distinguished three indications namely 1) imaging of a patient with hormone hypersecretion, 2) a chance finding of a neuroendocrine tumor or its metastases and the subsequent search for a primary (pancreatic) tumor, and 3) screening of asymptomatic mutation carriers. For these indications we searched in Pubmed, Medline and Embase databases for all English publications on imaging of islet cell tumors between 1995 and January 2010 and defined a Level of Evidence (LOE) for the applicability of each technique. Data were analyzed in a Forest plot for each technique separately and are arranged per imaging indication and per islet cell tumor subtype to give a clear overview of the available literature.

We show that LOEs are weak (2b at best) for all imaging techniques. Our analyses with Forest plots point towards especially a prominent role for endoscopic ultrasound for all three indications studied.

I. INTRODUCTION

Islet cell tumors of the pancreas are rare tumors, occurring in approximately one in 100,000 adults. They originate from the pancreatic islet cell lineage and can secrete one or more hormones or amines.[1] Up to 60% of these tumors are non-functioning; around 50% present with hepatic metastases at time of diagnosis.[2, 3] Tumors are classified as functioning or non-functioning, based on presence of symptoms caused by hormone production.[4]

Non-functioning tumors are generally detected in a late stage and present with non-specific symptoms or mass effects due to their (large) size or metastases. Functioning islet cell tumors are characterized according to the biological substance secreted. Insulinomas are typically small and in 90% benign tumors, presenting with hypoglycaemia. Gastrinomas can cause the Zollinger-Ellison syndrome, characterized by high gastric acid output, and are usually small and malignant.[1] Most gastrinomas arise in the gastrinoma triangle, comprising the head of the pancreas, the superior and descending portion of the duodenum and local lymph nodes.[5] Glucagonomas, which can cause diabetes and a characteristic rash, and VIPomas, which can be associated with severe diarrhea, are often large primary tumors and already metastasized at diagnosis.[1] Other subgroups of functioning islet cell tumors are even rarer, occurring in less than 0.1 per million adults.[1, 6]

Islet cell tumors can arise sporadically or as part of two hereditary cancer syndromes namely multiple endocrine neoplasia type 1 (MEN1) and von Hippel Lindau disease (VHL).[7, 8] Patients with an islet cell tumor have a chance of 5-30%, depending on the subtype of islet cell tumor, that an underlying genetic predisposition is present.[6] Carriers of a MEN1 mutation will develop islet cell tumors in 30-80%, those with a VHL gene mutation in 10-20%.

Diagnosing hormone or amine hypersecretion may help to confirm the suspicion of a functioning tumor in a patient with symptoms, but other causes of elevated hormone or amine levels have to be ruled out.[1] For non-functioning tumors extensive hormonal testing is usually little helpful. In either case, biochemical measurements do not provide tumor localization and thereby more direct proof of an islet cell tumor. Imaging is essential to localize the primary tumor, to detect metastases and to assess tumor response on treatment. Historically, visualization of pancreatic lesions has been difficult. The literature on the value of imaging of islet cell tumors presents a broad assortment of varying results for different imaging techniques. Interpreting the available imaging results is a challenge. Firstly due to the rarity of the disease most studies are performed in small and/or mixed patient cohorts. Secondly, many imaging techniques exist often without studies in which head to head comparisons were performed. Thirdly, clinically three indications can be distinguished for imaging of these tumors which are often all included in studies leading to confusing conclusions. To organize the heterogenous results described for the imaging of these tumors, we distinguished three indications namely 1) tumor localization and staging of a patient with symptomatic pancreatic hormone hypersecretion, 2) a chance finding of a neuroendocrine tumor or its metastases and the subsequent search for a primary (pancreatic) tumor localization and staging, and 3) screening in asymptomatic VHL and MEN1-mutation carriers.

In the present review, we give an overview of the performance of the various imaging techniques, their strength and weaknesses in relation to the three imaging indications described above and highlight standard as well as the place of newer techniques.

II. METHODS

We performed a non-systematic review of all publications between 1995 and January 2010 on imaging of pancreatic islet cell tumors. Articles were searched in the PubMed, Medline and Embase databases using a variety of search terms, including: imaging, visualization, localization, pancreatic neuroendocrine tumor or neoplasm, islet cell tumor, insulinoma, gastrinoma, glucagonoma, VIPoma and somatostatinoma. Only articles in the English language were included. Results from reviews without original data were excluded. The reference lists of all articles were checked for unknown publications. When more than 5 studies were available for an imaging technique, only studies with more than 10 patients for that technique were considered. When fewer studies were available, smaller studies and relevant case reports were also included. The full texts of the articles were reviewed, and whenever possible, we extracted and tabulated sensitivity and specificity values for the three imaging indications: 1) imaging of a patient with hormone hypersecretion, 2) a chance finding of a neuroendocrine tumor or its metastases and the subsequent search for a primary (pancreatic) tumor localization and staging, and 3) screening of mutation carriers of MEN1 and VHL. The number of patients in the studies was used as a weight factor in summarizing results for different imaging techniques and is represented by a square in the Forest plot analysis. For Forest plot calculations for CT scanning were performed for studies in which a multidector CT (MDCT) was used or, given the technical improvements in CT scanning, studies published in the last 7 years.

For the applicability of each imaging technique a Level of Evidence (LOE) was assigned, based on the system of the Oxford Centre of Evidence Based Medicine.[9] Level 1a evidence is considered definite; level 5 evidence is considered weak.

RESULTS

III. Anatomical imaging

A. Transabdominal and endoscopic ultrasound

Transabdominal ultrasound

Transabdominal ultrasound was one of the first imaging techniques available for the imaging of pancreatic neuroendocrine tumors. It is safe, non-invasive, relatively inexpensive and widely available. For tumor localization in a symptomatic patient transabdominal ultrasound can localize pancreatic insulinomas in 10-40% of the cases (range 9-79%).[10-21] Performance improves with increasing lesion size. In 120 patients with hyperinsulinism surgically confirmed tumors larger than 2 cm were detected with transabdominal ultrasound in 56%, but only 18% of those smaller than 1 cm.[10] Detection is also limited by interference of other intra-abdominal organs (for example bowel gas) and fat in obese patients.[11] Combining ultrasound with other imaging techniques improves detection rates; ultrasound plus magnetic resonance imaging (MRI) rendered a sensitivity of 97% in a study of 28 insulinoma patients with lesions of 0.8-4.3 cm at surgery.[11] Overall ultrasound has a LOE 2b for the detection of tumors in patients with hyperinsulinism. Pancreatic gastrinomas are detected by transabdominal ultrasound in 71% of 14 patients (LOE 2b).[20]

No studies have looked at the value of transabdominal ultrasound for tumor localization in patients with a chance tumor finding, or for the screening of MEN1 or VHL-patients.

One guideline still advocates transabdominal ultrasound as first imaging technique to localize non-functioning suspected islet cell tumors[22], despite the poor sensitivity described above. New developments, such as Doppler sonography[23] or the use of contrast agents[24, 25], can improve the performance of transabdominal ultrasound. These developments have not yet been investigated for the localization of pancreatic islet cell tumors. It

remains to be proven whether addition of these techniques can result in a good sensitivity for transabdominal ultrasound.

Endoscopic ultrasound

Endoscopic ultrasound (EUS) has evolved as a relevant technique to localize islet cell tumors.[26] Elastography, next to Doppler, may help distinguish tumors from their surrounding tissues because of their specific consistency[27], but has not yet been used in any of the current studies. An advantage of EUS is that it permits direct cytology to be obtained of the visualized lesion by fine needle aspiration (FNA). The yield of FNA may be lower for neuroendocrine tumors than for adenocarcinomas of the pancreas. In a study comparing the feasibility and value of FNA in solid pancreatic masses, the accuracy of FNA was 47% in neuroendocrine tumors (n = 15) and 81% for pancreatic adenocarcinoma (n = 59). This was possibly due to the vascular nature of neuroendocrine tumors, which resulted in purely hemorrhagic samples with few cells in 47%, making analysis impossible[28] and due to their low malignancy grade. When during EUS a FNA was performed with on-site assessment of the adequacy of the specimen a sensitivity and accuracy of both 83% was obtained in a retrospective study in 30 patients with suspected islet cell tumors.[29] Only one minor complication (abdominal pain) was reported. Based on their findings, these investigators advise that different strategies should be attempted to optimize the samples different strategies, for example, on-site assessment of the specimen.[29, 30]

For tumor localization in symptomatic patients the studies as illustrated in the Forest plot analyses show high sensitivities for EUS (Figure 1). The sensitivities are similar for all islet cell tumor subtypes. Most studies were small, with a median of 29 patients. Small tumors appear as uniformly hypoechoic masses, with distinct margins, but larger and malignant tumors can be inhomogenous, hyperechoic (Figure 2), and can have irregular margins.[12, 21, 31, 32]

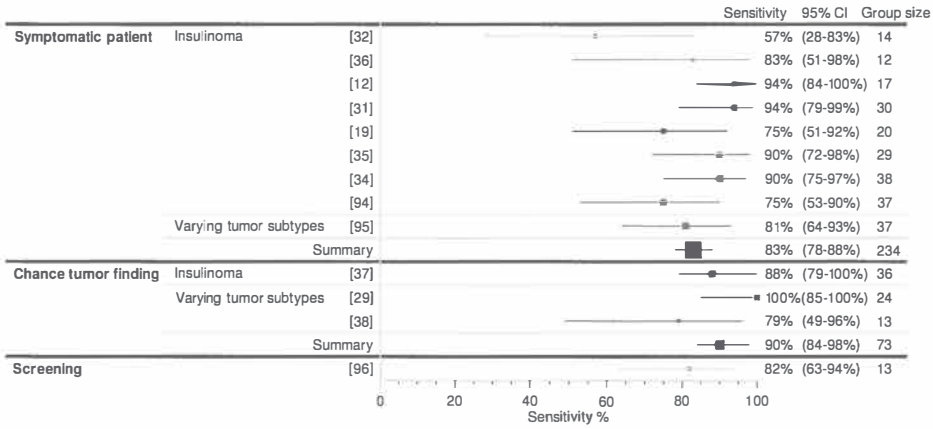

Figure 1. Results of endoscopic ultrasound presented in a Forest plot analysis. On the left side of this plot the reference of the study is mentioned, on the right side sensitivities from literature data are provided with their calculated confidence intervals and number of patients. Results are clustered per imaging indication. Within the different groups studies are clustered per tumor subtype and according to year of publishing. 95% CI: 95% Confidence Interval

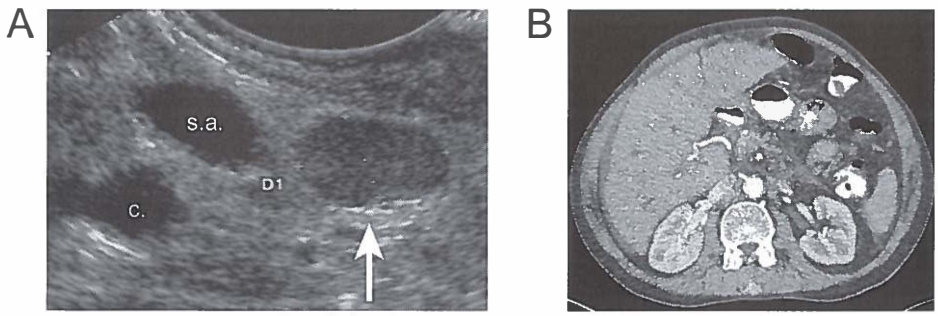

Figure 2. Patient with a small, 0.6 x 0.9 cm, metastasized glucagonoma, presenting with diabetes mellitus, icterus and a rash. A) Endoscopic ultrasound, showing the pancreatic tumor (arrow). On the left adjacent to the tumor the splenic artery (s.a.) and the hepatocaval confluence (c) are visible. B) The lesion is not visualized by computer tomography.

False-positive EUS findings in symptomatic patients can be caused by peripancreatic lymph nodes, imposing as tumoral nodes.[32-34] Reported false-negatives usually relate to very small or iso- or hyperechoic insulinomas.[35] The influence of size on the detection rates of insulinomas was confirmed in another study.[36] Two surgically proven insulinomas not detected by EUS had a mean diameter of 0.75 cm, while the smallest lesion that was detected by EUS measured 0.8 cm. Insulinomas in the pancreatic tail are more difficult to visualize than tumors in the pancreatic head (sensitivity 37-100% versus 83-100%).[32, 34] This likely relates to the variable distance of the endoscope, located in the gastric lumen, from the pancreatic tail due to the variable amounts of mesenteric fat. For insulinomas a negative EUS examination does not exclude a pancreatic tumor, given the negative predictive value of 43% found in a study with 36 patients.[37] Combining the results of EUS with MDCT, which permits acquisition of thinner slices, improved sensitivity to 100% in 32 patients with insulinomas measuring 0.9-9 cm at surgery.[31] The LOE for the performance of EUS to detect tumor in insulinoma patients is only 2b. None of the EUS studies allow for a separate evaluation of the EUS performance for only pancreatic gastrinomas. EUS with FNA on-site assessment of the adequacy of the specimen obtained a sensitivity of 90% and an accuracy of 90% in 10 patients suspected of a functional islet cell tumor.[30]

Also none of the EUS studies provide a separate evaluation of the EUS performance in patients with a chance finding of neuroendocrine tumor. Three studies report combined results for patients with symptoms or a chance finding of neuroendocrine tumor, which are in the same range as for symptomatic patients alone (Figure 1).[29, 37, 38] Median size of these studies is 24 patients. This study also showed that EUS may miss small tumors, as multiple tumors, although not precisely indicated, smaller than 0.2 cm were missed by EUS.[37]

There is only a LOE 3b for the performance of EUS for tumor detection in patients with a chance finding of neuroendocrine tumor.

For the screening of MEN1-carriers EUS performs well, identifying almost all tumors in one small study of 13 individuals (Figure 1). In 12 other patients EUS detected lesions in all patients, while CT and somatostatin receptors scintigraphy (SRS) could demonstrate them in only 1 and 2 patients, respectively.[39] EUS was the most sensitive technique, especially for the detection of lesions overall smaller than 1 cm. In most patients multiple small non-functioning tumors were found during surgery, some of which were missed even by EUS. No studies are performed as screening in VHL patients. For the screening of MEN1-mutation carriers with EUS there is a LOE 2b.

B. Computer tomography

CT is the most widely used imaging technique for the localization of islet cell tumors. As a consequence of their hypervascular nature, islet cell tumors typically are enhancing masses on contrast enhanced CT images during the arterial phase, in which the tumors are usually best visualized (Figure 3A).[40, 41] However, 4-8% of tumors are only visible during the portal-venous phase.[41, 42] Therefore, arterial phase and portal-venous phases are complementary, and both are recommended for the detection of islet cell tumors (LOE 2b).

For the tumor localization in a symptomatic patient Forest plot analyses show that the performance of CT varies widely between different studies (Figure 4). Patient numbers in these studies are low (median 30 patients). MDCT allows optimized scan protocols and improved sensitivity, from 29% for non-helical CT to 94% for MDCT with thin slices in insulinomas.[31] Most studies with conventional CT are in the lower range. This is certainly true for patients suspect for an insulinoma or in patients with varying islet cell tumor subtypes.

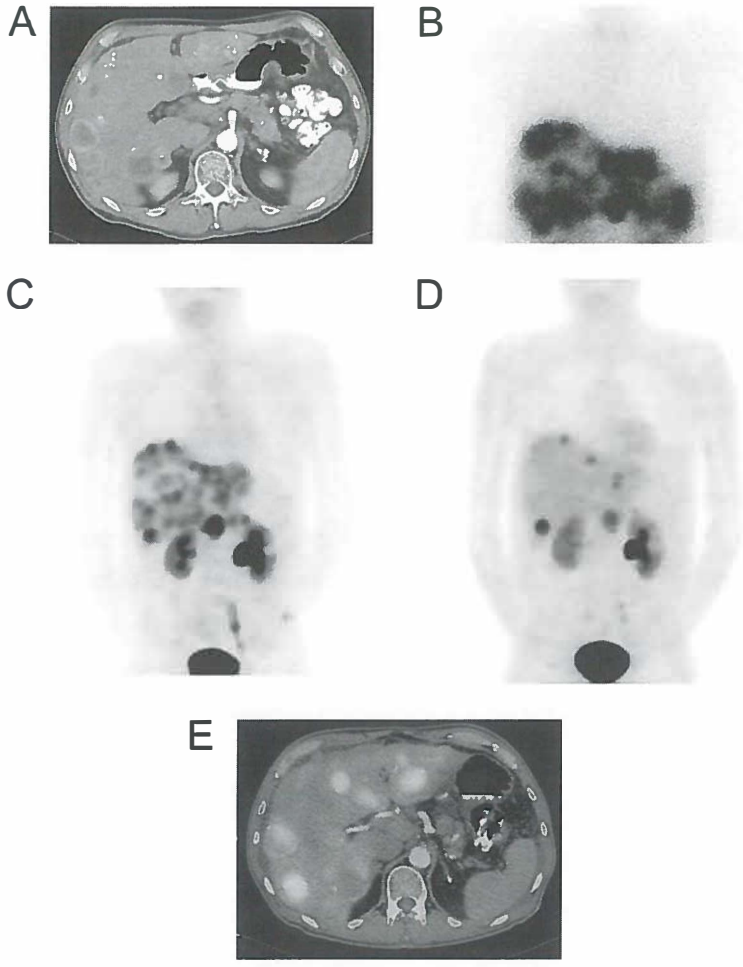

Figure 3. Illustration of yield of different imaging techniques in a patient with a metastasized non-functioning islet cell tumor, 2 x 2.7 cm. A lesion in the pancreas and liver metastases are visualized on all imaging techniques. **A.** Computer tomography shows precise anatomical location of the pancreatic lesion and of multiple liver metastases. **B.** Somatostatin receptor scintigraphy shows tracer uptake in pancreas and liver lesions. **C.** ^{11}C-HTP PET demonstrates uptake in the pancreas and multiple liver metastases. **D.** ^{18}F-DOPA PET shows lesions in the pancreas and liver, more lesions were observed with ^{11}C-HTP PET. **E.** A fusion image of ^{11}C-HTP PET and CT demonstrates multiple liver metastases.

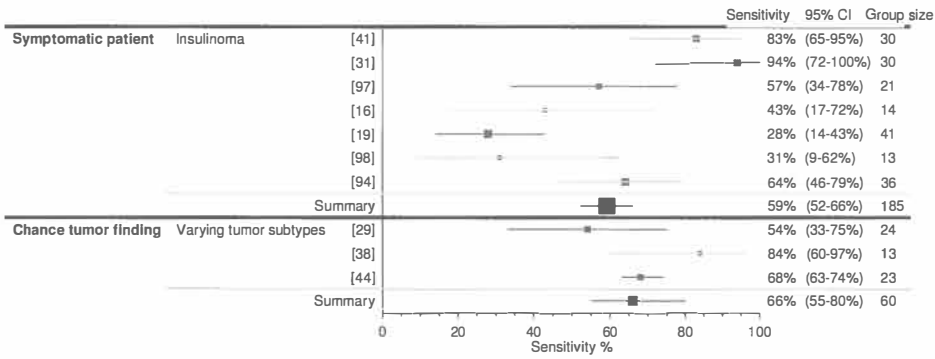

Figure 4. Results of computer tomography in publications published between 2003 and January 2010 and all MDCT studies presented in a Forest plot analysis. On the left side of this plot the reference of the study is mentioned, on the right side sensitivities from literature data are provided with their calculated confidence intervals and number of patients. Results are clustered per imaging indication. Within the different groups studies are clustered per tumor subtype and according to year of publishing. 95% CI: 95% Confidence Interval

Potential false-negatives include insulinomas adjacent to vessels, pedunculated morphology, non-enhancing lesions and insulinomas immediately adjacent to the small bowel.[41] Detection rate of insulinomas is also related to tumor size. In a study published in 1998 in 120 patients with hyperinsulinism (105 insulinomas) CT detected 20% of surgically proven tumors smaller than 1 cm, and 40% of tumors larger than 2 cm.[10] In another study published in 1999 in 66 patients with hyperinsulinism the detection rate of CT increased from 21% to 40% to 100% as tumor size increased from 1 cm to 3 cm and 6 cm.[14] The level of evidence for CT and MDCT for tumor localization in patients with hyperinsulinism is LOE 2b. Two studies published in 1995 and 1998 (12 and 14 patients respectively) provide detailed information about the value of CT for the detection of

pancreatic gastrinomas, which lies in the same range as for other islet cell tumor subtypes (60 and 93% respectively).[20, 43] The LOE for patients with gastrin hypersecretion is 2b.

None of the CT studies allows for a separate evaluation of the CT performance in patients with a chance finding of neuroendocrine tumor. Three studies include both patients with symptoms and those with a chance finding of neuroendocrine tumor (median 23 patients). MDCT shows an excellent sensitivity of 84% in varying subtypes of islet cell tumors.[38] For conventional CT the detection rates are low in these patients.[29, 44] False-positives were due to inflammatory non-neoplastic masses or aberrant pancreatic tissue.[38] There is a LOE2b for the performance of CT for tumor detection in patients with a chance finding of neuroendocrine tumor.

For the screening of islet cell tumors in MEN1-patients with CT misses a substantial number of lesions, as it could only identify lesions in 1 of 12 patients, that had demonstrated lesions on EUS.[39] No studies are available in VHL patients. There is a LOE 2b for the screening of MEN1-mutation carriers with CT.

C. Magnetic resonance imaging

The performance of MRI has greatly improved in recent years as shorter acquisition times resulted in less motion artefacts and higher signal-to-noise ratios. MRI for the detection of islet cell tumors should be performed with a 1.5 Tesla gradient system or higher, using a phased-array torso coil to improve the signal-to-noise ratio.[45]

For tumor localization in a symptomatic patient Forest plot analyses show that for all tumor subtypes MRI has sensitivities in the lower ranges (Figure 5). Although the difference between studies is wide, it is not as wide as for CT. Like for the other imaging techniques, studies are small (median number 21 patients).

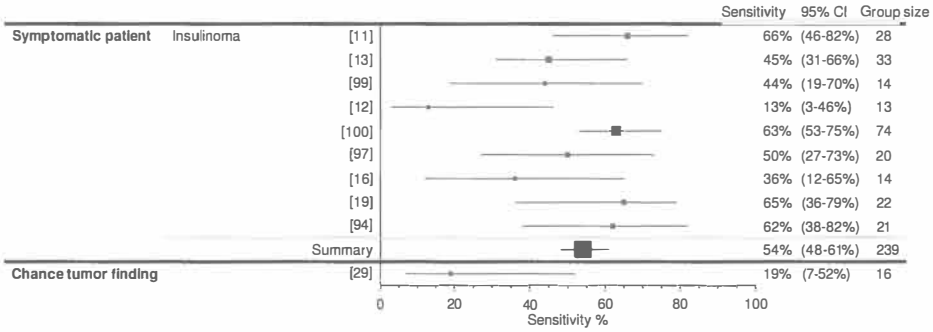

Figure 5. Results of magnetic resonance imaging presented in a Forest plot analysis. On the left side of this plot the reference of the study is mentioned, on the right side sensitivities from literature data are provided with their calculated confidence intervals and number of patients. Results are clustered per imaging indication. Within the different groups studies are clustered per tumor subtype and according to year of publishing. 95% CI: 95% Confidence Interval

In two studies (28 and 31 patients) in insulinomas the lesions located in the pancreatic head were easiest to detect, probably because the head is less affected by motion artefacts than the remaining pancreas.[11, 46] Other technical limitations include imaging in obese patients or those with irregular breathing.[47] MRI performs better with increasing lesion size.[11, 14] In 66 insulinoma patients the detection rate of MRI increased from 0 to 50 to 100% as lesion size increased from 1 to 2 to 3 cm.[14] However, a sensitivity of 85% was found in 20 patients with a functional islet cell tumor smaller than 2 cm. These lesions were confirmed at subsequent surgery (18 insulinomas, 2 gastrinomas).[47] No studies in gastrinomas could be analyzed in the Forest plot, since detailed information about the performance of MRI to detect pancreatic gastrinomas is lacking. In prospective studies the detection rates of MRI for tumor detection in symptomatic patients or staging in patients with evidence of a tumor or metastases equal those of CT (LOE 2b).[11, 42]

No studies are performed in patients with a chance finding of neuroendocrine tumor alone. Only one study includes both patients with a chance tumor finding and symptomatic patients. This small study including 16 patients found a low detection rate (LOE 2b).

Also no studies have looked at the value of MRI for the screening of MEN1 or VHL-patients.

IV. Molecular imaging

Functional molecular imaging is based on cellular properties, such as the presence of somatostatin receptors or the activity of metabolic pathways. Figure 6 shows a schematic depiction of the properties of islet cell tumors that are used to image these tumors. In case of somatostatin receptor imaging the tracer attaches itself to the somatostatin receptor on the cell membrane and this complex is subsequently internalized. The most widely available somatostatin receptor tracer is ^{111}In-DTPA-D-Phe-octreotide, which targets the somatostatin receptor subtype 2. The same type of mechanism is used for glucagon-like peptide 1 (GLP-1) imaging where the tracer ^{111}In-DOTA-exendin-4 binds the GLP-1 receptor and is then internalized. This is distinct from the several metabolic tracers to visualize neuroendocrine tumors. These metabolic tracers are transported into the cell via cell membrane bound transporters and are then intracellularly metabolized. [^{18}F]fluoro-2-deoxy-d-glucose (^{18}F-FDG) is transported into the cell by the glucose transporter, metabolized and trapped in the cytoplasm. Two other metabolic tracers ^{11}C-5-hydroxytryptophan (^{11}C-5-HTP) and [^{18}F]fluoro-dihydroxyphenylalanin (^{18}F-DOPA) are transported into the cell by the large amino acid transporter (LAT), decarboxylated by aromatic-L-amino acid decarboxylase (AADC) to ^{11}C-serotonin and ^{18}F-dopamine respectively, and transported into secretory vesicles by the vesicular monoamine transporter (VMAT).

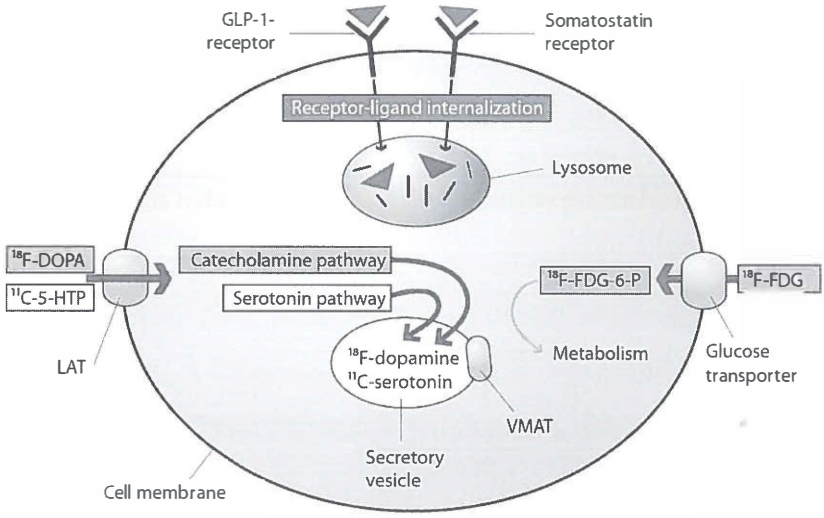

Figure 6. Schematic depiction of the different metabolic pathways by which neuroendocrine tumors can be visualized using nuclear medicine imaging techniques. This can be receptor based techniques and techniques which use the metabolic properties of these tumors. ^{11}C-5-HTTP: ^{11}C-5-hydroxytryptophan, ^{18}F-DOPA: ^{18}F-fluoro-dihydroxyphenylalanin, ^{18}F-FDG: ^{18}F-fluoro-2-deoxy-d-glucose, ^{18}F-FDG-6-P: ^{18}F-fluoro-2-deoxy-d-glucose-6-phosphate, GLP-1: glucagon-like peptide 1, LAT: large amino acid transporter, VMAT: vesicular monoamine transporter

We will first describe somatostatin receptor imaging, both with the conventional tracer ^{111}In-DTPA-D-Phe-octreotide and newer developments in both single photon emission tomography (SPECT) and positron emission tomography (PET tracers). Thereafter we will cover the various metabolic tracers visualized with PET.

A. Single photon emission tomography

Somatostatin receptor scintigraphy with ^{111}In-DTPA-D-Phe-octreotide

Functional nuclear medicine imaging with SRS is based on the fact that 70-100% of islet cell tumors express the human somatostatin

receptors.[48, 49] Most experience is available with ^{111}In-DTPA-D-Phe-octreotide. This gamma camera tracer specifically targets the somatostatin receptor subtype 2 and, to a lesser extent, subtype 5[50, 51] and is preferably used with SPECT. SRS has the advantage that it can almost ascertain the neuroendocrine nature of suspected lesions found on other imaging techniques (Figure 3B).

For tumor localization in a symptomatic patient Forest plot analyses show that the performance of SRS in insulinomas in 2 small studies (14 and 13 patients respectively) is highly variable (Figure 7). The main factors that determine the ability of SRS to detect a pancreatic lesion are its size, the receptor density of the lesion (especially subtype 2) and the target-to-background ratio. In insulinomas, the subtypes of somatostatin receptors, which are necessary for octreotide binding and thus visualization with SRS, are absent in 28% of cases, negatively influencing detection rates (LOE 2b).[49, 51-53]

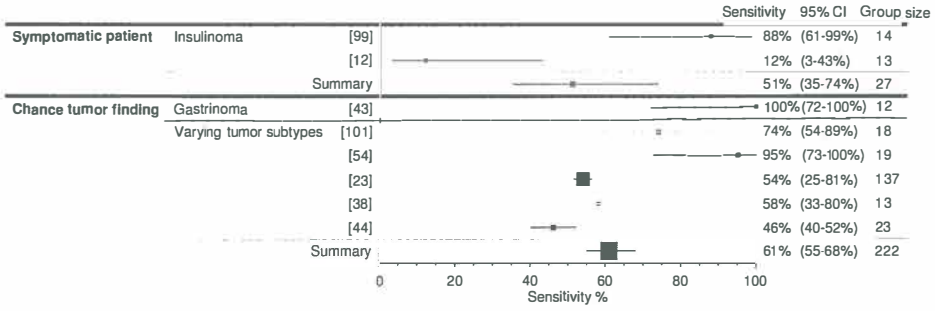

Figure 7. Results of somatostatin receptor scintigraphy presented in a Forest plot analysis. On the left side of this plot the reference of the study is mentioned, on the right side sensitivities from literature data are provided with their calculated confidence intervals and number of patients. Results are clustered per imaging indication. Within the different groups studies are clustered per tumor subtype and according to year of publishing. 95% CI: 95% Confidence Interval

No study allows for separate analysis of patients with a chance finding of neuroendocrine tumors, as all include symptomatic patients as well. One such study is available which evaluated SRS in pancreatic gastrinomas. In this study of 12 patients a perfect performance of SRS is found (LOE 2b) (Figure 7).[43] In groups with varying subtypes of islet cell tumors the Forest plot shows varying sensitivities, mainly in the mid to high ranges (Figure 7). Patient numbers in the studies are low (median 19 patients). Results of SRS modified treatment in 56% of 38 patients with suspected islet cell tumors.[54] Fusion of CT and SRS images improved detection rates in 23 patients with varying subtypes of islet cell tumors.[44] Routine co-registration of SRS with CT, which is becoming more common with the introduction of cameras equipped with a CT scanner (SPECT/CT), is therefore likely to result in a better interpretation of the findings in islet cell tumors and consequently in higher detection rates (LOE 2b).

When used for the screening of MEN-1 patients, SRS could only detect 2 out of 12 asymptomatic patients.[39] One study in VHL-patients included 27 patients with islet cell tumors, which were detected during screening, and SRS was positive in 16 of these patients.[55] SRS has a LOE 2b for the screening of mutation carriers.

Newer somatostatin receptor tracers

Newer somatostatin receptor tracers for gamma cameras and PET are currently being tested in mixed populations of patients with different neuroendocrine tumors, including islet cell tumors. Studies that investigate these tracers have included both symptomatic patients and patients with a chance tumor finding. As these studies do not allow a separate evaluation of only the islet cell tumor patients, no LOE has been assigned to these studies. Additionally no studies have yet looked at the value of these tracers in mutation-carriers.

The two SPECT tracers ^{99m}Tc-6-hydrazinopyridine-3-carbolic acid-Tyr3-octreotide (^{99m}Tc TOC) and ^{99m}Tc-6-hydrazinopyridine-3-carbolic acid-

Tyr3-Th8-octreotide (^{99m}Tc TATE) showed concordance in 12 patients with neuroendocrine tumors (5 islet cell tumors), with ^{99m}Tc TATE performing slightly better than ^{99m}Tc TOC.[56] These two tracers target somatostatin receptor subtypes 2 and 5, and show a higher tumor-to-background ratio and higher tumor uptake than ^{111}In-DTPA-D-Phe-octreotide.[57-59]

Glucagon-like peptide 1 scintigraphy

GLP-1-receptor scintigraphy uses the SPECT tracer ^{111}In-DOTA-exendin-4, a GLP-1 receptor agonist, to target the GLP-1 receptor. Its rationale is based on the fact that virtually all insulinomas expresss GLP-1 receptors.[60] GLP-1-receptor scintigraphy may offer new perspectives for these tumors, which are generally difficult to detect with imaging techniques used sofar. In 8 patients with hyperglycemia it has been used to localize an insulinoma which resulted in a LOE of 4.[61, 62]

B. Positron emission tomography

For PET imaging of neuroendocrine tumors a number of tracers, including somatostatin receptor tracers, are available. In comparison to gamma cameras, PET cameras have a better spatial resolution, and can therefore detect smaller tumors, resulting in better sensitivities.[63, 64] The most commonly used tracer in oncology is ^{18}F-FDG, which visualizes tumor glucose uptake. More recently, two other metabolic tracers, based on the intrinsic property of neuroendocrine tumors to take up, decarboxylate, and store amine precursors have been developed (Figure 6).

Somatostatin receptor imaging with PET

Somatostatin receptor tracers are also being developed for PET scanners. ^{68}Ga-DOTA-Tyr3-octreotide (^{68}Ga-DOTA-TOC) PET was superior to SRS and CT in 84 patients with different neuroendocrine tumors, including 25 islet cell tumors, who underwent these tests for initial

detection, staging or follow-up. ^{68}Ga-DOTA-TOC detected 23 of the pancreatic lesions, compared to 21 by SRS and 19 by CT.[65] ^{68}Ga-DOTA-Nal3-octreotide (^{68}Ga-DOTA-NOC) has the advantage that, in addition to targeting receptor subtypes 2 and 5, it also has a good affinity for the somatostastin receptor subtype 3. This may increase detection rate, since it will also visualize tumors lacking expression of receptor subtypes 2 and 5.[57] It showed more positive scans and lesions than ^{18}F-DOPA PET in 13 patients with neuroendocrine tumors (8 islet cell tumors) investigated for initial detection and staging.[66]

^{18}F-FDG PET

Casuistic evidence reports the value of ^{18}F-FDG PET for islet cell tumor detection.[67] One small study in 12 patients with varying subtypes of islet cell tumors has been performed, without clear specification of the indication. In this study only 53% of the tumors could be detected (LOE 2b).[68] For example, only 2 out of 5 insulinomas imaged with ^{18}F-FDG PET could be visualized by this technique.[68, 69] Tumors with a low glucose metabolism (such as well-differentiated neuroendocrine tumors) often show faint ^{18}F-FDG-uptake and are poorly visualised by PET, while more aggressive less-differentiated tumors (as demonstrated by a high Ki-67 expression) show better ^{18}F-FDG-uptake.[70-72]

^{18}F-FDG PET has not been performed for the screening of mutation-carriers. Based on to above data does also does not seem to be of interest.

^{11}C-5-HTP PET

PET using the serotonin precursor ^{11}C-5-HTP, another metabolic tracer, is compared to ^{18}F-FDG more specific for neuroendocrine tumors and showed promising results for the imaging of islet cell tumors (Figure 3C).

PET scanning with ^{11}C-5-HTP and the catecholamine precursor [^{11}C] dihydroxyphenylalanin (^{11}C-DOPA) were compared in 22 patients with

clinically and biochemically verified islet cell tumors (5 gastrinoma, 4 glucagonoma, 4 insulinoma, 1 VIPoma, 5 non-functioning). Both tracers showed the same number of lesions, but ^{11}C-5-HTP had higher tracer uptake per lesion (LOE 2b).[73]

One study is performed that includes patients with a chance finding of neuroendocrine tumors as well as patients that were imaged due to symptoms. In this study in 23 patients with different islet cell tumor subtypes referred for initial tumor detection or follow-up ^{11}C-5-HTP PET reached a sensitivity of 67%.[44] Combining ^{11}C-5-HTP PET with CT improved the sensitivity to 96%. The superior performance of ^{11}C-5-HTP PET compared to CT and SRS was confirmed in another study that included 10 patients with islet cell tumors (4 gastrinoma, 1 insulinoma, 5 non-functioning).[74] In 25 MEN-1 patients with positive biochemistry or positive CT/transabdominal ultrasound, ^{11}C-5-HTP PET could only identify tumors in 38%.[75] ^{11}C-5-HTP PET has a LOE 2b to detect an islet cell tumor in these groups with mixed imaging indications. Currently we are evaluating the value of ^{11}C-5-HTP PET for the screening of mutation-carriers (Dutch trial register number: NTR1668).

^{18}F-DOPA PET

The ^{18}F-labeled variant of the catecholamine precursor DOPA (^{18}F-DOPA) is also used as a metabolic PET tracer specific for neuroendocrine tumors (Figure 3D).

^{18}F-DOPA PET has shown varying results in patients with hyperglycemia. It localized the pancreatic lesion in 9 out of 10 patients with hyperinsulinemia (final histopathological diagnosis was n = 8 insulinomas, n = 2 nesidioblastosis)[76], but detected only 1 out of 6 patients in another study.[77] Co-administration of the aromatic-L-amino-acid decarboxylase (AADC) inhibitor carbidopa before ^{18}F-DOPA PET has been shown to result in higher tracer availability for tumor uptake, due to inhibition of renal decarboxylation and subsequent clearance of the decarboxylated tracers in

carcinoid tumors and pheochromocytoma.[78-81] In case of intrinsically absent tumor AADC-activity, tumor visualization might be affected negatively by pre-treatment with carbidopa.[82] Carbidopa masked the uptake of ^{18}F-DOPA in 2 out of 3 patients with hyperinsulinism and in one out of two patients with insulinoma.[83, 84] Therefore, the exact place of carbidopa coadministration with PET for islet cell tumors deserves further investigation. ^{18}F-DOPA PET has a LOE 2b for the detection of insulinomas.

One study is performed that included patients with a chance finding of neuroendocrine tumors, but it also includes patients that were imaged due to symptoms. ^{18}F-DOPA PET and ^{11}C-5-HTP PET were directly compared in 23 patients referred for initial detection or follow-up, in which ^{18}F-DOPA PET achieved a sensitivity of 41%, making it inferior to ^{11}C-5-HTP PET (67%) (LOE 2b).[44]

No studies have looked at the value of ^{18}F-DOPA PET for the screening of mutation-carriers.

V. DISCUSSION

This systematic review shows that EUS is the most sensitive imaging technique for all three imaging indications of islet cell tumors, but evidence for the application of all imaging techniques is weak. There is a considerable difference between the reported studies with regards to which subtypes of islet cell tumors were included and what the indication for imaging was. There for the results of these studies vary widely in sensitivities. Due to the rarity of the disease, most studies comprised only limited patient numbers, frequently missing a head-to-head comparison. These factors make clear interpretation of the data difficult.

Existing guidelines for the localization of the primary tumor and staging of islet cell tumors do not distinguish between symptomatic patients and patients with a chance finding of a neuroendocrine tumor.

Guidelines from the European Neuroendocrine Tumor Society recommend EUS followed by CT and SRS for imaging of gastrinoma, while for insulinoma CT, MRI and EUS are considered the most useful techniques, without one of those being clearly recommended above the other two.[85, 86] For other rare functioning islet cell tumors a combination of CT and SRS is recommended, while for non-functioning tumors a combination of transabdominal ultrasound with CT or MRI and SRS is advocated.[22, 87] The NCCN recommends CT or MRI for the localization of the primary tumor and staging for all subtypes of islet cell tumors, and SRS 'as appropriate'.[88] Our analyses with Forest plots point towards especially a prominent role for EUS. EUS has the best overall sensitivity to localize tumors in patients presenting with hormone hypersecretion. It shows also the best performance in patients with a chance finding of a neuroendocrine tumor. PET with ^{11}C-5-HTP or ^{18}F-DOPA (likely without carbidopa pre-treatment) has also a good sensitivity, but availability of these techniques is currently still limited while CT, MRI or SRS have only moderate detection rates. Although adding CT to EUS or PET does improve detection rates. Available information about the subtype of islet cell tumor should also be used to guide the choice of imaging technique, since for example SRS is of little value in patients with insulinoma.

For the screening of MEN1 international guidelines propose to use SRS and CT or MRI every 3 years. For VHL a yearly CT scan is advised, while SRS is not routinely recommended.[7, 8] Tumors in genetically predisposed individuals are usually multiple and small; therefore techniques with a high spatial resolution are required. A careful algorithm with implementation of new insights seems attractive, since repeated CT or SRS can result in a high cumulative radiation exposure.[89, 90] Radiation is a carcinogenic risk factor, which is especially undesirable for the individuals with an inherited predisposition for cancer. In this light, EUS is the best screening tool. Studies comparing CT, SRS, and EUS in MEN1 (14-22 patients) showed that EUS is the most sensitive technique, while the other

techniques detect only a small fraction of the patients.[39, 75, 91] This is especially true for the detection of lesions smaller than 1 cm in size. Therefore EUS deserves a prominent role in the screening of these individuals. No such studies are performed in VHL, but as in these patients the tumors are also small and multiple, EUS is probably also superior in VHL-patients. In VHL EUS-FNA offers the additional advantage that cytology can be obtained to distinguish between a cystadenoma, which are frequently seen in VHL-patients, and a solid islet cell tumor. Lastly, EUS carries no radiation exposure and is therefore safe to use in these patients.

Understanding biological and metabolic characteristics of islet cell tumors may help us understand why some tumors can be visualized with certain functional imaging techniques and why others cannot. Knowledge about tumor pathophysiology will provide new insights for the development of better tracers. In this light, the performance of ^{68}Ga-DOTA-labeled somatostatin analogues with PET scanning in patients with islet cell tumors deserves further investigation. It deserves also testing as screenings strategy in patients with hereditary tumors. This imaging technique has the potential to replace the SRS since its tracer has better receptor affinity than ^{111}In-DTPA-D-Phe-octreotide and PET has a better spatial resolution than SPECT. This may be a particular advantage for the imaging of insulinomas not expressing somatostatin receptor subtype 2.

The data available from clinical trials that fitted our inclusion criteria still have limitations. No separate sensitivities could be calculated for patients presenting with a chance finding of a neuroendocrine tumor or metastases as they were always analyzed in combination with symptomatic patients. Only one study provided separate sensitivity values for the detection of pancreatic gastrinomas. LOE was the same for all imaging techniques (2b), except for EUS to image patients with a chance tumor finding (LOE 3b). Therefore the LOEs could not be used to distinguish the best imaging technique. Consequently, the sensitivity value has to be used

to choose the best imaging technique. To determine the best imaging algorithm there is a great need of adequately sized prospective studies.

VI. CONCLUSION

Recent years have shown a fast evolution in pre-operative imaging techniques for islet cell tumors. With growing knowledge about these tumors we should now strive to develop new imaging algorithms to choose the right set of procedures in these patients. Imaging can be tailored depending on imaging indication (tumor detection in patients suspected of having an islet cell tumor or screening of mutation carriers) and tumor subtype. The insights gained in this review may serve as a starting-point to investigate the optimal imaging algorithm for (subtypes of) islet cell tumors.

REFERENCES

1. Oberg K, Eriksson B. Endocrine tumours of the pancreas. Best Pract Res Clin Gastroenterol 2005;19:753-781
2. Modlin IM, Oberg K, Chung DC, et al. Gastroenteropancreatic neuroendocrine tumours. Lancet Oncol 2008;9:61-72
3. Oberg K, Modlin IM. Non-functioning pancreatic endocrine tumors. In: Modlin IM, Oberg K, eds. A century of advances in neuroendocrine tumor biology and treatment. Hannover: Felsenstein CCCP, 2007;86-99
4. Kloppel G, Perren A, Heitz PU. The gastroenteropancreatic neuroendocrine cell system and its tumors: the WHO classification. Ann N Y Acad Sci 2004;1014:13-27
5. Stabile B, Morrow D, Passaro J. The gastrinoma triangle: Operative implications. Am J Surg 1984;147:25-31
6. Kaltsas GA, Besser GM, Grossman AB. The diagnosis and medical management of advanced neuroendocrine tumors. Endocr Rev 2004;25:458-511
7. Brandi M, Gagel R, Angeli A, et al. Guidelines for diagnosis and therapy of MEN Type 1 and Type 2. J Clin Endocrinol Metab 2001;86:5658-5671
8. Lonser R, Glenn G, Walther M, et al. Von Hippel-Lindau disease. Lancet 2003;361:2059-2067
9. Oberg K, Eriksson B. Endocrine tumours of the pancreas. Best Pract Res Clin Gastroenterol 2005;19:753-781
10. Kuzin NM, Egorov AV, Kondrashin SA, et al. Preoperative and intraoperative topographic diagnosis of insulinomas. World J Surg 1998;22:593-597
11. Angeli E, Vanzulli A, Castrucci M, et al. Value of abdominal sonography and MR imaging at 0.5 T in preoperative detection of pancreatic insulinoma: a comparison with dynamic CT and angiography. Abdom Imaging 1997;22:295-303
12. Zimmer T, Scherubl H, Faiss S, et al. Endoscopic ultrasonography of neuroendocrine tumours. Digestion 2000;62 Suppl 1:45-50

13. Brown C, Bartlett D, Doppman J, et al. Intraarterial calcium stimulation and intraoperative ultrasonography in the localization and resection of insulinomas. Surgery 1997;122:1189-1194
14. Boukhman MP, Karam JM, Shaver J, et al. Localization of insulinomas. Arch Surg 1999;134:818-822
15. Chavan A, Kirchhoff TD, Brabant G, et al. Role of the intra-arterial calcium stimulation test in the preoperative localization of insulinomas. Eur Radiol 2000;10:1582-1586
16. Grover AC, Skarulis M, Alexander HR, et al. A prospective evaluation of laparoscopic exploration with intraoperative ultrasound as a technique for localizing sporadic insulinomas. Surgery 2005;138:1003-1008
17. Machado MC, da Cunha JE, Jukemura J, et al. Insulinoma: diagnostic strategies and surgical treatment. A 22-year experience. Hepatogastroenterology 2001;48:854-858
18. Ravi K, Britton BJ. Surgical approach to insulinomas: are pre-operative localisation tests necessary? Ann R Coll Surg Engl 2007;89:212-217
19. Queiroz Almeida M, Machado MC, Correa-Giannella ML, et al. Endogenous hyperinsulinemic hypoglycemia: diagnostic strategies, predictive features of malignancy and long-term survival. J Endocrinol Invest 2006;29:679-687
20. Kisker O, Bastian D, Bartsch D, et al. Localization, malignant potential, and surgical management of gastrinomas. World J Surg 1998;22:651-657
21. Pitre J, Soubrane O, Palazzo L, et al. Endoscopic ultrasonography for the preoperative localization of insulinomas. Pancreas 1996;13:55-60
22. Falconi M, Plockinger U, Kwekkeboom DJ, et al. Well-differentiated pancreatic nonfunctioning tumors/carcinoma. Neuroendocrinology 2006;84:196-211
23. Rickes S, Unkrodt K, Ocran K, et al. Differentiation of neuroendocrine tumors from other pancreatic lesions by echo-enhanced power Doppler sonography and somatostatin receptor scintigraphy. Pancreas 2003;26:76-81
24. D'Onofrio M, Mansueto G, Vasori S, et al. Contrast-enhanced ultrasonographic detection of small pancreatic insulinoma. J Ultrasound Med 2003;22:413-417

25. D'Onofrio M, Mansueto G, Falconi M, et al. Neuroendocrine pancreatic tumor: value of contrast enhanced ultrasonography. Abdom Imaging 2004;29:246-258
26. Rosch T, Lightdale CJ, Botet JF, et al. Localization of pancreatic endocrine tumors by endoscopic ultrasonography. N Engl J Med 1992;326:1721-1726
27. Janssen J, Schlorer E, Greiner L. EUS elastography of the pancreas: feasibility and pattern description of the normal pancreas, chronic pancreatitis, and focal pancreatic lesions. Gastrointest Endosc 2007;65:971-978
28. Voss M, Hammel P, Molas G, et al. Value of endoscopic ultrasound guided fine needle aspiration biopsy in the diagnosis of solid pancreatic masses. Gut 2000;46:244-249
29. Ardengh JC, Paulo de AG, Ferrari PA. EUS-guided FNA in the diagnosis of pancreatic neuroendocrine tumors before surgery. Gastrointest Endosc 2004;60:378-384
30. Gines A, Vazquez-Sequeiros E, Soria M, et al. Usefulness of EUS-guided fine needle aspiration (EUS-FNA) in the diagnosis of functioning neuroendocrine tumors. Gastrointest Endosc 2002;56:291-296
31. Gouya H, Vignaux O, Augui J, et al. CT, endoscopic sonography, and a combined protocol for preoperative evaluation of pancreatic insulinomas. Am J Roentgenol 2003;181:987-992
32. Schumacher B, Lubke HJ, Frieling T, et al. Prospective study on the detection of insulinomas by endoscopic ultrasonography. Endoscopy 1996;28:273-276
33. Ruszniewski P, Amouyal P, Amouyal G, et al. Localization of gastrinomas by endoscopic ultrasonography in patients with Zollinger-Ellison syndrome. Surgery 1995;117:629-635
34. Sotoudehmanesh R, Hedayat A, Shirazian N, et al. Endoscopic ultrasonography (EUS) in the localization of insulinoma. Endocrine 2007;31:238-241
35. Kann PH, Ivan D, Pfutzner A, et al. Preoperative diagnosis of insulinoma: low body mass index, young age, and female gender are associated with negative imaging by endoscopic ultrasound. Eur J Endocrinol 2007;157:209-213

36. Ardengh JC, Rosenbaum P, Ganc AJ, et al. Role of EUS in the preoperative localization of insulinomas compared with spiral CT. Gastrointest Endosc 2000;51:552-555
37. Anderson MA, Carpenter S, Thompson NW, et al. Endoscopic ultrasound is highly accurate and directs management in patients with neuroendocrine tumors of the pancreas. Am J Gastroenterol 2000;95:2271-2277
38. Rappeport ED, Hansen CP, Kjaer A, et al. Multidetector computed tomography and neuroendocrine pancreaticoduodenal tumors. Acta Radiol 2006;47:248-256
39. Langer P, Kann PH, Fendrich V, et al. Prospective evaluation of imaging procedures for the detection of pancreaticoduodenal endocrine tumors in patients with multiple endocrine neoplasia type 1. World J Surg 2004;28:1317-1322
40. Van Hoe L, Gryspeerdt S, Marchal G, et al. Helical CT for the preoperative localization of islet cell tumors of the pancreas: value of arterial and parenchymal phase images. Am J Roentgenol 1995;165:1437-1439
41. Fidler JL, Fletcher JG, Reading CC, et al. Preoperative detection of pancreatic insulinomas on multiphasic helical CT. Am J Roentgenol 2003;181:775-780
42. Ichikawa T, Peterson MS, Federle MP, et al. Islet cell tumor of the pancreas: biphasic CT versus MR imaging in tumor detection. Radiology 2000;216:163-171
43. Schirmer WJ, Melvin WS, Rush RM, et al. Indium-111-pentetreotide scanning versus conventional imaging techniques for the localization of gastrinoma. Surgery 1995;118:1105-1113
44. Koopmans KP, Neels OC, Kema IP, et al. Improved staging of patients with carcinoid and islet cell tumors with 18F-dihydroxy-phenyl-alanine and 11C-5-hydroxy-tryptophan positron emission tomography. J Clin Oncol 2008;26:1489-1495
45. Noone TC, Hosey J, Firat Z, et al. Imaging and localization of islet-cell tumours of the pancreas on CT and MRI. Best Pract Res Clin Endocrinol Metab 2005;19:195-211
46. Catalano C, Pavone P, Laghi A, et al. Localization of pancreatic insulinomas with MR imaging at 0.5 T. Acta Radiol 1999;40:644-648

47. Thoeni RF, Mueller-Lisse UG, Chan R, et al. Detection of small, functional islet cell tumors in the pancreas: selection of MR imaging sequences for optimal sensitivity. Radiology 2000;214:483-490
48. Reubi JC, Schaer JC, Waser B, et al. Expression and localization of somatostatin receptor SSTR1, SSTR2, and SSTR3 messenger RNAs in primary human tumors using in situ hybridization. Cancer Res 1994;54:3455-3459
49. Reubi JC, Kvols L, Krenning E, et al. In vitro and in vivo detection of somatostatin receptors in human malignant tissues. Acta Oncol 1991;30:463-468
50. Krenning EP, Kwekkeboom DJ, Bakker WH, et al. Somatostatin receptor scintigraphy with [111In-DTPA-D-Phe1]- and [123I-Tyr3]-octreotide: the Rotterdam experience with more than 1000 patients. Eur J Nucl Med 1993;20:716-731
51. John M, Meyerhof W, Richter D, et al. Positive somatostatin receptor scintigraphy correlates with the presence of somatostatin receptor subtype 2. Gut 1996;38:33-39
52. Scherubl H, Bader M, Fett U, et al. Somatostatin-receptor imaging of neuroendocrine gastroenteropancreatic tumors. Gastroenterology 1993;105:1705-1709
53. Lamberts SW, Hofland LJ, van Koetsveld PM, et al. Parallel in vivo and in vitro detection of functional somatostatin receptors in human endocrine pancreatic tumors: consequences with regard to diagnosis, localization, and therapy. J Clin Endocrinol Metab 1990;71:566-574
54. Briganti V, Matteini M, Ferri P, et al. Octreoscan SPET evaluation in the diagnosis of pancreas neuroendocrine tumors. Cancer Biother Radiopharm 2001;16:515-524
55. Corcos O, Couvelard A, Giraud S, et al. Endocrine pancreatic tumors in von Hippel-Lindau disease: clinical, histological, and genetic features. Pancreas 2008;37:85-93
56. Cwikla J, Mikolajczak R, Pawlak D, et al. Initial direct comparison of 99mTc-TOC and 99mTc-TATE in identifying sites of disease in patients with proven GEP NETs. J Nucl Med 2008;49:1060-1065

57. Cescato R, Schulz S, Waser B, et al. Internalization of sst2, sst3, and sst5 Receptors: Effects of somatostatin agonists and antagonists. J Nucl Med 2006;47:502-511
58. Gabriel M, Decristoforo M, Donnemiller M, et al. An intrapatient comparison of 99mTc-EDDA/HYNIC-TOC with 111In-DTPA-octreotide for diagnosis of somatostatin receptor-expressing tumors. J Nucl Med 2003;44:708-716
59. Storch D, Behe M, Walter M, et al. Evaluation of [99mTc/EDDA/HYNIC0]octreotide derivatives compared with [111In-DOTA0,Tyr3, Thr8]octreotide and [111In-DTPA0]octreotide: does tumor or pancreas uptake correlate with the rate of internalization? J Nucl Med 2005;46:1561-1569
60. Jansen F, Vanderheyden J. The future of SPECT in a time of PET. Nucl Med Biol 2007;34:733-735
61. Rahmim A, Zaidi H. PET versus SPECT: strengths, limitations and challenges. Nucl Med Commun 2008;29:193-207
62. Gabriel M, Decristoforo C, Kendler D, et al. 68Ga-DOTA-Tyr3-octreotide PET in neuroendocrine tumors: comparison with somatostatin receptor scintigraphy and CT. J Nucl Med 2007;48:508-518
63. Ambrosini V, Tomassetti P, Castellucci P, et al. Comparison between 68Ga-DOTA-NOC and 18F-DOPA PET for the detection of gastro-entero-pancreatic and lung neuro-endocrine tumours. Eur J Nucl Med Mol Imaging 2008;35:1431-1438
64. Suzuki H, Kuwano H, Masuda N, et al. Diagnostic usefulness of FDG-PET for malignant somatostatinoma of the pancreas. Hepatogastroenterology 2008;55:1242-1245
65. Nakamoto Y, Higashi T, Sakahara H, et al. Evaluation of pancreatic islet cell tumors by fluorine-18 fluorodeoxyglucose positron emission tomography: comparison with other modalities. Clin Nucl Med 2000;25:115-119
66. Giorgi MC, Cunha RM, Soares J, Jr., et al. Dual-head gamma camera coincidence imaging in pancreatic cancer. Rev Esp Med Nucl 2004;23:90-94
67. Adams S, Baum R, Rink T, et al. Limited value of fluorine-18 fluorodeoxyglucose positron emission tomography for the imaging of neuroendocrine tumours. Eur J Nucl Med 1998;25:79-83

68. Pasquali C, Rubello D, Sperti C, et al. Neuroendocrine tumor imaging: can 18F-fluorodeoxyglucose positron emission tomography detect tumors with poor prognosis and aggressive behavior? World J Surg 1998;25:588-592
69. Kayani I, Bomanji JB, Groves A, et al. Functional imaging of neuroendocrine tumors with combined PET/CT using 68Ga-DOTATATE (DOTA-DPhe1,Tyr3-octreotate) and 18F-FDG. Cancer 1998;112:2447-2455
70. Ahlstrom H, Eriksson B, Bergstrom M, et al. Pancreatic neuroendocrine tumors: diagnosis with PET. Radiology 1995;195:333-337
71. Orlefors H, Sundin A, Garske U, et al. Whole-body (11)C-5-hydroxytryptophan positron emission tomography as a universal imaging technique for neuroendocrine tumors: comparison with somatostatin receptor scintigraphy and computed tomography. J Clin Endocrinol Metab 2005;90:3392-3400
72. Hellman P, Hennings J, Akerstrom G, et al. Endoscopic ultrasonography for evaluation of pancreatic tumours in multiple endocrine neoplasia type 1. Br J Surg 2005;92:1508-1512
73. Kauhanen S, Seppanen M, Minn H, et al. Fluorine-18-L-dihydroxyphenylalanine (18F-DOPA) positron emission tomography as a tool to localize an insulinoma or beta-cell hyperplasia in adult patients. J Clin Endocrinol Metab 2007;92:1237-1244
74. Tessonnier L, Sebag F, Ghander C, et al. Limited value of 18F-F-DOPA PET to localize pancreatic insulin-secreting tumors in adults with hyperinsulinemic hypoglycemia. J Clin Endocrinol Metab 2010;95:303-307
75. Brown WD, Oakes TR, DeJesus OT, et al. Fluorine-18-fluoro-L-DOPA dosimetry with carbidopa pretreatment. J Nucl Med 1998;39:1884-1891
76. Ishikawa T, Dhawan V, Chaly T, et al. Fluorodopa positron emission tomography with an inhibitor of catechol-O-methyltransferase: effect of the plasma 3-O-methyldopa fraction on data analysis. J Cereb Blood Flow Metab 1996;16:854-863
77. Orlefors H, Sundin A, Lu L, et al. Carbidopa pretreatment improves image interpretation and visualisation of carcinoid tumours with 11C-5-hydroxytryptophan positron emission tomography. Eur J Nucl Med Mol Imaging 2006;33:60-65

78. Timmers HJ, Hadi M, Carrasquillo JA, et al. The effects of carbidopa on uptake of 6-18F-fluoro-L-DOPA in PET of pheochromocytoma and extraadrenal abdominal paraganglioma. J Nucl Med 2007;48:1599-1606
79. Kema IP, Koopmans KP, Elsinga PH, et al. In Reply. J Clin Oncol 2008;26:5308-5309
80. Kauhanen S, Seppanen M, Nuutila P. Premedication with carbidopa masks positive finding of insulinoma and {beta}-cell hyperplasia in [18F]-dihydroxy-phenyl-alanine positron emission tomography. J Clin Oncol 2008;26:5307-5308
81. Ribeiro MJ, Boddaert N, Bellanne-Chantelot C, et al. The added value of [18F]fluoro-L-DOPA PET in the diagnosis of hyperinsulinism of infancy: a retrospective study involving 49 children. Eur J Nucl Med Mol Imaging 2007;34:2120-2128
82. Reubi JC, Waser B. Concomitant expression of several peptide receptors in neuroendocrine tumours: molecular basis for in vivo multireceptor tumour targeting. Eur J Nucl Med Mol Imaging 2003;30:781-793
83. Christ E, Wild D, Forrer F, et al. Glucagon-like peptide-1 receptor imaging for localization of insulinomas. J Clin Endocrinol Metab 2009;94:4398-4405
84. Wild D, Macke H, Christ E, et al. Glucagon-like peptide 1-receptor scans to localize occult insulinomas. N Engl J Med 2008;359:766-768
85. de Herder WW, Niederle B, Scoazec JY, et al. Well-differentiated pancreatic tumor/carcinoma: insulinoma. Neuroendocrinology 2006;84:183-188
86. Jensen RT, Niederle B, Mitry E, et al. Gastrinoma (duodenal and pancreatic). Neuroendocrinology 2006;84:173-182
87. O'Toole D, Salazar R, Falconi M, et al. Rare functioning pancreatic endocrine tumors. Neuroendocrinology 2006;84:189-195
88. NCCN clinical practice guidelines in oncology: Neuroendocrine tumors v.2.2009 National Comprehensive Cancer Network, http://www.nccn.org/professionals/physician_gls/PDF/neuroendocrine.pdf
89. Fazel R, Krumholz H, Wang Y, et al. Exposure to low-dose ionizing radiation from medical imaging procedures. N Engl J Med 2009;361:849-857
90. Sodickson A, Baeyens P, Andriole K, et al. Recurrent CT, cumulative radiation exposure, and associated radiation-induced cancer risks from CT of adults. Radiology 2009;251:175-184

91. Kann PH, Balakina E, Ivan D, et al. Natural course of small, asymptomatic neuroendocrine pancreatic tumours in multiple endocrine neoplasia type 1: an endoscopic ultrasound imaging study. Endocr Relat Cancer 2006;13:1195-1202
92. Kulke M, Lenz H, Meropol N, et al. Activity of sunitinib in patients with advanced neuroendocrine tumors. J Clin Oncol 2009;26:3403-3410
93. Yao J, Lombard-Bohas C, Baudin E, et al. Daily oral everolimus activity in patients with metastatic pancreatic neuroendocrine tumors after failure of cytotoxic chemotherapy: A phase II trial. J Clin Oncol 2010;28:69-76
94. Roland CL, Lo CY, Miller BS, et al. Surgical approach and perioperative complications determine short-term outcomes in patients with insulinoma: results of a bi-institutional study. Ann Surg Oncol 2008;15:3532-3537
95. Varas Lorenzo MJ, Miquel Collell JM, Maluenda Colomer MD, et al. Preoperative detection of gastrointestinal neuroendocrine tumors using endoscopic ultrasonography. Rev Esp Enferm Dig 2006;98:828-836
96. Wamsteker E, Gauger P, Thompson N, et al. EUS detection of pancreatic endocrine tumors in asymptomatic patients with type 1 multiple endocrine neoplasia. Gastrointest Endosc 2003;58:531-535
97. Wiesli P, Brandle M, Schmid C, et al. Selective arterial calcium stimulation and hepatic venous sampling in the evaluation of hyperinsulinemic hypoglycemia: potential and limitations. J Vasc Interv Radiol 2004;15:1251-1256
98. Won JG, Tseng HS, Yang AH, et al. Intra-arterial calcium stimulation test for detection of insulinomas: detection rate, responses of pancreatic peptides, and its relationship to differentiation of tumor cells. Metabolism 2003;52:1320-1329
99. Schillaci O, Massa R, Scopinaro F. 111In-pentetreotide scintigraphy in the detection of insulinomas: importance of SPECT imaging. J Nucl Med 2000;41:459-462
100. Chen X, Cai WY, Yang WP, et al. Pancreatic insulinomas: diagnosis and surgical treatment of 74 patients. Hepatobiliary Pancreat Dis Int 2002;1:458-461

101. Krausz Y, Bar-Ziv J, de Jong RB, et al. Somatostatin-receptor scintigraphy in the management of gastroenteropancreatic tumors. Am J Gastroenterol 1998;93:66-70

Chapter 3

^{18}F-DOPA PET is superior to conventional imaging with ^{123}I-metaiodobenzylguanidine scintigraphy, computer tomography, and magnetic resonance imaging in localizing tumors causing catecholamine excess

Helle-Brit Fiebrich[1], Adrienne H. Brouwers[2], Michiel N. Kerstens[3], Milan E. J. Pijl[4], Ido P. Kema[5], Johan R. de Jong[2], Pieter L. Jager[6], Philip H. Elsinga[2], Rudi A. J. O. Dierckx[2], Jacqueline E. van der Wal[7], Wim J. Sluiter[3], Elisabeth G. E. de Vries[1], Thera P. Links[3]

Departments of [1]Medical Oncology, [2]Nuclear Medicine and Molecular Imaging, and [3]Endocrinology, University Medical Center Groningen, Groningen, The Netherlands, [4]Department of Radiology, Martini Hospital, Groningen, The Netherlands, [5]Department of Laboratory Medicine, University Medical Center Groningen, Groningen, The Netherlands, [6]Department of Nuclear Medicine, Hamilton Health Sciences and McMaster University, Hamilton, ON, Canada
[7]Department of Pathology, University Medical Center Groningen, Groningen, The Netherlands

J Clin Endocrinol Metab 2009, 94:3922-3930

ABSTRACT

Context

Catecholamine excess is rare, but symptoms may be life-threatening.

Objective

To investigate the sensitivity of 6-[F-18]fluoro-L-dihydroxyphenylalanine positron emission tomography (^{18}F-DOPA PET), compared to ^{123}I-metaiodobenzylguanidine (^{123}I-MIBG) scintigraphy and CT/MRI for tumor localization in patients with catecholamine excess.

Design and Setting

All consecutive patients with catecholamine excess visiting the UMCG, Groningen, between March 2003 and January 2008 were eligible.

Patients

48 patients were included. The final diagnosis was pheochromocytoma in 40, adrenal hyperplasia in 2, paraganglioma in 2, ganglioneuroma in 1, unknown in 3.

Main Outcome Measures

Sensitivities and discordancy between ^{18}F-DOPA PET, ^{123}I-MIBG and CT or MRI, were analyzed for individual patients and lesions. Metanephrines and 3-methoxytyramine in plasma and urine, uptake of ^{18}F-DOPA with PET were measured to determine the whole-body metabolic burden and

correlated with biochemical tumor activity. Gold standard was a composite reference standard.

Results

^{18}F-DOPA PET showed lesions in 43 patients, ^{123}I-MIBG in 31 and CT/MRI in 32. Patient-based sensitivity for ^{18}F-DOPA PET, ^{123}I-MIBG and CT/MRI was 90, 65 and 67% (P<.01 for ^{18}F-DOPA PET vs. both ^{123}I-MIBG and CT/MRI, P=1.0 ^{123}I-MIBG vs. CT/MRI). Lesion-based sensitivities were 73, 48 and 44% (P<.001 for ^{18}F-DOPA PET vs. both ^{123}I-MIBG and CT/MRI, P=.51 ^{123}I-MIBG vs. CT/MRI). The combination of ^{18}F-DOPA PET with CT/MRI was superior to ^{123}I-MIBG with CT/MRI (93 vs. 76%, P<.001). Whole-body metabolic burden measured with ^{18}F-DOPA PET correlated with plasma normetanephrine (r=0.82), and urinary normetanephrine (r=0.84), and metanephrine (r=0.57).

Conclusion

To localize tumors causing catecholamine excess ^{18}F-DOPA PET is superior to ^{123}I-MIBG scintigraphy and CT/MRI.

INTRODUCTION

Catecholamine excess caused by catecholamine-producing tumors is rare, but clinically important since its symptoms may be life-threatening. Patients can often be cured by surgical removal of the tumor. The most frequent catecholamine-producing tumors are pheochromocytomas, which arise from chromaffin cells of the adrenal medulla (80 - 85%) or extra-adrenal paraganglia (15 - 20%).[1] However, also other tumors such as ganglioneuromas can produce the clinical symptoms of catecholamine excess. Catecholamine excess is detected by measuring catecholamines and their metabolites in plasma or 24-h urine samples. Imaging techniques are used to localize the primary tumor and to search for metastases. In case of pheochromocytomas most tumors are benign but 10-20% are malignant.[1,2] Ruling out metastatic disease before initial surgery is important, because the presence of metastases affects treatment.

Computer tomography (CT) and magnetic resonance imaging (MRI) demonstrate good sensitivities in detecting adrenal pheochromocytoma, but exhibit lower sensitivities for extra-adrenal or metastatic disease.[1, 3] Functional imaging methods allow further characterization of detected lesions and provide whole-body images. The standard functional imaging technique for catecholamine-producing tumors is scintigraphy with $^{123/131}$I-labeled meta-iodobenzylguanidine (MIBG), which combines a high sensitivity and high specificity.[1, 4, 5] However, sensitivity is lower for malignant pheochromocytoma, and small pheochromocytomas may be missed because of limited spatial resolution of single photon emission computed tomography (SPECT) with $^{123/131}$I-MIBG.[6, 7]

Positron emission tomograpy (PET) imaging with a variety of different tracers has shown that 6-[F-18]fluorodeoxyglucose (FDG) has a high sensitivity in a subset of patients with metastatic disease and underlying *succinate dehydrogenase D* (SDHD)-mutation, but limited

sensitivity and specificity in the more common benign pheochromocytomas.[6, 8-10] More specific imaging of catecholamine-producing tumors is possible with the catecholamine precursor 6-[F-18]fluoro-L-dihydroxyphenylalanine (^{18}F-DOPA) or the catecholamine ^{18}F-fluorodopamine. Small studies have confirmed the feasibility of ^{18}F-DOPA as tracer for staging of pheochromocytomas.[10-13] ^{18}F-fluorodopamine showed an excellent sensitivity superior to ^{123}I-MIBG, in a retrospective study in 53 patients with known or suspected benign and malignant pheochromocytomas.[14] In a small study in 12 pheochromocytoma patients ^{18}F-DOPA PET has also shown good performance relative to ^{123}I-MIBG scintigraphy.[10] However, most studies in the past have based inclusion of patients on the (suspected) presence of a pheochromocytoma or paraganglioma. They have not addressed this issue from the even more basic clinical relevant question: a patient presenting with catecholamine excess.

The aim of this prospective study was to investigate the sensitivity of ^{18}F-DOPA PET to visualize lesions in a large group of patients with catecholamine excess compared with ^{123}I-MIBG scintigraphy and CT/MRI. In addition we correlated ^{18}F-DOPA PET findings with catecholamine plasma and urine markers.

PATIENTS AND METHODS

All consecutive patients with proven catecholamine excess who visited the UMCG, Groningen, between March 2003 and January 2008 were asked to participate in this study (Figure 1). Each patient underwent extensive biochemical analysis and conventional imaging with CT and/or MRI and ^{123}I-MIBG in the UMCG or the referring hospital, and an ^{18}F-DOPA PET scan in the UMCG. Data for age, gender, medication, biochemical measurements, the presence of genetic mutations (succinate

dehydrogenase B (SDHB), SDHD, von Hippel Lindau (VHL), neurofibromatosis type 1 (NF1) and the rearranged during transfection (RET)-gene) and histology were collected. Patients were classified as having malignant disease in case of recurrence or presence of metastases. The study was approved by the local medical ethics committee. All patients or their legal representatives gave written informed consent.

^{123}I-MIBG and ^{18}F-DOPA PET imaging

^{123}I-MIBG imaging was performed according to guidelines of the Dutch Society of Nuclear Medicine.[15] In brief, before administration of ^{123}I-MIBG (200-370 MBq) medication interfering with ^{123}I-MIBG-uptake has to be stopped and thyroid uptake of possibly formed free ^{123}I is blocked with sodium or potassium iodide or perchlorate. Planar whole-body images are acquired 24 hours after injection of ^{123}I-MIBG, but can additionally be performed at 4 and 48 hours after injection. In case SPECT images are performed, this is done at 24 hours after injection.

^{18}F-DOPA was locally produced as described previously.[16] Patients, allowed to continue all medication, fasted for 6 hours before the examination. Whole-body 2D-PET images were acquired 60 minutes after the intravenous administration of ^{18}F-DOPA (180 $\pm$ 50 MBq), on a Siemens ECAT HR+ positron camera (Siemens, Knoxville, TN) with attenuation correction (7 – 10 bed positions of 5 minutes emission and 3 minutes transmission scan, total scanning time approximately 60 minutes). Images were reconstructed using the OSEM algorithm 8 subsets, 2 iterations. For the reduction of tracer decarboxylation, subsequent renal clearance and to increase tracer uptake in tumor cells patients received 2 mg/kg carbidopa orally as pre-treatment 1 hour prior to the ^{18}F-DOPA injection.[12, 17, 18]

CT/MRI

In all patients either CT or MRI were performed, based on the preferences of the treating physician. CT-examinations were performed using a spiral or multislice scanner, both before and after administration of intravenous contrast agent. MRI-examinations were performed on a 1.5 Tesla scanner using various T1 and T2-weighted sequences, including series after administration of an intravenous gadolinium agent. In the majority of MRI-examinations in- and opposed phase T1-weighted sequences were available. Reconstructed slice thickness varied between 3-10 mm. In accordance with current clinical practice and to keep radiation exposure low, all patients had their upper abdomen scanned and if there was suspicion of lesions elsewhere, the involved body region was also analyzed.

Image interpretation

One nuclear medicine physician (AHB), blinded for other imaging and biochemical information, interpreted the ^{123}I-MIBG scans and ^{18}F-DOPA PET scans during separate reading sessions. Lesions were graded semi-quantitatively using liver uptake (LU) as reference (scores: 0 = uptake absent; 1 = uptake less than LU; 2 = equal to LU; 3 = moderately more intense than LU; 4 = markedly more intense than LU) (19). Lesions were classified as positive using the following criteria: adrenal uptake more intense than LU (score 3-4) and any non-physiologic extra-adrenal focal uptake. Scans were considered positive if at least one positive lesion was found.

We determined a 'whole-body metabolic burden' (WBMB) to serve as an image-derived index for overall tumor activity per patient.[20] In order to make the WBMB independent of body weight and injected dose, standardized uptake values (SUV) were used.[21] For each tumor lesion the metabolic burden (MB) was calculated as:

$MB = SUV_{mean} \times volume$.

The WBMB was calculated as the sum of the MB of each tumor lesion in the PET image. Both SUV_{mean} and tumor volume were obtained from the PET image using a volume of interest (VOI) that was defined as the tumor volume enclosed by a 40% isodensity surface.[22]

All CT and MRI scans were assessed by a radiologist, (MEJP) blinded for all other imaging and biochemical data. Adrenals were classified as normal, hyperplastic or suspect for pheochromocytoma. Other lesions were graded as benign or metastatic tumor. Criteria for classifying a lesion as pheochromocytoma were: a hyperintense signal on T2-weighted MRI images, strong enhancement after gadolinium administration, enhancement with intravenous contrast on CT, localization, size (of adrenal gland or lymph node) and infiltrative growth pattern.[4] Enhancement at CT and MRI was visually noted, comparing the series before and after administration of the contrast agent. Level of certainty was expressed on a scale of 1-5 (1 = not tumor, 2 = probably not tumor, 3 = equivocal, 4 = probably tumor, 5 = definitely tumor). Lesions with scores of 4 and 5 were regarded as positive findings. CT and MRI data were analyzed together.

Composite Reference standard

As a composite reference standard for presence of tumor lesions, all available clinical information on cytology, histology, follow-up and imaging (CT/MRI, ^{123}I-MIBG and ^{18}F-DOPA PET) was used.[23, 24] This is considered the optimal gold standard, as cytological or histological verification of every lesion is neither feasible nor justifiable in these patients. Whenever possible, new findings on PET were verified with additional investigations.

Biochemical markers

Concentrations of markers of catecholamine metabolism, i.e. normetanephrine, metanephrine and 3-methoxytyramine were determined in plasma (free fractions) and in a 24-h urine sample (total fractionated metanephrines) (upper reference limits of metanephrine, normetanephrine, 3-methoxytyramine are 1.07, 0.33, 0.17 nmol/liter in plasma and 260, 99, 197 μmol/mol creatinine in urine, respectively) as described earlier.[25, 26] Serum concentrations of chromogranin A were measured using a radioimmunoassay (Cga-React, Cis Bio International, Marcoule, France) (upper limit 100 mg/liter).

Catecholamine-producing tumors can produce either predominantly norepinephrine or epinephrine. Metanephrine concentrations in plasma and urine were used to determine catecholamine-secretion phenotype, as described earlier.[27]

Effect on treatment

All imaging modalities were considered for treatment decisions and all treatments were documented. In particular, it was evaluated whether additional information provided by ^{18}F-DOPA PET had changed treatment decisions. Treatment for pheochromocytoma and paraganglioma consisted of surgery for benign pheochromocytomas or solitary recurrence, according to international guidelines.[5, 28] Surgical debulking of malignant tumors was performed if technically possible, and additional palliative medical treatment was given, including ^{131}I-MIBG administration for metastatic MIBG-positive lesions.[5]

Data and statistical analysis

The routine clinical use of ^{18}F-DOPA PET was considered to be of relevance in case sensitivity would increase from 71% (estimated sensitivity

for ^{123}I-MIBG based on the comparative study by Hoegerle[10]) to 95% with ^{18}F-DOPA PET, using McNemar's test for comparison with 90% power, with a discordancy rate of 24% ^{18}F-DOPA PET-positive but ^{123}I-MIBG-negative patients and 2% of patients positive on ^{123}I-MIBG scintigraphy but negative on ^{18}F-DOPA PET and $P < 0.05$, two-sided. The required number to study this was calculated to be at least 43 patients.

Analysis was performed at the level of individual patients and individual lesions, both for the total group of patients and for subgroups based on benign vs. malignant pheochromocytoma and hereditary vs. non-hereditary tumors. If the number of lesions in one region exceeded five, the number of lesions was truncated at five lesions for that region to avoid bias when calculating sensitivity.[23, 24] ^{18}F-DOPA PET and ^{123}I-MIBG scintigraphy are whole-body modalities, while CT and MRI are primarily directed at the areas of clinical interest. In order to eliminate bias towards whole-body imaging methods, only body areas for which all three imaging modalities were available, have been evaluated for sensitivity calculations.

Patient-based sensitivity was determined as the number of patients with a positive test (at least one lesion detected) divided by the total number of patients. Lesion-based sensitivity was calculated as the number of positive lesions by an individual technique divided by the total number of lesions using the composite reference standard, both for the total group of patients and for subgroups. For correlations, Spearman's r test was calculated. A P value was considered significant in case of values < 0.05, two-sided. Statistical tests were performed using the SPSS package version 14.0

RESULTS

Patient characteristics

Forty-eight patients were screened and included (Figure 1, Table 1). In 43 patients SPECT ^{123}I-MIBG was performed. No patients used medication known to interfere with ^{123}I-MIBG-uptake around the time of imaging.[29] Median time between ^{18}F-DOPA PET and ^{123}I-MIBG was 19 days. All scans were performed within 3 months, except for one patient with a 121 day interval. In addition to CT/MRI of the upper abdomen, CT/MRI of the lower abdomen was performed in 40 patients, CT/MRI of the thorax in 14 and of the head and neck in three. Genetic testing was performed in 32 patients.

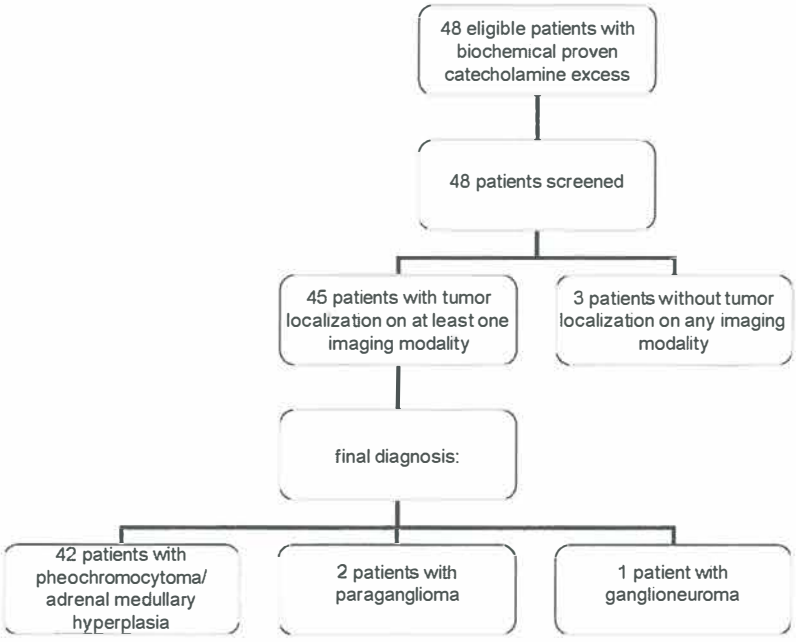

Figure 1. Flow diagram schematically showing patient recruitment.

Table 1. Patient characteristics (n = 48)

Characteristics	Value
Sex (N of patients) male/female	20/28
Median age in years (range)	46 (5 - 79)
MEN2a/VHL/NF1/SDHD/SDHB (N of patients with genetic mutation)	7/3/2/1/2
Suspected tumor/known tumor	30/18
Adrenal/Extra-adrenal tumor (N of patients)	42/3
Benign/Malignant tumor (N of patients)	24/21
Adrenergic/Noradrenergic phenotype (N of patients)	32/16
Biochemical analysis (median, range)	
Urinary normetanephrine (μmol/mol) (N = 44)	540 (44 - 18,704)
Urinary metanephrine (μmol/mol) (N = 44)	200 (14 - 9229)
Urinary 3-methoxytyramine (μmol/mol) (N = 36)	184 (47 - 3708)
Plasma free normetanephrine (nmol/liter) (N = 30)	3.8 (0.17 - 70.1)
Plasma free metanephrine (nmol/liter) (N = 30)	0.72 (0.01 - 27.5)
Plasma free 3-methoxytyramine (nmol/liter) (N = 25)	0.15 (0.01 - 6.8)
Chromogranin A (mg/liter) (N = 28)	87 (15 - 4250)

Patient-based analysis

^{18}F-DOPA PET was positive in 43 patients, ^{123}I-MIBG in 31 and CT/MRI in 32..

Patient-based analysis showed ^{18}F-DOPA PET to be superior in identifying affected patients compared to ^{123}I-MIBG ($P < 0.01$) and versus CT/MRI ($P < 0.01$) as it had the highest sensitivity (Table 2).

A representative patient is shown in Figure 2. There was no statistically significant difference between the sensitivity of ^{123}I-MIBG and CT/MRI ($P = 1.0$).

Table 2. Patient based analysis of imaging performances

	Number of patients with positive lesions/total number of patients	Sensitivity % (95% CI)
CT/MRI	32/48	67% (52 - 80)
^{18}F-DOPA PET	43/48	90% (77 - 97)
^{123}I-MIBG	31/48	65% (49 - 78)

Lesions were solely demonstrated by ^{18}F-DOPA PET in nine patients and by ^{123}I-MIBG in one. The clinical and biochemical characteristics, including ratios of the biochemical markers, of the three patients in whom all imaging modalities were negative were in the same range as from the patients with positive scans.

Figure 2. Imaging of a patient with a known metastatic pheochromocytoma. (A) ^{18}F-DOPA PET shows increased uptake in the left adrenal gland and three lesions in the spine (arrows). (B) Fusion image of ^{18}F-DOPA PET and CT shows uptake in the region of the left adrenal gland, without anatomical substrate. (C) CT image of the region of the left adrenal gland. ^{123}I-MIBG imaging was negative (not shown).

Lesion-based analysis

A total of 124 lesions were detected by all imaging methods together. Seventeen patients had one lesion, eight had two, three had four and four patients had five or more lesions. In lesion-based analysis, ^{18}F-DOPA PET had the highest sensitivity compared to the other imaging modalities (Table 3) (^{18}F-DOPA PET ($P < 0.001$) vs. ^{123}I-MIBG and vs. CT/MRI ($P < 0.001$)). Performance of ^{123}I-MIBG and CT/MRI did not differ ($P = 0.51$). In addition, the combination of ^{18}F-DOPA PET and CT/MRI had the highest sensitivity (93%) for detecting tumor lesions, as CT/MRI detected lesions missed by nuclear medicine techniques and vice versa. The sensitivity of the ^{18}F-DOPA PET/CT/MRI combination was higher than the combination of ^{123}I-MIBG and CT/MRI (sensitivity 94 vs. 76%, $P < 0.001$).

^{18}F-DOPA PET showed more lesions in 23 patients, while ^{123}I-MIBG performed better in three patients, all three with malignant pheochromocytoma. In 18 patients both methods showed the same number of lesions. We observed no difference in regional sensitivity for the detection of metastases for the different techniques. Lesions missed by ^{18}F-DOPA PET were mostly abdominally or retroperitonally located, size ranging from 12-24mm. Except for one adrenal pheochromocytoma of 18 mm, none of these lesions was histologically verified. CT/MRI missed mainly adrenal lesions < 2cm, especially in patients with hereditary disease or local recurrence, and ossal lesions.

Sensitivities in subgroups of patients with benign or malignant pheochromocytoma and in patients with hereditary or non-hereditary disease showed that ^{18}F-DOPA PET is superior to ^{123}I-MIBG or CT/MRI in all subgroups (Table 3). The performance of imaging modalities did not differ significantly between benign and malignant pheochromocytoma and hereditary and non-hereditary pheochromocytoma. The clinical and biochemical characteristics, including ratios of the separate biochemical markers, of the three patients in whom ^{123}I-MIBG was superior to ^{18}F-DOPA PET were not different from the other patients with malignant

Table 3. Lesion based sensitivities of imaging modalities

	Sensitivity (95% CI)	Sensitivity benign pheochromocytoma (95% CI)	Sensitivity malignant pheochromocytoma (95% CI)	Sensitivity hereditary pheochromocytoma (95% CI)	Sensitivity non-hereditary pheochromocytoma (95% CI)	Total detected number of lesions per mentioned modality
CT/MRI	44 (35 - 54)	70 (51 - 85)	45 (33 - 57)	48 (27-70)	50 (39 - 61)	55
^{18}F-DOPA PET	73 (65 - 81)	85 (68 - 95)	73 (62 - 83)	87 (66 - 97)	72 (61 - 81)	91
^{123}I-MIBG	48 (39 - 57)	52 (33 - 69)	56 (45 - 68)	39 (20 - 62)	55 (44 - 65)	59
^{18}F-DOPA PET + CT/MRI	94 (88 - 97)	100 (87 - 97)	93 (85 - 97)	100 (84 - 99)	93 (86 - 98)	116
^{123}I-MIBG + CT/MRI	76 (67 - 83)	76 (56 - 90)	85 (76 - 92)	57 (34 - 77)	90 (81 - 95)	94

pheochromocytoma. Neither catecholamine-secretion phenotype, nor serum chromogranin-level predicted scan performance.

Treatment consisted of surgical resection of primary tumor (n = 27) or metastases (n = 5) in a total of 32 patients and surgery combined with ^{131}I-MIBG-therapy in three, ^{131}I-MIBG-therapy alone in three, chemotherapy in one, symptomatic medical therapy in three and watchful waiting in six. Final diagnosis (by histology) was pheochromocytoma in 40 patients, adrenal hyperplasia in two, paraganglioma in two, ganglioneuroma in one, and remained unknown in three since no lesions were detected. The latter three patients presented with typical complaints of pheochromocytoma and a catecholamine excess, but until now no tumor could be localized.

Imaging with ^{18}F-DOPA PET influenced treatment decisions in 14 patients (29%). It localized solitary tumors (n = 7), indicated the neuroendocrine nature of inconclusive lesions on CT/MRI (n = 2) or inconclusive uptake on ^{123}I-MIBG (n = 2), resulting in the decision to proceed to surgical resection (Figure 3). In three patients surgery was cancelled because of multiple otherwise unknown metastases. Removed lesions (n = 7) that were only visible on ^{18}F-DOPA PET were all histopathologically confirmed to be neuroendocrine tumor.

Correlations between PET imaging and catecholamine metabolism

Biochemical characteristics (Table 1), including ratios of the biochemical markers, did not differ between patients with benign and malignant pheochromocytoma.

Median SUV_{max} was 3.2 (range: 1.3 - 31.9), while median SUV_{mean} was 2.2 (0.88 – 19.8). Median total tumor volume was 11.3 cm^3 (0 - 515 cm^3). Together they resulted in a median WBMB of 65 (0 - 3229) cm^3.

The WBMB correlated with the 24-h urinary excretion of total (free +conjugated) normetanephrine (r = 0.84, P < 0.001), metanephrine (r = 0.57, P < 0.01), and 3-methoxytyramine (r = 0.65, P < 0.01) as well as plasma free

levels of normetanephrine (r = 0.82, P < 0.001), 3-methoxytyramine (r = 0.51, P = 0.01) and chromogranin A (r = 0.49, P < 0.01).

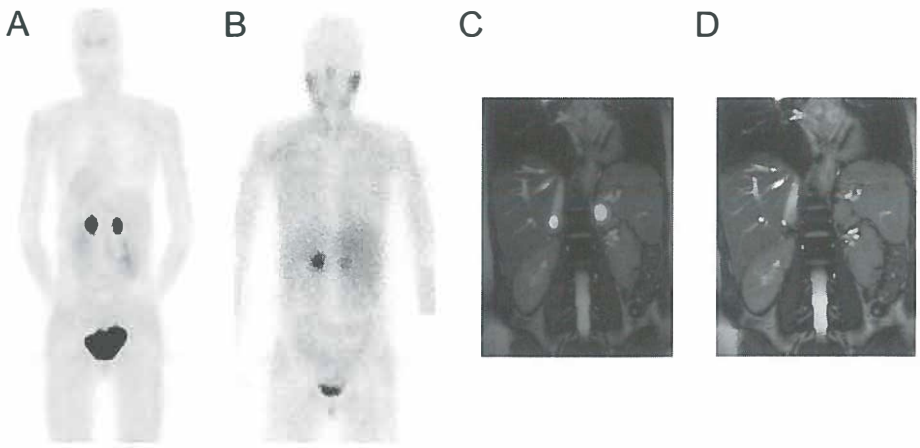

Figure 3. Patient with bilateral pheochromocytoma. (A) ^{18}F-DOPA PET shows increased uptake in both adrenal glands. (B) ^{123}I-MIBG imaging: asymmetric ^{123}I uptake in the adrenals: the left adrenal shows markedly increased uptake, whereas uptake in the right adrenal can easily be mistaken as physiological. (C) Fusion of ^{18}F-DOPA PET and MRI shows uptake in both adrenal glands. (D) MRI showing the left adrenal pheochromocytoma.

DISCUSSION

This study compared the performance of ^{18}F-DOPA PET and ^{123}I-MIBG scintigraphy and CT/MRI in patients with catecholamine excess, and found that ^{18}F-DOPA PET was superior to all other modalities. In addition, ^{18}F-DOPA PET plus CT/MRI was superior to ^{123}I-MIBG scintigraphy plus CT/MRI. ^{18}F-DOPA PET plus CT/MRI was found to be the optimal combination of imaging procedures to localize catecholamine-producing tumors. Furthermore, we showed that WBMB, measured with ^{18}F-DOPA PET, correlated with metabolic tumor activity, determined with biochemical markers.

In this study we have addressed the problem of imaging of catecholamine-producing tumors from the most basic clinical relevant question. Therefore, we included all patients with proven catecholamine excess and not just patients with a (suspected) pheochromocytoma or paraganglioma. The most common final diagnosis in our study was pheochromocytoma, while only a few patients had another diagnosis. Since all diagnostic techniques have their limitations, it is possible that tumor lesions in the three patients with negative imaging studies were still too small to be visualized or that the biochemical tests were false-positive.[30] As pheochromocytoma and paraganglioma together constitute the majority of catecholamine-producing tumors, most imaging studies are performed in patients with known pheochromocytoma and paraganglioma. To our knowledge, no studies investigating PET imaging in ganglioneuroma have been performed.[31]

Previous small studies (9 to 25 patients) have reported sensitivities ranging from 50-100% for ^{18}F-DOPA PET in pheochromocytoma and paraganglioma.[10-13] In the present study in the patients with benign (n = 21) and malignant (n = 19) pheochromocytoma, both on a patient and lesion-based level, we observed excellent sensitivities for ^{18}F-DOPA PET (95% patient-based and 85% lesion-based). This contrasts with previous studies in 9 to 30 patients that have reported lower sensitivity for PET with ^{18}F-DOPA or ^{18}F-fluorodopamine in metastatic pheochromocytoma and paraganglioma.[6, 11, 12] These previous findings have stimulated the use of the broader imaging tracer ^{18}F-FDG PET, which visualizes glucose metabolism, and ^{18}F-FDG PET has been suggested to be superior for imaging of metastatic pheochromocytoma or paraganglioma, especially for patients with an underlying *SDHB*-mutation. It has been demonstrated that ^{18}F-FDG PET can detect malignant pheochromocytoma and paraganglioma lesions that are missed on imaging with more specific tracers like ^{18}F-DOPA.[6, 11] However, ^{18}F-FDG PET is not suitable as first-line tracer in patients presenting with catecholamine excess, in view of a low sensitivity (58% in

12 benign pheochromocytoma).[8] In addition, although ^{18}F-FDG PET was found to be superior to ^{18}F-fluorodopamine PET in two groups of 30 patients with a *SDHB*-mutation, the latter performed better in 41 metastatic *SDHB*-negative patients.[6, 32] The excellent sensitivity of ^{18}F-DOPA PET for metastatic disease in our study may be due to the fact that only two patients were *SDHB*-mutation positive in our study, compared to 45 - 100% of the patients in previous studies.[6, 12]

Handling of the tracer by the tumor cell may well explain why ^{18}F-DOPA is a more suitable tracer for catecholamine-producing tumors than ^{18}F-fluorodopamine. ^{18}F-DOPA is transported into the cell by the large amino acid transporter 2 (LAT2), than decarboxylated by aromatic-L-amino acid decarboxylase (AADC) to ^{18}F-fluorodopamine and transported into storage vesicles by VMAT. This pathway is active in many neuroendocrine tumors, making ^{18}F-DOPA suitable to image a wide range of neuroendocrine tumors. ^{18}F-fluorodopamine is transported into the cell not by LAT2 but by the dopamine transporter DAT, and thereafter immediately transported into storage vesicles by VMAT. The fact that LAT2 is constitutionally expressed in all cells, and AADC is highly expressed by most neuroendocrine tumors, whereas VMAT and DAT are variably expressed, potentially explains why ^{18}F-DOPA could perform superior to ^{18}F-fluorodopamine.[33-35] In our study ^{18}F-DOPA PET improved staging by detecting 36 unkown lesions and changed treatment decision in 14 patients. This suggests that routine implementation of ^{18}F-DOPA PET in patients with catecholamine excess is likely to influence patient management.

Pretreatment with carbidopa has been shown to increase the tumor-to-background ratio of tracer uptake.[12, 18, 19] This has lead to an enhanced sensitivity of ^{18}F-DOPA PET for pheochromocytomas and paragangliomas.[12] In the other studies of ^{18}F-DOPA PET in pheochromocytomas and paragangliomas no carbidopa pre-treatment was given[10, 11] or only in a small number of patients, without mentioning the

effect of carbidopa in these patients.[13]. We feel that all studies with ^{18}F-DOPA PET should be performed with carbidopa to maximize the potential of this imaging technique.

The correlation between WBMB measured with ^{18}F-DOPA PET and biochemical activity of catecholamine-producing tumors, as determined with biochemical markers, confirms that uptake of the catecholamine precursor ^{18}F-DOPA is enhanced by overactivity of the catecholamine synthesis pathway and illustrates the tumor burden.[36] Noradrenergic tumors secrete more catecholamines than adrenergic tumors of comparable size.[27, 37] This might explain why we found stronger correlations between tumor burden and normetanephrine than metanephrine, in accordance with previous studies, which used tumor diameter[27] and tumor mass[37] as a measure of tumor burden. However, one recent study did not find a correlation between SUV_{max} and biochemical markers.[13] In our opinion, this is not surprising for SUV_{max} is not a marker that represents total tumor burden, but a single measurement point, representing the maximum uptake in one single voxel. Biochemical markers on the other hand do represent a total tumor burden. WBMB, as used in our study, is a more real marker of tumor burden, than SUV_{max}. Therefore it is not surprising to find a correlation between biochemical markers and WBMB.

Shortcomings of this study are the fact that only three patients with extra-adrenal tumors were included. Furthermore, not all lesions were histologically verified, which would be the optimal gold standard, since we feel histological verification of every lesion is neither feasible nor justifiable in these patients.

In conclusion, ^{18}F-DOPA PET is superior to both ^{123}I-MIBG scintigraphy and CT/MRI for the localization of catecholamine-producing tumors. The combination of ^{18}F-DOPA PET and CT/MRI is most informative in the diagnostic work-up of patients with catecholamine excess.

REFERENCES

1. Lenders JW, Eisenhofer G, Mannelli M, et al. Phaeochromocytoma. Lancet 2005;20:665-675
2. Eisenhofer G, Bornstein SR, Brouwers FM, et al. Malignant pheochromocytoma: current status and initiatives for future progress. Endocr Relat Cancer 2004;11:423-436
3. Brink I, Hoegerle S, Klisch J, et al. Imaging of pheochromocytoma and paraganglioma. Fam Cancer 2005;4:61-68
4. Ilias I, Pacak K Current approaches and recommended algorithm for the diagnostic localization of pheochromocytoma. J Clin Endocrinol Metab 2004;89:479-491
5. Pacak K, Eisenhofer G, Ahlman H, et al. Pheochromocytoma: recommendations for clinical practice from the First International Symposium. October 2005. Nat Clin Pract Endocrinol Metab 2007;3:92-102
6. Timmers HJ, Kozupa A, Chen CC, et al. Superiority of fluorodeoxyglucose positron emission tomography to other functional imaging techniques in the evaluation of metastatic SDHB-associated pheochromocytoma and paraganglioma. J Clin Oncol 2007;25:2262-2269
7. van der Harst E., de Herder WW, Bruining HA, et al. [(123)I]metaiodobenzylguanidine and [(111)In]octreotide uptake in benign and malignant pheochromocytomas. J Clin Endocrinol Metab 2001;86:685-693
8. Shulkin BL, Thompson NW, Shapiro B, et al. Pheochromocytomas: imaging with 2-[fluorine-18]fluoro-2-deoxy-D-glucose PET. Radiology 1999;212:35-41
9. Ilias I, Yu J, Carrasquillo JA, et al. Superiority of 6-[18F]-fluorodopamine positron emission tomography versus [131I]-metaiodobenzylguanidine scintigraphy in the localization of metastatic pheochromocytoma. J Clin Endocrinol Metab 2003;88:4083-4087
10. Hoegerle S, Nitzsche E, Altehoefer C, et al. Pheochromocytomas: detection with 18F DOPA whole body PET--initial results. Radiology 2002;222:507-512

11. Taieb D, Tessonnier L, Sebag F, et al. The role of 18F-FDOPA and 18F-FDG-PET in the management of malignant and multifocal pheochromocytomas. Clinical Endocrinology 2008;69:580-586
12. Timmers HJ, Hadi M, Carrasquillo JA, et al. The effects of carbidopa on uptake of 6-18F-fluoro-L-DOPA in PET of pheochromocytoma and extraadrenal abdominal paraganglioma. J Nucl Med 2007;48:1599-1606
13. Imani F, Agopian V, Auerbach M, et al. ^{18}F-FDOPA PET and PET/CT accurately localize pheochromocytomas. J Nucl Med 2009;50:513-519
14. Ilias I, Chen CC, Carrasquillo JA, et al. Comparison of 6-18F-Fluorodopamine PET with 123I-Metaiodobenzylguanidine and 111In-Pentetreotide Scintigraphy in Localization of Nonmetastatic and Metastatic Pheochromocytoma. J Nucl Med 2008;49:1613-1619
15. MIBG-scintigrafie, In: Barneveld PC, Van Urk eds Aanbevelingen 2007 Nucleaire Geneeskunde. Neer: Kloosterhof acquisitie services, 2007; 60-63
16. De Vries EFJ, Luurtsema G, Brussermann M, et al. Fully automated synthesis module for the high yield one-pot preparation of 6-[18F]fluoro-L-DOPA. Appl Radiat Isot 1999;51:389-394
17. Ishikawa T, Dhawan V, Chaly T, et al. Fluorodopa positron emission tomography with an inhibitor of catechol-O-methyltransferase: effect of the plasma 3-O-methyldopa fraction on data analysis. J Cereb Blood Flow Metab 1996;16:854-863
18. Orlefors H, Sundin A, Lu L, et al. Carbidopa pretreatment improves image interpretation and visualisation of carcinoid tumours with 11C-5-hydroxytryptophan positron emission tomography. Eur J Nucl Med Mol Imaging 2006;33:60-65
19. Cecchin D, Lumachi F, Marzola MC, et al. A meta-iodobenzylguanidine scintigraphic scoring system increases accuracy in the diagnostic management of pheochromocytoma. Endocr Relat Cancer 2006;13:525-533
20. Berkowitz A, Basu S, Srinivas S, et al. Determination of whole-body metabolic burden as a quantitative measure of disease activity in lymphoma: a novel approach with fluorodeoxyglucose-PET. Nucl Med Commun 2008;29:521-526
21. Thie JA Understanding the standardized uptake value, its methods, and implications for usage. J Nucl Med 2004;45:1431-1434

22. Erdi YE, Mawlawi O, Larson SM, et al. Segmentation of lung lesion volume by adaptive positron emission tomography image thresholding. Cancer 1997;80:2505-2509
23. Koopmans KP, de Vries EG, Kema IP, et al. Staging of carcinoid tumours with 18F-DOPA PET: a prospective, diagnostic accuracy study. Lancet Oncol 2006;7:728-734
24. Koopmans KP, Neels OC, Kema IP, et al. Improved staging of patients with carcinoid and islet cell tumors with 18F-dihydroxy-phenyl-alanine and 11C-5-hydroxy-tryptophan positron emission tomography. J Clin Oncol 2008;26:1489-1495
25. de Jong WH, Graham KS, van der Molen JC, et al. Plasma free metanephrine measurement using automated online solid-phase extraction HPLC tandem mass spectrometry. Clin Chem 2007;53:1684-1693
26. Kema IP, Meiborg G, Nagel GT, et al. Isotope dilution ammonia chemical ionization mass fragmentographic analysis of urinary 3-O-methylated catecholamine metabolites. Rapid sample clean-up by derivatization and extraction of lyophilized samples. J Chromatogr 1993;617:181-189
27. Eisenhofer G, Lenders JWM, Goldstein DS, et al. Pheochromocytoma catecholamine phenotypes and prediction of tumor size and location by use of plasma free metanephrines. Clin Chem 2005;51:735-744
28. National Cancer Institute: PDQ: Pheochromocytoma treatment, 3/2008 update.
http://www.cancer.gov/cancertopics/pdq/treatment/pheochromocytoma/HealthProfessional/
29. Solanki KK, Bomanji J, Moyes J, et al. A pharmacological guide to medicines which interfere with the biodistribution of radiolabelled meta-iodobenzylguanidine (MIBG). Nucl Med Commun 1992;13:513-521
30. Lenders JW, Pacak K, Walther MM, et al. Biochemical diagnosis of pheochromocytoma: which test is best? JAMA 2002;287:1427-1434
31. Ilias I, Shulkin B, Pacak K New functional imaging modalities for chromaffin tumors, neuroblastomas and ganglioneuromas. Trends Endocrinol Metab 2005;16:66-72
32. Zelinka T, Timmers HJ, Kozupa A, et al. Role of positron emission tomography and bone scintigraphy in the evaluation of bone involvement in

metastatic pheochromocytoma and paraganglioma: specific implications for succinate dehydrogenase enzyme subunit B gene mutations. Endocr Relat Cancer 2008;15:311-323

33. Kolby L, Bernhardt P, Levin-Jakobsen AM, et al. Uptake of meta-iodobenzylguanidine in neuroendocrine tumours is mediated by vesicular monoamine transporters. Br J Cancer 2003;89:1383-1388
34. Cleary S, Brouwers FM, Eisenhofer G, et al. Expression of the noradrenaline transporter and phenylethanolamine N-methyltransferase in normal human adrenal gland and phaeochromocytoma. Cell Tissue Res 2005;322:443-453
35. Lemmer K, Ahnert-Hilger G, Hopfner M, et al. Expression of dopamine receptors and transporter in neuroendocrine gastrointestinal tumor cells. Life Sci 2002;71:667-678
36. Eisenhofer G, Huynh TT, Hiroi M, et al. Understanding catecholamine metabolism as a guide to the biochemical diagnosis of pheochromocytoma. Rev Endocr Metab Disord 2001;2:297-311
37. Eisenhofer G, Keiser H, Friberg P, et al. Plasma metanephrines are markers of pheochromocytoma produced by catechol-o-methyltransferase within tumors. J Clin Endocrinol Metab 1998;83:2175-2185

Chapter 4

Myocardial metastases of islet cell tumors visualized by ^{11}C-5-hydroxytryptophan PET

Helle-Brit Fiebrich[1], Adrienne H. Brouwers[2], Iwan C.C. van der Horst[3], Koen V.J.M. Vanghillewe[4], Klaas-Pieter Koopmans[2], Pieter L. Jager[4], Philip H. Elsinga[2], Rudi A.J.O. Dierckx[2], and Elisabeth G. E. de Vries[1]

Departments of [1]Medical Oncology, [2]Nuclear Medicine and Molecular Imaging, [3]Cardiology, University Medical Center Groningen and University of Groningen, Groningen, the Netherlands
[3]Department of Radiology, Martini Hospital, Groningen, the Netherlands
[4]Department of Nuclear Medicine, Hamilton Health Sciences and McMaster University, Canada

Submitted

ABSTRACT

Objective: Thus far one patient with a cardiac metastasis from an islet cell tumor has been reported. This is likely an underestimation due to restrictions of the used imaging methods and a lack of awareness of their possible existence. ^{11}C-5-hydroxytryptophan positron emission tomography (^{11}C-5-HTP-PET) fused with CT is currently the most sensitive imaging technique to detect islet cell tumors, which may identify cardiac metastases in these patients.

Design & Patients: A renewed analysis of all ^{11}C-5-HTP-PET scans performed in patients with metastasized islet cell tumors was performed between October 2005 and July 2009. When lesions suspect for cardiac metastases were identified with ^{11}C-5-HTP-PET, chest-CT scans were reviewed and fused with the ^{11}C-5-HTP-PET scans.

Setting: University hospital

Main outcome measure: Myocardial uptake on ^{11}C-5-HTP-PET suspect for cardiac metastases

Results: Five of 26 patients (19%) had ≥1 lesion suspect for cardiac metastases on ^{11}C-5-HTP-PET. None showed symptoms of cardiac involvement. One cardiac lesion was also discernible on CT after fusion with PET. These CT scans, not ECG-gated, provided suboptimal information. Three of five patients with and 12 of 14 patients without cardiac metastases showed ECG-changes.

Conclusion: Cardiac metastases of islet cell tumors are likely more frequent than currently observed. Increased awareness is necessary when evaluating

these patients for metastatic disease. Cardiac metastases may best be identified with ^{11}C-5-HTP-PET.

INTRODUCTION

Pancreatic islet cell tumors are rare neoplasms of the pancreas, originating from the pancreatic islet cell lineage and can be associated with a clinical syndrome due to hormone hypersecretion. At the time of diagnosis approximately 50% of islet cell tumors have already metastasized, especially to the liver.[1] However, when evaluating a patient for metastases, the heart is seldom considered. Based on the information from the literature myocardial metastases are rare as only one case of myocardial metastases from an islet cell tumor has been reported.[2] Also the incidence of metastases in the heart in carcinoid tumors, a similar low grade neuroendocrine tumor, is considered to be low.[3] However, the low incidence can well be an underestimation due to the restrictions of the used imaging methods.

We have reported a case where myocardial carcinoid metastases were identified by imaging with the catecholamine precursor 6-fluoro-[^{18}F]L-dihydroxyphenylalanine positron emission tomography (^{18}F-DOPA PET), but not by conventional imaging.[4] In addition, we recently discovered a patient with an islet cell tumor that showed cardiac metastases on ^{11}C-5-hydroxytryptophan (^{11}C-5-HTP) PET, alerting us to the possibility that the prevalence of cardiac metastases in these patients might be higher than suspected. It is possible that in patients with islet cell tumors, similar to carcinoid patients, the number of myocardial metastases is underestimated due to the lack of sensitive imaging modalities.

^{11}C-5-HTP PET scanning is based on the intrinsic property of neuroendocrine tumors to take up, decarboxylate, and store amine precursors, such as the serotonin precursor ^{11}C-5-HTP. This technique is currently considered as the most sensitive imaging modality for diagnosing islet cell tumors (up to 100%), being superior to ^{18}F-DOPA PET and somatostatin receptor scintigraphy.[5] In nuclear medicine, 6-[fluoride-

18]fluorodeoxyglucose (^{18}F-FDG) is the most widely used PET tracer for the imaging of tumors. This tracer visualizes tissue with increased glycolysis, such as tumor, but also in a number of other tissues such as the heart or the brain. Against such a strong physiological background pathological uptake due to metastases is only very rarely discernible. Therefore, nuclear medicine physicians are not accustomed to look for, and find, metastases in the heart. We decided to re-analyze all patients with metastasized islet cell tumors that underwent ^{11}C-5-HTP PET with regard to myocardial metastases, including those patients reported earlier in a publication.[5]

PATIENTS AND METHODS

Since October 2005 ^{11}C-5-HTP PET is available for imaging of islet cell tumors in the University Medical Center Groningen. Until July 2009 154 ^{11}C-5-HTP PET scans had been performed, 97 of which for (suspected) islet cell tumors. From a database of all ^{11}C-5-HTP PET scans performed in the University Medical Center Groningen between October 2005 and July 2009 all patients with an islet cell tumor that had received a ^{11}C-5-HTP PET scan, were identified. The ^{11}C-5-HTP PET scans of all patients, which showed metastasised disease, were reviewed with thorough inspection of the heart by an experienced nuclear medicine specialist (A.H.B.). Focal increased uptake in the heart, which was higher than the normal diffuse, slight uptake in the myocardium was considered as suspect for cardiac metastases. Both conventional whole-body images and short and long axis reconstructions were reviewed.

For all patients standardised uptake values (SUVs) were determined as a measure of tumor tracer uptake. A volume of interest (VOI) was semi-automatically drawn over the whole heart, including suspected cardiac lesions. SUVs were calculated using the formula: SUV = activity

concentration [MBq/ml] / injected dose per gram [MBq/g]. SUVmax was defined as the pixel with the highest ^{11}C-5-HTP-uptake in the VOI. In case of patients with suspect cardiac lesions, SUVmax over the heart was SUVmax of the lesion, as this was the hottest area in the heart. If more than one suspect cardiac lesion was seen, then the SUVmax of both lesions was measured, in which case the highest SUVmax was taken as the SUVmax over the heart. SUVmean was obtained from the PET image using a VOI that was defined as the tumor volume enclosed by a 70% isodensity surface. SUVmean was calculated as the mean SUV of all pixels with an activity of 70 to 100% of the SUVmax within the VOI. The SUVmax over the heart was divided by the SUVmean to determine a ratio as a measurement of heterogeneity/homogeneity of cardiac uptake.

All patients had, as part of their tumor staging, also undergone a computer tomography (CT) scan of the chest at the same time, that were reviewed by an experienced radiologist (K.V.J.M.V.). In addition, the CT scan was, if possible, fused with the ^{11}C-5-HTP PET scan. The resulting images were discussed in a multidisciplinary setting.

The charts of the selected patients were reviewed for data on clinical follow up, cardiac risk profile (including hypertension, diabetes, dyslipidaemia and a history of cardiovascular disease) and standard twelve-lead electrocardiograms (ECGs). The ECGs (MAC 500, General Electrics, the Netherlands) were recorded by certified technicians with patients in supine position. ECGs were examined by a cardiologist blinded for the data to determine rhythm, heart rate, QRS axis, PR interval, QRS duration, QT-interval, and ST segment. ECGs could show more than one abnormality.

Data of 17 patients from the present analysis were reported earlier by us.[5] However, data on the heart had in retrospect not been examined so thoroughly. Patients participated in that study evaluating the diagnostic sensitivity of ^{11}C-5-HTP PET and ^{18}F-DOPA PET in patients with carcinoid tumors and islet cell tumors. The study was approved by the medical ethical committee, all patients gave informed consent.

^{11}C-5-HTP was produced locally as described earlier.[6] Patients fasted for 2 h before the examination. For the reduction of tracer decarboxylation and subsequent renal clearance and to increase tracer uptake in tumor cells all patients received 2 mg/kg carbidopa orally as pre-treatment 1 h prior to the ^{11}C-5-HTP injection.[7-9]

Whole body 2D-PET images were acquired 10 min after the intravenous (IV) administration of ^{11}C-5-HTP (200 - 400 MBq, with an estimated mean radiation dose of 0.34 mSv per 100 MBq) on a Siemens ECAT HR+ PET camera (Siemens) with attenuation correction (7-10 bed positions of 5 min emission and 3 min transmission scan).

CT of the chest (4-16 slice, Siemens Somatom Sensation) with an estimated mean radiation dose of 8-20 mSv[10] was performed using oral contrast and IV contrast (Visipaque, 120 mL, 2.5 mL/s) enhancement. The reconstruction interval was 0.75-10 mm.

RESULTS

Twenty-six patients (17 males, 9 females) with a metastasised islet cell tumor who had been analyzed by a ^{11}C-5-HTP PET scan were identified. Of these patients 22 had a non-functioning islet cell tumor, two had a glucagonoma, one an insulinoma and one a gastrinoma. Median age was 57 years (range: 17-75). Median follow-up after the ^{11}C-5-HTP PET scan was 32 months (range: 3-44 months). Out of these patients five patients (19%) were identified that had one or more lesion suspect for myocardial metastases. The characteristics of those five patients are shown in Table 1.

Out of these patients, only patient 5 had a history of prior ischemic cardiac disease for which he had received a bypass operation 12 years earlier, the others did not have cardiac risk factors. None of the patients showed any clinical signs or symptoms indicating possible cardiac problems or metastases at the time of the ^{11}C-5-HTP PET scan. One patient

Table 1. Characteristics of the 5 patients who showed myocardial metastases on the ^{11}C-5-HTP PET scan

	Patient Sex (Age in years)	Clinical signs/ symptoms	^{11}C-5-HTP PET	CT-scan	ECG	Echocardiography	Treatment	Outcome
1	M (60)	none	2 cardiac lesions, lesions in liver and left supraclavicular region	negative, heart partly in field of view	normal	-	chemotherapy	alive
2	M (62)	none	1 cardiac lesion, 1 lesion in pancreas and liver each	negative, thick slices	premature ventricular complexes, U wave	no signs of metastases	chemotherapy	alive
3	M (65)	none	2 cardiac lesions, and widespread abdominal and ossal metastases	2 lesions visible	Diffuse negative T-waves, left axis	-	chemotherapy	alive
4	M (53)	none	1 cardiac lesion, abdominal and ossal metastases	negative, heart partly in field of view	sinus tachycardia	-	-	death (acute)
5	M (59)	none	1 cardiac lesion, multiple liver lesions	negative, breathing artefacts	normal	-	-	death due to progression

in the group of patients without focal myocardial uptake on the ^{11}C-5-HTP PET scan had a typical cardiac risk profile, while none of these patients had a history of cardiac disease.

The cardiac metastases in all patients showed relatively low uptake of ^{11}C-5-HTP in comparison to the other lesions. Median cardiac SUVmax and SUVmean in hearts without possible metastases were lower than in patients with suspect cardiac lesions on ^{11}C-5-HTP PET (Table 2). This resulted in a higher SUVmax/SUVmean ratio in the latter group, suggesting less homogenous uptake of ^{11}C-5-HTP.

Three out of five patients with possible cardiac metastases had atypical changes on their ECG, i.e. sinus tachycardia (n=1), left axis (n=1), premature ventricular complexes (n=1), diffuse negative T-waves (n=1), and U-wave (n=1). In 14 out of 21 patients without possible cardiac metastases on the ^{11}C-5-HTP PET scan, an ECG was available.

Table 2. Cardiac SUVs (including the possible cardiac lesions) on ^{11}C-5-HTP PET

	Patients without suspect cardiac uptake	**Patients with suspect cardiac uptake**
SUVmax (whole heart): median (range)	1.9 (1.1-3.0)	2.6 (1.9-4.8)*
SUVmean: median (range)	1.7 (1.0-2.6)	1.7 (1.4-2.2)
SUVmax suspect lesions: median (range)		2.6 (1.9-4.8)
SUVmax/SUVmean ratio: median (range)	1.1 (1.1-1.2)	1.4 (1.3-2.3)

SUV: standardised uptake value

*In these patients cardiac SUVmax is the SUVmax of the hottest cardiac lesion.

A total of two ECGs of these patients were without changes. Observed changes were atrial fibrillation (n=1), sinus tachycardia (n=2), sinus bradycardia (n=3), premature ventricular complexes (n=1), left axis (n=1), right axis (n=1), right bundle branch block (n=2), QT-interval prolonging

(n=3), and U-wave (n=9). None of these patients took any medication that might have caused the ECG changes.

Three patients had clear focally increased uptake in the heart region on the ^{11}C-5-HTP PET scan, while two had equivocal lesions. Short and long axis reconstructions did not render clearer results than conventional whole-body images due to lack of counts in the field of view. In one patient the cardiac lesions were also discernable on the CT scan after fusion of the ^{11}C-5-HTP PET images with the CT images (Figure 1).

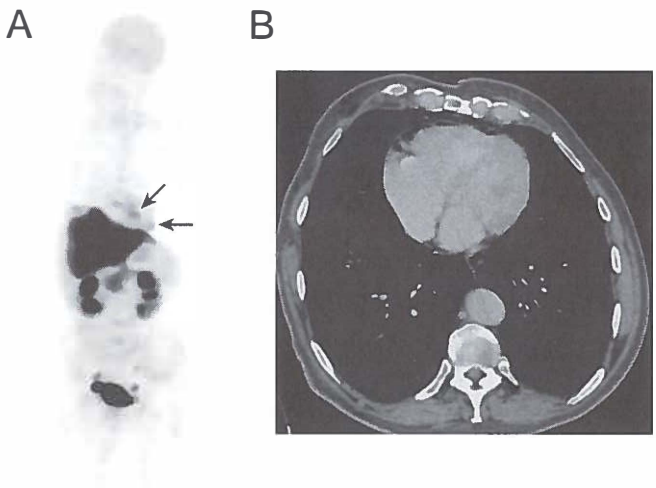

Figure 1. Patient 3 **A.** ^{11}C-5-HTP PET scan showing two cardiac metastases (arrows), both confirmed by CT scan, and extensive liver metastases. Diffuse physiological uptake in the pancreas and excretion via the kidneys, ureters and bladder. **B.** Fusion image of CT and ^{11}C-5-HTP PET showing one of the cardiac metastases.

Even though CT scans of the chest were available for all patients with suspected cardiac metastases, they were not ECG-gated. Considering the limitations due to slice thickness and the presence of movement artifacts which obscured the images or the fact that the heart had only partly been scanned they allowed only suboptimal interpretation of the

heart. As a result of this, no other cardiac lesions could be confirmed with CT. In patient 2 echocardiography was performed when the ^{11}C-5-HTP PET scan indicated possible cardiac involvement, but this failed to confirm the presence of cardiac metastases. Cardiac MRI was not possible due to pedical screws placed in the thoracic spine following corporectomy for a metastasis in vertebrae Th1. Unfortunately, because of the retrospective nature of this study, patients 4 and 5 had already died at the time of this analysis and no autopsy was performed, leaving only the CT scans available for evaluation.

Patient 1, 2, 3 are currently still in follow-up. Patient 4 died acutely at home, while patient 5 died due to progression of disease.

DISCUSSION

In this study we systematically investigated the presence of cardiac metastases in patients with an islet cell tumor using the most sensitive technique, namely ^{11}C-5-HTP PET, for imaging of islet cell tumors and argued that cardiac metastases in patients with islet cell tumors are likely more frequent than reported in literature.

We showed that when doctors are aware of the possibility of cardiac metastases and consequently thoroughly inspect the heart, lesions suspect for cardiac metastases can be found. Metastases to the heart are not frequently discovered in cancer patients premortem. However, in postmortem studies cardiac metastases are found in up to 25% of all cancer patients.[11][The low premortem detection rate can either be explained by the fact that 90% of cardiac metastases are clinically silent[12, 13] and/or by the fact that they are underestimated due to the restrictions of the commonly used imaging methods, as the vast majority of these metastases is small.[3, 11] The combination of these factors has lead to a lack of awareness of physicians concerning the presence of cardiac metastases in cancer patients.

For the detection of cardiac metastases regardless of tumor type echocardiography is recommended.[12] However, lesions smaller than 1.0 cm are difficult to identify with echocardiography.[3] Pericardial effusion, another sign of metastases, is non-specific. This might be the reason that echocardiography is not routinely performed in the diagnostic work-up of patients with islet cell tumors. Other possible diagnostic imaging methods to detect cardiac metastases are CT and MRI. A drawback of these methods is the necessity of synchronizing data acquisition to the cardiac cycle to ensure optimal visualization of the heart, which can be achieved by ECG gating.[14] However; ECG gating is not routinely performed for tumor staging scans, as was the case in our patients. The resulting imaging artifacts make identification of cardiac metastases difficult and thus radiologists are not accustomed to look for them in routine staging scans. For islet cell tumors we have the unique possibility of a tracer to specifically visualize the neuroendocrine tumor cell metabolism. The result is little interfering physiological uptake and clear tumor visualization, also within the heart. Given the high sensitivity of ^{11}C-5-HTP PET for the detection of islet cell tumors in general[5] and keeping in mind the limitations of conventional imaging for cardiac imaging, ^{11}C-5-HTP PET can likely detect more myocardial metastases than conventional imaging. When lesions suspect for myocardial metastases of an islet cell tumor are found on ^{11}C-5-HTP PET, conventional imaging specifically directed on the heart can be performed for confirmation. In this, ^{11}C-5-HTP PET/CT, if gated, may be an attractive option, since the imaging in one session allows for optimal fusion results. Alternatively, an additional cardiac MRI can be performed when suspicion is raised based on the ^{11}C-5-HTP PET and is not readily confirmed by the CT data.

We found ECG-changes in three out of five patients with cardiac metastases. These observed abnormalities were non-specific, i.e. we could not identify a relation between the location of the metastases and the observed abnormalities. On the other hand in twelve out of fourteen (86%)

patients without cardiac metastases ECG changes were also observed. In contrast to carcinoid tumors, islet cell tumors rarely produce serotonin.[15] Thus, without cardiac metastases, patients with an islet cell tumor have a chance similar to that of the general population to display changed ECG-patterns. The majority of cancer patients with cardiac metastases have evidence of ECG changes, such as ST-T-wave-changes or arrhythmias.[16] These ECG changes are most likely the result of mass lesions involving the myocardium or pericardium, possibly infiltrating the conducting system.[11, 12, 16] However, these are frequently asymptomatic, as only 1% of all cancer patients with cardiac metastases develop clinical symptoms related to intracavitary or intramyocardial metastases.[17] When left untreated, these may eventually lead to a 'sudden cardiac death.[18] In this light the QT-interval prolongation is of interest. In our patients without cardiac metastases a prolonged QT-interval (after correction for heart rate) U-waves on the ECG were more frequently observed. Therefore, we cannot underline a relation between cardiac metastases and cardiac arrhythmias due to QT prolongation. In few patients with an islet cell tumor an autopsy is performed to examine the conducting system and search for cardiac metastases as possible cause of death. Therefore, this cause of death may be more frequent than we know and should be considered. It has been reported that in patients with cardiac involvement the incidence of abnormal ECGs increased as death approached.[19] Serial ECG recordings during follow-up and the relation with changes, such as the QT-interval, might identify patients at risk for sudden death. The discovery of cardiac metastases may thus have significant impact on the prognosis of an individual patient.

In this study we could confirm the presence of cardiac metastases with CT in one patient. Even if not all islet cell tumor patients identified in this study would indeed have cardiac metastases, we still feel that they are far more common than previously reported. Considering the potential consequences, doctors should be more aware of the possibility of metastatic

involvement of the heart and should consider this when evaluating patients with a metastatic islet cell tumor.

CONCLUSION

This study shows that cardiac metastases of islet cell tumors likely occur more frequently than previously reported. Special attention should be paid to this when evaluating patients with metastatic disease of islet cell tumors. To identify patients with cardiac metastases a ^{11}C-5-HTP PET scan may best be performed, as this is currently the most sensitive imaging technique to image islet cell tumors. Suspect lesions should then be verified by anatomical imaging with preferably ECG-gated MRI or CT.

REFERENCES

1 Modlin IM, Oberg K, Chung DC, et al. Gastroenteropancreatic neuroendocrine tumours. Lancet Oncol 2008;9:61-72

2 Sparrow PJ, Kurian JB, Jones TR, et al. MR imaging of cardiac tumors. Radiographics 2005;25:1255-76

3 Pellikka PA, Tajik AJ, Khandheria BK, et al. Carcinoid heart disease. Clinical and echocardiographic spectrum in 74 patients. Circulation 1993;87:1188-1196

4 Fiebrich HB, Brouwers AH, Links TP, et al. Images in cardiovascular medicine: myocardial metastases of carcinoid visualized by 18F-dihydroxy-phenyl-alanine positron emission tomography. Circulation 2008;118:1602-1604

5 Koopmans KP, Neels OC, Kema IP, et al. Improved staging of patients with carcinoid and islet cell tumors with 18F-dihydroxy-phenyl-alanine and 11C-5-hydroxy-tryptophan positron emission tomography. J Clin Oncol 2008;26:1489-1495

6 Orlefors H, Sundin A, Garske U, et al. Whole-body (11)C-5-hydroxytryptophan positron emission tomography as a universal imaging technique for neuroendocrine tumors: comparison with somatostatin receptor scintigraphy and computed tomography. J Clin Endocrinol Metab 2005;90:3392-3400

7 Bergstrom M, Lu L, Marquez M, et al. Modulation of organ uptake of 11C-labelled L-DOPA. Nucl Med Biol 1997;24:15-19

8 Neels OC, Koopmans KP, Jager PL, et al. Manipulation of [11C]-5-hydroxytryptophan and 6-[18F]fluoro-3,4-dihydroxy-L-phenylalanine accumulation in neuroendocrine tumor cells. Cancer Res 2008;68:7183-7190

9 Orlefors H, Sundin A, Lu L, et al. Carbidopa pretreatment improves image interpretation and visualisation of carcinoid tumours with 11C-5-hydroxytryptophan positron emission tomography. Eur J Nucl Med Mol Imaging 2006;33:60-65

10 International Commission on Radiological Protection: ICRP Publication 87: Managing patient dose in computed tomography. ICRP Online. Elsevier, 2001. http://icrp.org

11 Reynen K, Kockeritz U, Strasser RH. Metastases to the heart. Ann Oncol 2004;15:375-381

12 Butany J, Nair V, Naseemuddin A, et al. Cardiac tumours: diagnosis and management. Lancet Oncol 2005;6:219-228

13 Shapiro LM. Cardiac tumours: diagnosis and management. Heart 2001;85:218-222

14 Altbach MI, Squire SW, Kudithipudi V, et al. Cardiac MRI is complementary to echocardiography in the assessment of cardiac masses. Echocardiography 2007;24:286-300

15 O'Grady HL, Conlon KC. Pancreatic neuroendocrine tumours. Eur J Surg Oncol 2008;34:324-32.

16 Cates CU, Virmani R, Vaughn WK, et al. Electrocardiographic markers of cardiac metastasis. Am Heart J 1986;112:1297-1303

17 Roberts WC. Primary and secondary neoplasms of the heart. Am J Cardiol 1997;80:671-682

18 Shehata BM, Thomas JE, Doudenko-Rufforny I. Metastatic carcinoid to the conducting system-is it a rare or merely unrecognized manifestation of carcinoid cardiopathy? Arch Pathol Lab Med 2002;126:1538-1540

19 Glancy DL, Roberts WC. The heart in malignant melanoma. A study of 70 autopsy cases. Am J Cardiol 1968;21:555-571

Chapter 4a

Myocardial metastases of carcinoid visualized by ^{18}F-DOPA PET

Helle-Brit Fiebrich[1], MD, Adrienne H. Brouwers[2], MD, PhD, Thera P. Links[3], MD, PhD, Elisabeth G. E. de Vries[1], MD, PhD

Departments of [1]Medical Oncology, [2]Nuclear Medicine and Molecular Imaging and [3]Endocrinology, University Medical Center Groningen, Groningen, The Netherlands

Circulation 2008, 18:1602-1604

Carcinoids are rare tumors arising from neuroendocrine cells, which can produce and secrete hormones. Carcinoid disease may comprise cardiac involvement, with right-sided endocardial and valvular fibrous lesions of the heart.[1] This so-called carcinoid heart disease may present with cardiac failure and arrhythmias. More uncommonly, myocardial metastases are diagnosed in carcinoid disease. The reported incidence of myocardial carcinoid metastases among patients with metastatic carcinoid disease is 4%.[2] These metastases are usually discovered during screening for distant metastatic disease or carcinoid heart disease, but may also present with arrhythmias. However, the incidence may be underestimated as a consequence of limited resolution of the used imaging techniques. In the past, myocardial metastases have been located with ultrasonography and somatostatin receptor scintigraphy (SRS). Lesions smaller than 1.0 cm are difficult to identify with ultrasonography and although good sensitivity (92%) has been reported for SRS, it is by no means perfect.[3, 4] New imaging techniques, such as the ^{18}F-DOPA PET scan, can be of additional value in diagnosing these rare metastases of carcinoid disease, as shown in the following case report.

A 60-year old man presented with diarrhea, abdominal pain and weight loss, but no cardiac complaints. Physical examination revealed no abnormalities apart from a slight hepatomegaly. Laboratory values showed mild anemia, an elevated serotonin level in platelets of 41 nmol/10^9 platelets (upper reference limit 5.4 nmol/10^9 platelets) and urinary 5-hydroxyindoleacetic acid level of 15.2 mmol/mol creatinine (upper reference limit 3.8 mmol/mol creatinine).

SRS with planar imaging of the whole body and SPECT imaging of abdomen and chest 24 hours after injection of 200 MBq ^{111}In-octreotide showed uptake in abdomen, bones, ribs and left supraclavicular region (Figure 1A).

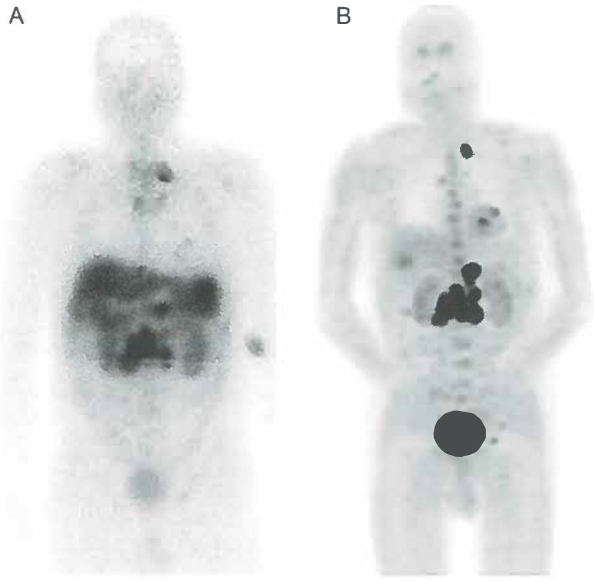

Figure 1. A, SRS planar imaging of the whole body shows uptake in abdomen, skeletal lesions and left supraclavicular region. **B**, the ^{18}F-DOPA PET scan shows uptake in the abdomen, bone metastases and two lesions in the heart.

An ^{18}F-DOPA PET scan revealed uptake in the abdomen, bone metastases and two lesions in the heart (Figure 1B). The ECG showed a sinus bradycardia of 52 beats per minute during metoprolol for hypertension, but was otherwise normal (Figure 2).

Echocardiography showed no tumor lesions and no abnormalities of right ventricular function or valves, indicative of carcinoid heart disease.

An MRI of the heart demonstrated two myocardial lesions in the left ventricle. Fusion of ^{18}F-DOPA PET and MRI confirmed the presence of two lesions in the left ventricular myocardium (Figure 3A). In retrospect, one myocardial lesion was also visible on SRS (Figure 3B; fusion of MRI and SRS).

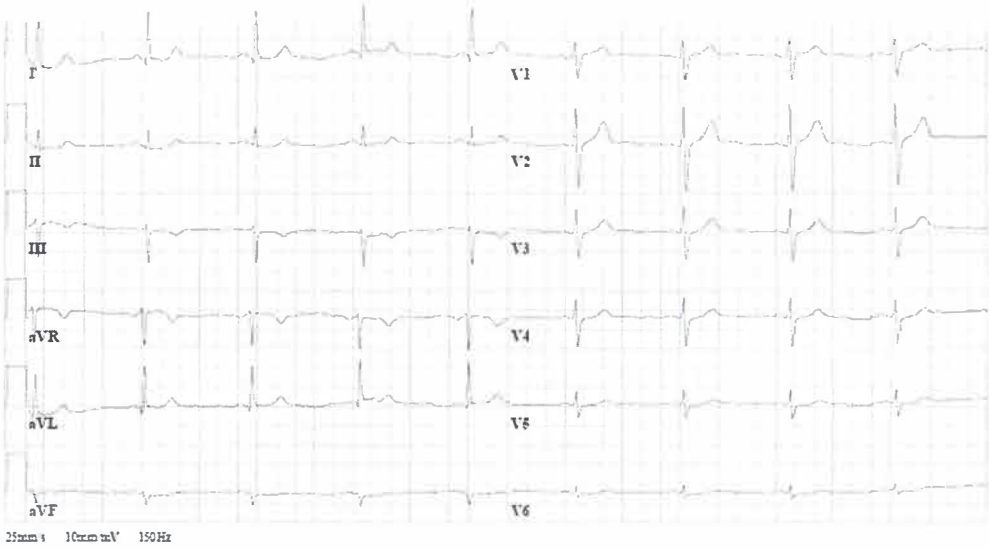

Figure 2. ECG showing sinus bradycardia.

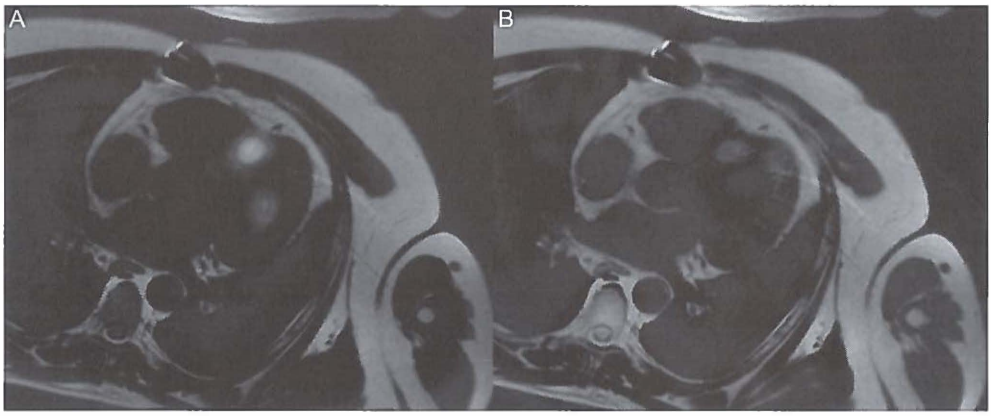

Figure 3. A, fusion of ^{18}F-DOPA PET and MRI confirms the presence of two lesions in the left ventricular myocardium. **B**, fusion of MRI and SRS shows only one myocardial lesion.

Given the absence of cardiac problems, no surgical intervention was considered for the cardiac lesions. The primary ileal tumor was surgically removed and confirmed to be a carcinoid. Follow-up ^{18}F-DOPA PET and

MRI scans one year later showed unchanged metastases including the cardiac lesions and no new metastases.

PET scanning using the catecholamine precursor ^{18}F-DOPA was recently shown to be of diagnostical value in carcinoid disease. Imaging with ^{18}F-DOPA is based on the intrinsic property of neuroendocrine tumors to take up amine precursors, such as ^{18}F-DOPA. The combination of this specific tracer with the high resolution provided by PET, shows an excellent sensitivity of detection of neuroendocrine tumor lesions (up to 96%), which is higher than the sensitivity with SRS in carcinoid patients.[4] This can be explained by the limited spatial resolution and the lack of somatostatin-receptor expression in a number of tumors. Consequently, in carcinoid patients with cardiac complaints, a ^{18}F-DOPA PET scan should be considered, to demonstrate or rule our myocardial metastases.

The treatment for myocardial metastases usually consists of watchful waiting or surgical removal. Recently, a case of successful external beam irradiation has been reported. In our patient absence of complaints and stable cardiac lesions justify watchful waiting.

REFERENCES

1. Bhattacharyya S, Davar J, Dreyfus G, et al. Carcinoid heart disease. Circulation 2007;116:2860-2865
2. Pellikka PA, Tajik AJ, Khandheria BK, et al. Carcinoid heart disease. Clinical and echocardiographic spectrum in 74 patients. Circulation 1993;87:1188-1196
3. Pandya UH, Pellikka PA, Enriquez-Sarano M, et al. Metastatic carcinoid tumor to the heart: echocardiographic-pathologic study of 11 patients. J Am Coll Cardiol 2002;40:1328-1332
4. Koopmans KP, Neels OC, Kema IP, et al. Improved staging of patients with carcinoid and islet cell tumors with ^{18}F-dihydroxy-phenyl-alanine and ^{11}C-5-hydroxy-tryptophan Positron Emission Tomography. J Clin Oncol 2008;26:1489-1495

Chapter 5

Combining ^{18}F-DOPA and ^{18}F-FDG PET for distinction of non-carcinoid malignancies in carcinoid patients

Helle-Brit Fiebrich[1] MD, Adrienne H. Brouwers[2] MD, PhD, Klaas Pieter Koopmans[2] MD, PhD, Elisabeth G. E. de Vries[1] MD, PhD

Departments of [1]Medical Oncology, [2]Nuclear Medicine and Molecular Imaging, University Medical Center Groningen, Groningen, The Netherlands

European Journal of Cancer 2009, 45: 2312-2315

ABSTRACT

Aim

Carcinoid patients frequently develop a second primary malignancy (SPM), which can deserve full treatment. Distinguishing a SPM from carcinoid lesions is therefore important. Differentiation can be achieved using the difference in uptake between different positron emission tomography (PET) tracers.

Methods and Results

Between January 2005 and August 2008 105 carcinoid patients were seen at the Department of Medical Oncology for treatment and follow-up. We identified 3 patients who presented with a new SPM in whom differentiation between carcinoid lesions and the SPM was guided by functional imaging of the catecholamine pathway with 6-fluoro-[^{18}F]L-dihydroxyphenylalanine (^{18}F-DOPA) PET and [^{18}F]fluoro-2-deoxy-d-glucose (^{18}F-FDG) PET as radiotracer for the glucose metabolism. All 3 patients had metastatic carcinoid disease and localised adenocarcinoma based on the PET-scans. For the adenocarcinoma they received curative treatment.

Conclusion

The difference in uptake between these PET techniques can be used for decision making when a primary or metastatic SPM is suspected.

INTRODUCTION

Carcinoids are rare neuroendocrine tumours. They often display a relative indolent behavior, resulting in a long survival. In up to 46% of patients with carcinoid tumours, another non-carcinoid primary malignancy is diagnosed.[1] Given the relative long survival, even in case of metastatic disease, such a second primary malignancy (SPM) can deserve full treatment. Distinguishing lesions of a SPM from a carcinoid metastasis is therefore important, and may have therapeutic consequences. We will illustrate this in three patients in whom decision making was guided by functional imaging of the catecholamine pathway, with 6-fluoro-[^{18}F]L-dihydroxyphenylalanine (^{18}F-DOPA) positron emission tomography (PET) and [^{18}F]fluoro-2-deoxy-d-glucose (^{18}F-FDG) PET as radiotracer for the glucose metabolism.

PATIENTS AND METHODS

All carcinoid patients with metastatic disease seen between January 2005 and August 2008 at the Department of Medical Oncology for treatment and follow-up were included in this retrospective study. The charts of all patients were reviewed to identify patients that had presented with a new SPM during this period. The patients with a new SPM who received both a ^{18}F-DOPA PET scan and a ^{18}F-FDG PET scan to distinguish between the carcinoid lesions and the SPM in order to make a decision about possible curative surgery were further analysed. Clinical follow-up data of these patients were obtained.

^{18}F-FDG PET was performed as described previously.[2] Since 2005 ^{18}F-DOPA PET is available at the University Medical Center Groningen and is used as part of the routine work-up for staging of carcinoid tumours. ^{18}F-

DOPA was locally produced.[3] For the ^{18}F-DOPA PET scan the patients fasted for 6 h before the examination and were allowed to continue all medication. Whole body 2D-PET images were acquired 60 min after the intravenous administration of ^{18}F-DOPA (180 $\pm$ 50 MBq), on a Siemens ECAT HR+ positron camera (Siemens, Knoxville, TN) with attenuation correction (7–10 bed positions of 5 min emission and 3 min transmission scan, total scanning time approximately 60 min). Images were reconstructed using the OSEM algorithm 2 subsets, 8 iterations. One hour prior to the ^{18}F-DOPA injection patients received 2 mg/kg carbidopa orally to increase tumour-to-background ratio of tracer uptake.[4-6]

RESULTS

Hundred five patients with a metastatic carcinoid tumour were identified, 49 men and 56 women with an average age of 62 years. Median follow-up since diagnosis of the carcinoid tumour was 3 years. Fifteen patients (14%) had an additional diagnosis of a SPM, most commonly located in the gastrointestinal tract (n = 4 patients) and the genitourinary tract (n = 4 patients). In 6 patients a metachronous carcinoid was detected 2 to 22 years after the non-carcinoid malignancy, while in 4 patients a synchronous, asymptomatic carcinoid was discovered during surgery for a non-carcinoid malignancy. In 5 patients a metachronous SPM was discovered 2-10 years after diagnosis of the carcinoid tumour was made. In 3 of these patients the SPM was diagnosed between 2005 and 2008, after ^{18}F-DOPA PET became available in our hospital for the routine care of carcinoid tumours. These 3 patients underwent both a ^{18}F-DOPA PET and a ^{18}F-FDG PET scan.

Patient 1 is a 56-year old woman with a carcinoid of the ampulla of Vater was treated with a pancreaticoduodenectomy. Four years later, a

liver metastasis was found on a CT scan. Six years after initial diagnosis she experienced bloody stools due to a rectal adenocarcinoma. The known liver metastasis was reconfirmed on CT scan and ^{18}F-DOPA PET scan and found to be stable (Figure 1a). On the ^{18}F-FDG PET, faint uptake in the liver lesion and intense uptake in the rectum was seen (Figure 1b).

No other sites of increased ^{18}F-FDG uptake were visualised. At this moment no somatostatin receptor scintigraphy (SRS) was performed as a 2 years earlier the SRS showed fewer lesions than the ^{18}F-DOPA PET at that moment. It was concluded that the liver metastasis originated from the carcinoid, and not from the adenocarcinoma. This was histologically confirmed by a liver biopsy. A curative resection of the rectal tumour was performed, which was histologically confirmed to be an adenocarcinoma of the rectum.

Patient 2 is a 61-year old man with a carcinoid of the small intestine and liver metastases. Resection of the primary carcinoid tumour proved impossible because of its proximity to mesenterial arteries. Ten years later, he presented with bloody stools due to a rectal adenocarcinoma. ^{18}F-DOPA PET demonstrated uptake in the primary carcinoid tumour and liver metastases, while ^{18}F-FDG PET showed faint uptake in all carcinoid lesions, but intense uptake in the rectum and physiological uptake in the colon. No recent SRS was performed. It was concluded that the metastatic disease originated from the carcinoid, and not from the adenocarcinoma. A curative resection of the rectal tumour was performed, which was histologically confirmed to be an adenocarcinoma of the rectum. Three years have passed without any signs of new lesions originating from the adenocarcinoma.

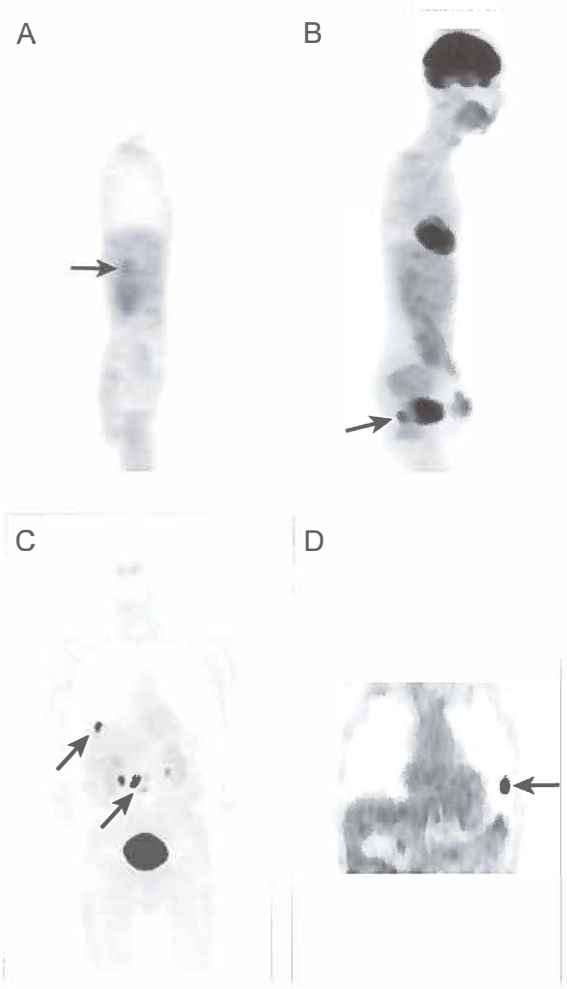

Figure 1. Patient 1 (a,b): (a) On ^{18}F-DOPA-PET one liver lesion (arrow). (b) ^{18}F-FDG-PET shows faint uptake in liver lesion, intense rectal-uptake (arrow). Patient 3 (c,d): (c) ^{18}F-DOPA-PET reveals four abdominally located metastases (arrows). (d) ^{18}F-FDG-PET showing uptake in left lung (arrow).

Patient 3 is a 74-year old man with a carcinoid of the small intestine and metastases in liver and abdominal lymph nodes. One year later, on a routine chest CT scan, a previously unknown lesion suspect for lung cancer was discovered. This patient was a smoker. The ^{18}F-DOPA PET showed

uptake in a liver lesion and three abdominal lesions, while no lung uptake was observed (Figure 1c). SRS showed the same liver lesion as were also seen on ^{18}F-DOPA PET and some vague uptake approximately in the midline of the abdomen on the site where the three abdominal lesions were seen on the ^{18}F-DOPA PET scan and no lung uptake. However, the lung lesion did show up on ^{18}F-FDG PET (Figure 1d). It was concluded that the liver- and abdominal lesions originated from the carcinoid, and not from the pulmonary tumour. This lesion was surgically removed and histology showed a planocellular non-small cell lung cancer (NSCLC). Three years later still no signs of metastases of the lung cancer have been discovered.

DISCUSSION

The most common site of a SPM in carcinoid patients is the gastrointestinal tract, followed by the genitourinary tract and lung/bronchial system.[7] SPMs are usually the more aggressive malignancy. Consequently, most patients with both a carcinoid tumour and a SPM die from the SPM.[1] Differentiation between metastases from either the carcinoid, or the SPM, may be difficult. Our findings illustrate that combining two different radiotracers for functional PET imaging can be helpful in these cases. Absence of proof of metastases of the adenocarcinomas supported the decision for surgery with curative intent in all cases.

^{18}F-FDG PET imaging can detect fast-growing tumours with a high glucose metabolism (such as colorectal cancer and NSCLC), with a sensitivity of 95%.[8] In contrast, tumours with a low metabolic rate (such as carcinoid tumours) often show faint ^{18}F-FDG uptake and are poorly visualised by PET, with detection rates of 25-75%.[9-15]

Imaging with ^{18}F-DOPA is based on the exclusive property of neuroendocrine cells to take up and decarboxylate amine precursors. An

excellent sensitivity of 96% for detection of carcinoid tumour lesions is obtained with ^{18}F-DOPA PET, which is higher than that of SRS. [16-18]

Previous studies have shown that less differentiated neuroendocrine tumours, as determined by a higher Ki-67 index, are more likely to show higher uptake of ^{18}F-FDG on PET, while showing lower uptake on imaging, which specifically shows neuroendocrine tumours, such as SRS.[9,15,19] Theoretically, lesions on ^{18}F-FDG PET might also be due to de-differentiation of secondary lesions which, were initially a well-differentiated carcinoid. However, the ^{18}F-FDG PET-positive lesions in our patients were not previously seen, for example on ^{18}F-DOPA PET, which should have been the case if they were indeed initially a well-differentiated carcinoid. Secondly, to our knowledge, no studies exist describing dedifferentiation of carcinoid tumors. In this study we did not take biopsies of all metastatic lesions to rule out the possibility of a false negative ^{18}F-FDG PET scan, as cytological and histological verification runs a risk of bleeding complications in the highly vascular carcinoid lesions. While this risk has certainly to be accepted for establishing an initial diagnosis, during the course of the disease in case of several metastatic lesions using the combination of PET tracers can be extremely helpful. Especially considering the excellent sensitivities of the PET techniques and the fact that no new or rapidly growing lesions have been discovered so far, the chance of a false negative ^{18}F-FDG PET scan seems small. The possibility of distinguishing lesions without the need of taking biopsies with the associated risks is the great advantage of the combined use of these two radiotracers.

In conclusion, the difference in uptake between ^{18}F-FDG and ^{18}F-DOPA in tumour lesions can be used to make the distinction between metastases from the carcinoid tumour or the SPM. This may clearly have therapeutic consequences, allowing curative treatment for non-metastasised SPMs, even in case of metastatic carcinoid disease.

REFERENCES

1. Gerstle JT, Kauffman GL, Jr., Koltun W A The incidence, management, and outcome of patients with gastrointestinal carcinoids and second primary malignancies. J Am Coll Surg 1995;180:427-432
2. de Groot JW, Links TP, Jager PL, et al. Impact of 18F-fluoro-2-deoxy-D-glucose positron emission tomography (FDG-PET) in patients with biochemical evidence of recurrent or residual medullary thyroid cancer. Ann Surg Oncol 2004;11:786-794
3. De Vries EFJ, Luurtsema G, Brussermann M, et al. Fully automated synthesis module for the high yield one-pot preparation of 6-[18F]fluoro-L-DOPA. Appl Radiat Isot 1999;51:389-394
4. Brown WD, Oakes TR, DeJesus OT, et al. Fluorine-18-fluoro-L-DOPA dosimetry with carbidopa pretreatment. J Nucl Med 1998;39:1884-1891
5. Ishikawa T, Dhawan V, Chaly T, et al. Fluorodopa positron emission tomography with an inhibitor of catechol-O-methyltransferase: effect of the plasma 3-O-methyldopa fraction on data analysis. J Cereb Blood Flow Metab 1996;16:854-863
6. Orlefors H, Sundin A, Lu L, et al. Carbidopa pretreatment improves image interpretation and visualisation of carcinoid tumours with 11C-5-hydroxytryptophan positron emission tomography. Eur J Nucl Med Mol Imaging 2006;33:60-65
7. Habal N, Sims C, Bilchik AJ Gastrointestinal carcinoid tumors and second primary malignancies. J Surg Oncol 2000;75:310-316
8. Wood KA, Hoskin PJ, Saunders MI Positron emission tomography in oncology: a review. Clin Oncol (R Coll Radiol) 2007;19:237-255
9. Adams S, Baum R, Rink T, et al. Limited value of fluorine-18 fluorodeoxyglucose positron emission tomography for the imaging of neuroendocrine tumours. Eur J Nucl Med 1998;25:79-83
10. Belhocine T, Foidart J, Rigo P, et al. Fluorodeoxyglucose positron emission tomography and somatostatin receptor scintigraphy for diagnosing and staging carcinoid tumours: correlations with the pathological indexes p53 and Ki-67. Nucl Med Commun 2002;23:727-734

11. Chong S, Lee KS, Kim BT, et al. Integrated PET/CT of pulmonary neuroendocrine tumors: diagnostic and prognostic implications. Am J Roentgenol 2007;188:1223-1231
12. Daniels CE, Lowe VJ, Aubry MC, et al. The utility of fluorodeoxyglucose positron emission tomography in the evaluation of carcinoid tumors presenting as pulmonary nodules. Chest 2007;131:255-260
13. Erasmus JJ, McAdams HP, Patz EF, Jr., et al. Evaluation of primary pulmonary carcinoid tumors using FDG PET. Am J Roentgenol 1998,170:1369-1373
14. Le Rest C, Bomanji JB, Costa DC, et al. Functional imaging of malignant paragangliomas and carcinoid tumours. Eur J Nucl Med 2001;28:478-482
15. Kayani I, Bomanji JB, Groves A, et al. Functional imaging of neuroendocrine tumors with combined PET/CT using 68Ga-DOTATATE (DOTA-DPhe1,Tyr3-octreotate) and 18F-FDG. Cancer 2008;112:2447-2455
16. Koopmans KP, Neels OC, Kema IP, et al. Improved staging of patients with carcinoid and islet cell tumors with 18F-dihydroxy-phenyl-alanine and 11C-5-hydroxy-tryptophan positron emission tomography. J Clin Oncol 2008;26:1489-1495
17. Koopmans KP, de Vries EG, Kema IP, et al. Staging of carcinoid tumours with 18F-DOPA PET: a prospective, diagnostic accuracy study. Lancet Oncol 2006;7:728-734
18. Hoegerle S, Altehoefer C, Ghanem N, et al. Whole-body 18F dopa PET for detection of gastrointestinal carcinoid tumors. Radiology 2001;220:373-380
19. Pasquali C, Rubello D, Sperti C, et al. Neuroendocrine tumor imaging: can 18F-fluorodeoxyglucose positron emission tomography detect tumors with poor prognosis and aggressive behavior? World J Surg 1998;22:588-592

Chapter 6

Total ^{18}F-DOPA PET tumor uptake reflects metabolic endocrine tumor activity in patients with a carcinoid tumor

Helle-Brit Fiebrich[1], Johan R. de Jong[2], Ido P. Kema[3], Klaas Pieter Koopmans[2], Wim Sluiter[4], Rudi A.J.O. Dierckx[2], Annemiek M. Walenkamp[1], Thera P. Links[4], Adrienne H. Brouwers[2], Elisabeth G.E. de Vries[1]

Departments of [1]Medical Oncology, [2]Nuclear Medicine and Molecular Imaging, [3]Laboratory Medicine, [4]Endocrinology, University Medical Center Groningen, Groningen, The Netherlands

Submitted

ABSTRACT

Positron emission tomography (PET) using 6-[F-18]fluoro-L-dihydroxyphenylalanine (^{18}F-DOPA) has an excellent sensitivity to detect carcinoid tumor lesions. ^{18}F-DOPA-tumor uptake and the levels of biochemical tumor markers are mediated by tumor endocrine metabolic activity. Therefore we evaluated whether total ^{18}F-DOPA-tumor uptake on PET, defined as the whole-body metabolic burden (WBMTB) reflects tumor load per patient, as measured with tumor markers.

Methods

77 consecutive carcinoid patients who underwent a ^{18}F-DOPA PET scan in two previously published studies were analyzed. For all tumor lesions mean standardized uptake values (SUVs) at 40% of the maximal SUV and tumor volume on ^{18}F-DOPA PET were determined and multiplied to calculate a metabolic burden per lesion. WBMTB was the sum of the metabolic burden of all individual lesions per patient. As tumor markers served 24-hour urinary serotonin, urine and plasma 5-hydroxindole acetic acid (5HIAA); catecholamines (nor)epinephrine, dopamine and their metabolites, measured in urine and plasma, and serum chromogranin A.

Results

All but one were evaluable for WBMTB, 74 patients had metastatic disease. ^{18}F-DOPA PET detected 979 lesions. SUVmax on ^{18}F-DOPA PET varied up to 29-fold between individual lesions within the same patients. WBMTB correlated with urinary serotonin (r = 0.68) and urinary and plasma 5HIAA (r = 0.78 and 0.66). WBMTB also correlated with urinary norepinephrine, epinephrine, dopamine and plasma dopamine, but not with serum chromogranin A.

Conclusion

Tumor load per patient measured with ^{18}F-DOPA PET correlates with tumor markers of the serotonin and catecholamine pathway in urine and plasma in carcinoid patients and reflects metabolic tumor activity.

INTRODUCTION

Carcinoids are rare tumors arising from neuroendocrine cells, which can produce and secrete a variety of biochemical markers, including serotonin and 5-hydroxindole acetic acid (5-HIAA), the main metabolite of serotonin. Carcinoid tumors can produce several other markers including catecholamines in 48% of patients.[1-3] Measuring urinary 5-HIAA excretion is currently the cornerstone in the diagnosis and response evaluation of metastatic carcinoid tumors, in combination with data provided by computer tomography (CT) and magnetic resonance imaging (MRI).[4] Recently, it has been suggested that serum chromogranin A is a better marker than urinary 5-HIAA excretion for follow-up of carcinoid patients.[5, 6] The disadvantage of urinary 5-HIAA is that the collection of 24-hour urine samples can be unrealiable and is inconvenient for the patient.[7] Therefore a more convenient and accurate marker is of interest. But in contrast to 5-HIAA, serum chromogranin A does not reflect the metabolic status of these tumors.[6, 8]

The intrinsic property of neuroendocrine tumor cells to take up and decarboxylate amine precursors, which is reflected in the secretory activity of these tumors, is also used for positron emission tomography (PET) imaging of these tumors. PET using the catecholamine precursor 6-[F-18]fluoro-L-dihydroxyphenylalanine (^{18}F-DOPA) has an excellent sensitivity to detect carcinoid tumor lesions.[9-11] In the intracellular accumulation of ^{18}F-DOPA by neuroendocrine tumors several essential steps play a role. ^{18}F-DOPA is transported into the cell by the L-type amino acid transporter (LAT) and then decarboxylated by aromatic-L-amino acid decarboxylase (AADC), resulting in the formation of ^{18}F-dopamine. This is subsequently transported into specific storage vesicles by vesicular monoamine transporter and protected from enzymatic degradation. Unstored ^{18}F-dopamine is subject to degradation in the cytosol and the

formed metabolites leave the cell via diffusion.[12] The increased demand for precursors by the overactive secretory pathways in carcinoid tumors induces high ^{18}F-DOPA-uptake in tumor cells.[13, 14]

Currently, functional information of PET is increasingly being incorporated into staging and follow-up. This information complements the anatomical information, such as exact size and location of lesions, provided by CT and MRI.[15-18] Whether ^{18}F-DOPA-PET can also complement biochemical tumor makers or become a surrogate marker is as yet unknown.

Attempts to quantitate metabolic disease activity are usually based on the maximum standardized uptake value (SUVmax) and the mean standardized uptake value (SUVmean) within a certain volume of interest (VOI). PET imaging additionally opens ways to analyze whole-body metabolic tumor burden (WBMTB) as quantitative measure of the overall tumor load. This approach was used with ^{18}F-FDG PET in non-Hodgkin's lymphoma to measure the treatment response after chemotherapy with glucose uptake in the tumor. With PET WBMTB was the best measure of overall response when compared with SUVmax and SUVmean.[19]

In order to study whether the metabolic endocrine tumor activity measured by biochemical markers in plasma and urine correlates with metabolic activity, as measured on ^{18}F-DOPA PET, the aim of the present study was to evaluate in a group of patients who underwent ^{18}F-DOPA PET as well as careful collection of relevant biochemical tumor markers whether total ^{18}F-DOPA-tumor uptake on PET, reflects the tumor load per patient, as measured with the tumor markers.

PATIENTS AND METHODS

Patients

For this study we selected all consecutive patients with a carcinoid tumor (n=77) who underwent ^{18}F-DOPA PET as well as a careful collection of relevant biochemical tumor markers in two previously published ^{18}F-DOPA PET studies of our institute (between October 2003 and February 2007).[9, 10] The inclusion criteria for these studies were patients with a strong suspicion of a carcinoid tumor, based on clinical and biochemical findings, and patients with histopathologically proven carcinoid tumor, with a clinical indication for (re)staging. All patients had to have at least one abnormal lesion on conventional imaging. These previous studies were designed to evaluate the diagnostic sensitivity of ^{18}F-DOPA PET and ^{11}C-5-hydroxytryptophan (^{11}C-5-HTP) PET in patients with carcinoid tumors. Extended biochemical analyses were performed and charts were checked for the presence of somatostatin analogue treatment. The studies were approved by the medical ethical committee, all patients gave informed consent.

^{18}F-DOPA PET

^{18}F-DOPA was locally produced and performed as described earlier.[9, 10, 20] In short, whole body 2D-PET images were acquired 60 min after the intravenous administration of ^{18}F-DOPA (180 $\pm$ 50 MBq). The patients fasted for 6 h before the examination and were allowed to continue all medication. For the reduction of tracer decarboxylation and subsequent renal clearance and to increase tracer uptake in tumor cells all patients received 2 mg/kg carbidopa orally as pre-treatment 1 h prior to the ^{18}F-DOPA injection.[21-23]

Image analysis

The ^{18}F-DOPA PET scans were reviewed. For each patient, a WBMTB was determined as the sum of the metabolic burden (MB) of each tumor lesion in the PET image.[19] In order to make the MB independent of body weight and injected dose the SUV was used, which is defined as:
SUV = activity concentration [MBq/ml] / injected dose per gram [MBq/g]
In turn, the MB was calculated as: MB = SUVmean x volume of tumor lesion. Both SUVmean and tumor volume were obtained from the PET image using a VOI that was defined as the tumor volume enclosed by a 40% isodensity surface.[24, 25] This VOI was semi-automatically drawn. First, the tumor was fully enclosed by a hand-drawn ellipsoid. In this pre-selected volume the maximum SUV was established. Finally, the VOI contained all voxels with values over 40% of the maximum.

Biochemical analysis

Tumor markers measured for serotonin metabolism were serotonin levels in a 24-h urine collection, urinary and plasma 5-HIAA levels.[26] As markers for catecholamine metabolism we determined urinary and plasma concentrations of adrenalin, noradrenalin and dopamine, and urinary concentrations of the major catecholamine metabolites homovanillic acid (HVA), 3,4-dihydroxyphenylacetic acid (DOPAC), vanillylmandelic acid (VMA), vanillic acid (VA), 3-methoxy-4-hydroxyphenylethylene glycol (MHPG) metanephrine, normetanephrine and 3-methoxytyramine (3-MT) in a 24-h urine collection.[27-29] Serum chromogranin A was determined using a radioimmunoassay (Cga-React, Cis Bio International, Gif-sur-Yvette, France) as a marker for general neuroendocrine tumor activity (reference interval 20-100 mg/L).
All laboratory analyses were performed within 3 months of the ^{18}F-DOPA PET scan in the original studies.[9, 10]

Statistical analysis

For correlations between WBMTB and biochemical data, Spearman's *r* test was calculated. Significance level was 0.05, two-sided. The statistical tests were carried out using the SPSS package version 14.0.

RESULTS

Seventy-four patients had metastatic disease. In 76 of 77 carcinoid patients the tumor volume with ^{18}F-DOPA PET generated by the computer using the SUVmean seemed to correlate well with the visual tumor volume (Figure 1). In one patient visual inspection of the computer generated tumor volume showed a gross underestimation of the visually identified tumor volume due to enormously heterogeneous uptake in the metastases. This patient had an extremely large tumor load in the liver and upper abdomen, consisting of confluent lesions with varying uptake-intensities in different parts of the tumor. As a result, the less avid lesions, which had uptake-values below the 40% threshold of the SUVmax of the hottest lesion, were not included in the lesion volume by the computer algorithm. Therefore, this patient was excluded from further analysis.

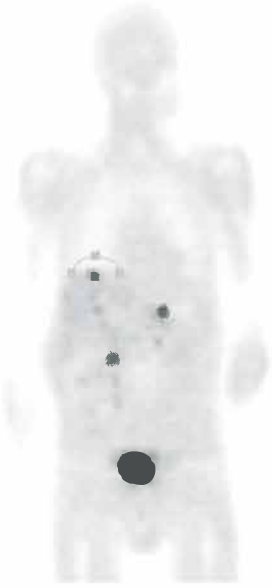

Figure 1. Example of a ^{18}F-DOPA PET scan of a patient with a semi-automatically generated volume of interest (VOI) of a carcinoid lesion.

A total of 979 lesions were detected by ^{18}F-DOPA PET (Table 1). ^{18}F-DOPA PET tumor uptake was shown to vary greatly between carcinoid lesions within individual patients. Within patients SUVs of different lesions showed a large variance; this range was wider for SUVmax than for SUVmean, as the former is more sensitive to outliers. Median difference between the SUVmax of different lesions within one patient of 11.6 (range 0.1-28.7) and the SUVmean of 7.2 (0.2-19.7) (Figure 2).

Table 1. Patient and lesion characteristics

Number of evaluable patients	76
New patients vs. patients with known disease (N of patients)	30/46
Somatostatin analogue treatment (N of patients)	28
Interferon treatment (N of patients)	2
Number of ^{18}F-DOPA PET positive lesions	979
Median number per patient (range)	12 (0-85)
SUVmax, median (range)	3.9 (0.8-33.4)
SUVmean, median (range)	2.6 (0.5-22.7)
Volume in cm^3, median (range)	7.6 (0.55-2308)
WBMTB in cm^3, range	712 (0-19,000)

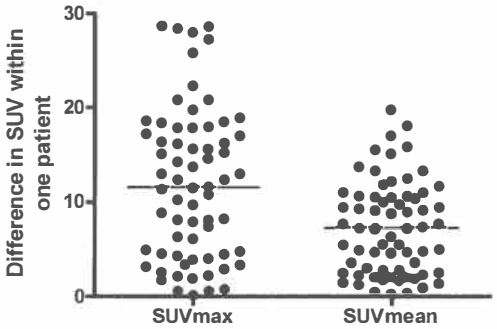

Figure 2. Difference between highest and lowest SUVmax and SUVmean within individual patients, each dot representing one patient. Horizontal bars represent the median values.

This resulted in up to a 29-fold differences for SUVmax and a 25-fold for SUVmean within individual patients. This wide range was caused by difference in size and probable difference in metabolic activity of the lesions. In addition, there was a wide range of measured SUVs between different patients; this range was also wider for SUVmax (0.8-33.4) than for SUVmean (0.5-22.7). The large variability was also reflected in widely differing WBMTB between patients (Figure 3). The latter was caused by varying numbers of lesions between patients as well as by varying uptake intensities.

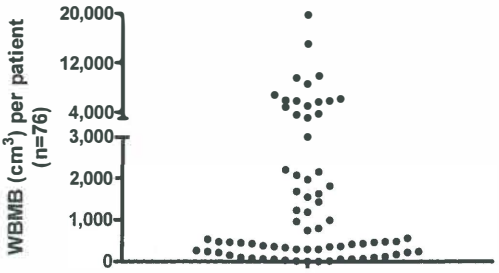

Figure 3. Distribution of whole-body metabolic burden for all individual patients (n=76), each dot representing one patient.

Urinary serotonin and/or 5-HIAA levels were elevated in 64 patients (84%). WBMTB showed significant correlations with both urinary serotonin and its metabolite 5-HIAA in urine and plasma (Table 2). The strongest correlation was found between WBMTB and 24-hour urinary 5-HIAA. There was no difference in strength of correlations between newly diagnosed patients and patients during follow-up.

Elevated levels of catecholamines and/or their metabolites were found in 35 patients (46%). The single most frequently elevated marker was 3-MT, which was elevated in 17 patients (22%). We found significant correlations between WBMTB and the urinary levels of the three main catecholamines norepinephrine, epinephrine and dopamine (Table 2).

There was no difference between newly diagnosed patients and patients known with a carcinoid tumor.

Serum levels of chromogranin A did not correlate with WBMTB (P = 0.14).

Levels of the three major catecholamines norepinephrine, epinephrine and dopamine in 24-hour urine were significantly correlated with urinary 5-HIAA and serotonin levels (data not shown).

Table 2. Significant correlations between biochemical markers and ^{18}F-DOPA PET in total group.

	Correlation coefficient	**Variance explained by correlation**
Urinary serotonin	0.59	0.35
Urinary 5-HIAA	0.78	0.61
Plasma 5-HIAA	0.66	0.44
Urinary norepinephrine	0.53	0.28
Urinary epinephrine	0.38	0.14
Urinary dopamine	0.41	0.17
Urinary 3-MT	0.44	0.19
Plasma dopamine	0.39	0.15

DISCUSSION

We demonstrated that whole-body metabolic tumor burden, as measured with ^{18}F-DOPA-tumor uptake on PET, correlates with biochemical tumor markers in patients with a carcinoid tumor, thus reflecting metabolic endocrine tumor activity. Tracer uptake correlated with urinary and plasma markers of both the serotonin and the

catecholamine pathway, and presented a whole-body image of the specific sites where endocrine production is occurring. ^{18}F-DOPA PET tumor uptake was shown to vary greatly between carcinoid lesions within individual patients, up to 29-fold differences between individual lesions were observed. In addition, there was also great inter-patient variance.

The strongest correlation was found between WBMTB and urinary 5-HIAA levels. This is interesting considering the fact that urinary 5-HIAA is the most widely used marker for follow-up and response assessment of carcinoid tumors.

Currently, there is some debate about the optimal tumor marker for follow-up and management of patients with a carcinoid tumor. Serum chromogranin A has been suggested to replace urinary 5-HIAA.[5, 6] Chromogranin A plays an important role in the regulation of storage and secretion of hormones and peptides. It is localized in the secretory granules of most neuroendocrine cells.[30] Chromogranin A was shown to correlate with tumor load in patients with carcinoid tumors.[31, 32] Here we show that chromogranin A does not reflect the metabolic activity of these tumors, since the whole-body metabolic tumor activity on ^{18}F-DOPA PET did correlate with carefully collected urinary 5-HIAA but not with serum chromogranin A. As WBMTB is the product of tumor volume x metabolic tumor activitity, and chromogranin A is known to correlate with tumor burden, it follows that it does not correlate with metabolic tumor activity. This is in accordance with previous studies which show that chromogranin A fails to reflect the metabolic activity of carcinoid tumors.[6, 8] Our study provided a controlled setting in which a careful collection of all biochemical markers was performed. For routine follow-up reliable urinary 5-HIAA measurements to determine metabolic tumor activity are more difficult to obtain. In view of this an automatically generated WBMTB may prove an interesting marker, since it has demonstrated a good correlation with the metabolic activity of the carcinoid tumor. The additional advantage is that it is a one-stop diagnostic modality where excellent tumor localization and

information about the metabolic tumor activity are both obtained with one scan.

In our patients we found a correlation between WBMTB and catecholamine markers, but these correlations were weaker than those found between WBMTB and serotonin markers. About half of our patients had elevated catecholamine levels, which is conform the numbers found in literature.[1-3] This is less than the 84% of patients who had elevated serotonin or 5-HIAA. Intrinsic tumor catecholamine production explains at least partly the elevated catecholamine levels in these patients. In about two-thirds of carcinoid tumors at least one of the enzymes necessary for catecholamine synthesis is present.[2] These enzymes are focally distributed within the tumor, indicating that a small subpopulation of carcinoid cells could be responsible for the catecholamine synthesis in these patients.[2] Catecholamine levels can also be influenced by sympathoadrenal activation and medication, which could provide an alternative explanation for elevated catecholamine levels in these patients. These influences affect catecholamines proportionally much stronger than their metabolites.[33]

Several factors can influence SUVs, thereby influencing the strength of the correlation between tumor uptake and biochemical markers. Firstly, the time after injection is an important variable that can influence SUVs. A previous study on ^{18}F-DOPA PET in carcinoid tumors found that SUVs did not differ when measured after either 30 or 90 minutes, indicating that a plateau phase is already reached at 30 minutes.[34] This was confirmed in other ^{18}F-DOPA PET studies, which showed that most tumor uptake occurred in the first 30 minutes and that uptake then remained constant for at least 100 minutes.[35-37] Thus, SUVs measured after 60 minutes, as was done in our study, render adequate and reliable measures of tumor tracer uptake. A second factor is the amount of available tracer. Pre-treatment with carbidopa, a peripheral inhibitor of AADC is known to improve image quality for ^{18}F-DOPA PET due to higher tumor-to-background ratios. Carbidopa further improves lesion detection through increased SUV values

of lesions.[21-23, 35] The fact that ^{18}F-DOPA uptake is visible in other structures in our scans serves as a visual control for sufficient tracer availability, otherwise most ^{18}F-DOPA would go to the tumor, as this is the most active tissue.

In conclusion, total tumor load per patient defined as whole-body metabolic tumor burden measured with ^{18}F-DOPA PET correlates with biochemical markers, reflecting metabolic tumor activity in carcinoid patients. It is a one-stop diagnostic tool, providing both a measure of the metabolic tumor activity and a whole-body overview of the specific sites where endocrine production is occurring. In future, WBMTB could serve as alternative assessment parameter to evaluate disease extent and biochemical activity in carcinoid patients. Future studies should investigate the use of this new parameter for follow-up or for the assessment of treatment response.

REFERENCES

1. Modlin IM, Kidd M, Latich I, et al. Current status of gastrointestinal carcinoids. Gastroenterology 2005;128:1717-1751
2. Meijer WG, Copray SC, Hollema H, et al. Catecholamine-synthesizing enzymes in carcinoid tumors and pheochromocytomas. Clin Chem 2003;49:586-593
3. Feldman JM Increased dopamine production in patients with carcinoid tumors. Metabolism 1985;34:255-260
4. Eriksson B, Kloppel G, Krenning E, et al. Consensus guidelines for the management of patients with digestive neuroendocrine tumors--well-differentiated jejunal-ileal tumor/carcinoma. Neuroendocrinology 2008;87:8-19
5. Korse C, Taal B, de Groot C, et al. Chromogranin-A and N-terminal pro-brain natriuretic peptide: an excellent pair of biomarkers for diagnostics in patients with neuroendocrine tumor. J Clin Oncol 2009;27:4293-4299
6. Korse CM, Bonfrer JM, Aaronson NK, et al. Chromogranin A as an alternative to 5-hydroxyindoleacetic acid in the evaluation of symptoms during treatment of patients with neuroendocrine tumors. Neuroendocrinology 2009;89:296-301
7. O'Toole D, Grossman A, Gross D, et al. ENETS consensus guidelines for the standards of care in neuroendocrine tumors: biochemical markers. Neuroendocrinology 2009;90:194-202
8. Woltering E, Hilton RSB, Zolfoghary C, et al. Validation of serum versus plasma measurements of chromogranin A levels in patients with carcinoid tumors: lack of correlation between absolute chromogranin A levels and symptom frequency. Pancreas 2006;33:250-254
9. Koopmans KP, de Vries EG, Kema IP, et al. Staging of carcinoid tumours with 18F-DOPA PET: a prospective, diagnostic accuracy study. Lancet Oncol 2006;7:728-734
10. Koopmans KP, Neels OC, Kema IP, et al. Improved staging of patients with carcinoid and islet cell tumors with 18F-dihydroxy-phenyl-alanine and 11C-5-hydroxy-tryptophan positron emission tomography. J Clin Oncol 2008;26:1489-1495

11. Hoegerle S, Altehoefer C, Ghanem N, et al. Whole-body 18F dopa PET for detection of gastrointestinal carcinoid tumors. Radiology 2001;220:373-380
12. Eisenhofer G, Huynh TT, Hiroi M, et al. Understanding catecholamine metabolism as a guide to the biochemical diagnosis of pheochromocytoma. Rev Endocr Metab Disord 2001;2:297-311
13. Meijer WG, Copray SC, Hollema H, et al. Catecholamine-synthesizing enzymes in carcinoid tumors and pheochromocytomas. Clin Chem 2003;49:586-593
14. Gilbert JA, Bates LA, Ames MM Elevated aromatic-L-amino acid decarboxylase in human carcinoid tumors. Biochem Pharmacol 1995;50:845-850
15. Berghmans T, Dusart M, Paesmans M, et al. Primary tumor standardized uptake value (SUVmax) measured on fluorodeoxyglucose positron emission tomography (FDG-PET) is of prognostic value for survival in non-small cell lung cancer (NSCLC): a systematic review and meta-analysis (MA) by the European Lung Cancer Working Party for the IASLC Lung Cancer Staging Project. J Thorac Oncol 2008;3:6-12
16. Wahl R, Jacene H, Kasamon Y, et al. From RECIST to PERCIST: Evolving considerations for PET response criteria in solid tumors. J Nucl Med 2009;50:122S-150
17. Schwarz-Dose J, Untch M, Tiling R, et al. Monitoring primary systemic therapy of large and locally advanced breast cancer by using sequential positron emission tomography imaging with [18F]Fluorodeoxyglucose. J Clin Oncol 2009;27:535-541
18. Prior JO, Montemurro M, Orcurto MV, et al. Early prediction of response to sunitinib after imatinib failure by 18F-Fluorodeoxyglucose positron emission tomography in patients with gastrointestinal stromal tumor. J Clin Oncol 2009;27:439-445
19. Berkowitz A, Basu S, Srinivas S, et al. Determination of whole-body metabolic burden as a quantitative measure of disease activity in lymphoma: a novel approach with fluorodeoxyglucose-PET. Nucl Med Commun 2008;29:521-526

20. De Vries EFJ, Luurtsema G, Brussermann M, et al. Fully automated synthesis module for the high yield one-pot preparation of 6-[18F]fluoro-L-DOPA. Appl Radiat Isot 1999;51:389-394
21. Brown WD, Oakes TR, DeJesus OT, et al. Fluorine-18-fluoro-L-DOPA dosimetry with carbidopa pretreatment. J Nucl Med 1998;39:1884-1891
22. Ishikawa T, Dhawan V, Chaly T, et al. Fluorodopa positron emission tomography with an inhibitor of catechol-O-methyltransferase: effect of the plasma 3-O-methyldopa fraction on data analysis. J Cereb Blood Flow Metab 1996;16:854-863
23. Orlefors H, Sundin A, Lu L, et al. Carbidopa pretreatment improves image interpretation and visualisation of carcinoid tumours with 11C-5-hydroxytryptophan positron emission tomography. Eur J Nucl Med Mol Imaging 2006;33:60-65
24. Erdi YE, Mawlawi O, Larson SM, et al. Segmentation of lung lesion volume by adaptive positron emission tomography image thresholding. Cancer 1997;80:2505-2509
25. Jentzen W, Freudenberg L, Eising EG, et al. Segmentation of PET volumes by iterative image thresholding. J Nucl Med 2007;48:108-114
26. Kema IP, Meijer WG, Meiborg G, et al. Profiling of tryptophan-related plasma indoles in patients with carcinoid tumors by automated, on-line, solid-phase extraction and HPLC with fluorescence detection. Clin Chem 2001;47:1811-1820
27. Kema IP, Meiborg G, Nagel GT, et al. Isotope dilution ammonia chemical ionization mass fragmentographic analysis of urinary 3-O-methylated catecholamine metabolites. Rapid sample clean-up by derivatization and extraction of lyophilized samples. J Chromatogr 1993;617:181-189
28. Willemsen JJ, Ross HA, Wolthers BG, et al. Evaluation of specific high-performance liquid-chromatographic determinations of urinary metanephrine and normetanephrine by comparison with isotope dilution mass spectrometry. Ann Clin Biochem 2001;38:722-730
29. Willemsen JJ, Ross HA, Wolthers BG, et al. Evaluation of specific high-performance liquid-chromatographic determinations of urinary adrenaline and noradrenaline by comparison with isotope dilution mass spectrometry. Ann Clin Biochem 2001;38:356-364

30. Deftos L Chromogranin A: Its role in endocrine function and as an endocrine and neuroendocrine tumor marker. Endocr Rev 1991;12:181-188
31. Nobels F, Kwekkeboom D, Coopmans W, et al. Chromogranin A as serum marker for neuroendocrine neoplasia: comparison with neuron-specific enolase and the {alpha}-subunit of glycoprotein hormones. J Clin Endocrinol Metab 1997;82:2622-2628
32. Janson ET, Holmberg L, Stridsberg M, et al. Carcinoid tumors: Analysis of prognostic factors and survival in 301 patients from a referral center. Ann Oncol 1997;8:685-690
33. Eisenhofer G, Rundqvist B, Friberg P Determinants of cardiac tyrosine hydroxylase activity during exercise-induced sympathetic activation in humans. Am J Physiol 1998;274:R626-R634
34. Becherer A, Szabo M, Karanikas G, et al. Imaging of advanced neuroendocrine tumors with (18)F-FDOPA PET. J Nucl Med 2004;45:1161-1167
35. Timmers HJ, Hadi M, Carrasquillo JA, et al. The effects of carbidopa on uptake of 6-18F-fluoro-L-DOPA in PET of pheochromocytoma and extraadrenal abdominal paraganglioma. J Nucl Med 2007;48:1599-1606
36. Schiepers C, Chen W, Cloughesy T, et al. 18F-FDOPA kinetics in brain tumors. J Nucl Med 2007;48:1651-1661
37. Bergstrom M, Eriksson B, Oberg K, et al. In vivo demonstration of enzyme activity in endocrine pancreatic tumors: decarboxylation of carbon-11-DOPA to carbon-11-dopamine. J Nucl Med 1996;37:32-37

Chapter 7

Everolimus induces rapid plasma glucose normalization in insulinoma patients by effects on tumor as well as normal tissues

Helle-Brit Fiebrich[1], Ester J.M. Siemerink[1], Adrienne H. Brouwers[2], Geke A.P. Hospers[1], Elisabeth G.E. de Vries[1]

Departments of [1]Medical Oncology, [2]Nuclear Medicine and Molecular Imaging, University Medical Center Groningen, Groningen, The Netherlands

Submitted

To the editor:

Recently, the expression profiling evidence for a role of the phosphatidylinositol 3-kinase (PI3K)/Akt/mammalian target of rapamycin (mTOR) pathway, which integrates signals from growth factors and nutrients to regulate cell growth, proliferation and survival, in islet cell tumors was highlighted in this journal.[1] In addition, two recent phase II studies showed antitumor efficacy of the mTOR-inhibitor everolimus in patients with mixed islet cell tumors.[2,3] Additionally everolimus has been reported to induce stunningly rapid control of hypoglycemias in four patients with malignant insulinomas.[4] The precise mechanism by which glucose normalization was achieved is not yet unravelled. Therefore, we closely monitored glucose and (pro)insulin levels in three patients with malignant symptomatic insulinomas. In addition, we visualized and quantified with positron emission tomography (PET) the glucose metabolism using [^{18}F]fluoro-2-deoxy-d-glucose as tracer (^{18}F-FDG-PET).

The patient characteristics are summarized in Table 1. Two patients were therapy-naive, one had previously received chemotherapy and peptide receptor radionuclide therapy. All patients had severe hypoglycaemic episodes despite by frequent meals and octreotide. Patient 1 and 2 were dependent on continuous glucose infusions to achieve normal glucose levels. Therefore treatment with 10 mg everolimus daily orally, provided by Novartis Pharma AG, Basel, Switzerland, on a compassionate need basis was initiated. In case of grade 3 toxicity according to the CTCAE, version 3.0 the dose was temporarily reduced to 5 mg daily.

Venous plasma glucose was measured daily in the first month and weekly thereafter with an APEC glucose analyzer (APEC Inc., Danvers, MA), serum insulin and proinsulin levels before start of treatment and monthly thereafter.

Table 1. Characteristics of the patients, previous therapy, and biochemical response to everolimus

Patient	Sex, Age (years)	Previous therapy	Insulin in mE/L / proinsulin in pmol/L (elevation above normal, x-fold)			Tumor response and progression free survival
			Pretreatment	1 month	5 months	
1	M, 60	-	75/328 (4.4/45)	45/110 (2.7/15)	57/110 (3.4/15)	Stable disease for 8 months
2	F, 75	-	43/322 (2.5/44)	37/76 (2.2/10)	23/46 (1.4/6)	Stable disease for 8+ months
3	M, 55	3 cycles 5-FU + streptozocin 6 cycles PPRT	107/254 (6.3/35)	38/110 (2.3/15)	130/115 (7.7/16)	Stable disease for 5 months

M: male, F: female, 5-FU: 5-fluorouracil, PPRT: peptide receptor radionuclide therapy

Serum insulin was determined with a DSL-1600 insulin radio-immunoassay (upper level of normal 16.9 mU/L) (Beckman Coulter; Brea, CA) and intact proinsulin (upper level of normal 7.3 pmol/L) as described previously.[5]

The patients underwent computer tomography (CT) scanning before start of treatment, after 2 months and 3 monthly thereafter to determine tumor response according to RECIST 1.1.[6] ^{18}F-FDG-PET was performed at the same time points plus at 2 and 5 weeks. The ^{18}F-FDG-uptake was quantitated as the maximum standardized uptake value (SUVmax) in regions of interest.[7] To quantify glucose-uptake in tumor and normal tissues SUVmax values were calculated for the three hottest tumor lesions, the myocardium, and forearm muscles.

After start of everolimus clinical condition and self-reported well-being improved in all patients. Before everolimus therapy during hypoglycemic episodes, insulin levels were 2.5-6.3-fold elevated compared to the upper limit of normal and proinsulin levels 35-45-fold (Table 1). Glucose levels normalized already on day 4, 8, and 14 respectively (Figure 1) and the continuous glucose infusions could be discontinued. In the heavily pre-treated patient this effect subsided after 13 weeks and was temporarily restored by increasing the octreotide dose to 200 μg three times daily. Insulin levels were lower but still elevated in all after 4 weeks (Figure 1, Table 1). This reduction further persisted in two patients, but increased again in patient 3 after 5 weeks.

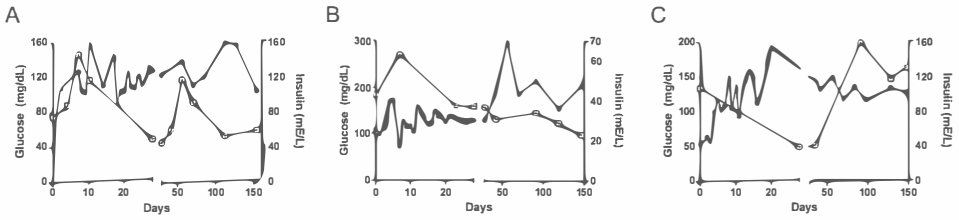

Figure 1. showing the plasma glucose (●) and serum insulin (□) levels per patient. **A**. patient 1, **B.** patient 2, **C**. patient 3

All patients experienced stable disease for respectively 5, 8, and 8+ months. Figure 2 shows the changes in tumor size per patient. ^{18}F-FDG-PET visualized the tumor lesion in the pancreas and more liver lesions than CT in all patients (Figure 3).

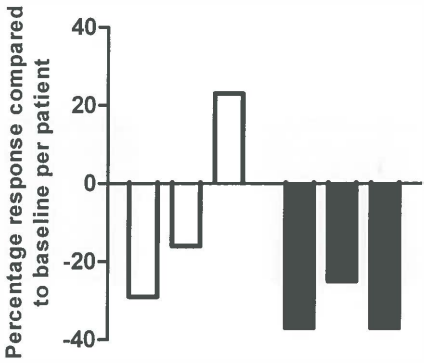

Figure 2. Waterfall plot showing the percentage response in size and maximum standardized uptake values respectively after 5 months per patient on CT (white bars) and ^{18}F-FDG-PET (black bars).). Bars from left to right patient 1 to 3.

^{18}F-FDG-PET before treatment showed abnormally high myocardial and muscle uptake in all patients, which largely normalized during treatment. After 2 weeks everolimus ^{18}F-FDG-uptake in tumor and muscles decreased, with a SUVmax decrease in tumor and muscle of 26 ± 14% (mean ± SD) and 19 ± 41%, respectively (Figure 4). ^{18}F-FDG-uptake of tumor and muscle further decreased on subsequent scans, on average 31 ± 13% (mean ± SD) and 27 ± 41%, respectively after 5 months.

In our patients everolimus controlled hypoglycemia already within 14 days. Concomitantly, (pro)insulin levels decreased, but remain abnormally elevated while the initially elevated ^{18}F-FDG-uptake in the tumor and muscles on PET decreases as well.

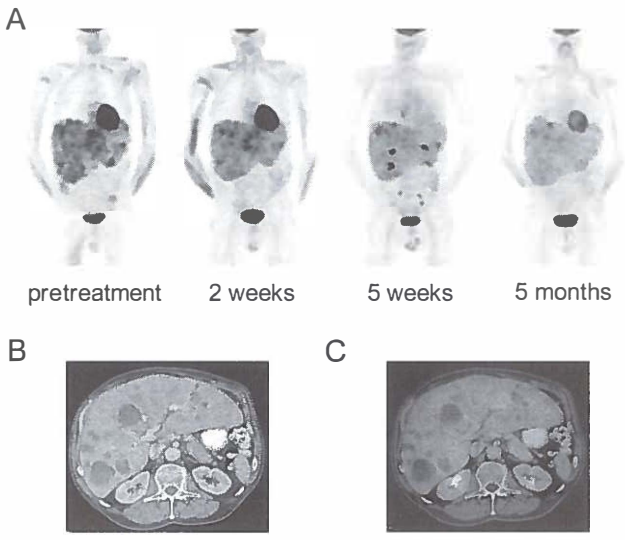

Figure 3. Patient 1. **A.** ^{18}F-FDG-PET scans. Pathological uptake in the liver lesions and physiological uptake in the muscles and myocardium decreases during treatment with everolimus. **B.** Pre-treatment CT scan showing a pancreatic mass and multiple liver lesions. **C.** Fusion of the pre-treatment CT and ^{18}F-FDG-PET confirming uptake in the pancreatic and liver lesions.

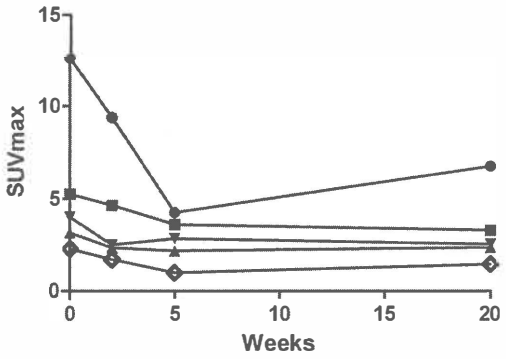

Figure 4. Maximum standardized uptake values decrease on the repeated ^{18}F-FDG-PET scans. Physiological uptake in the myocardium (●) and forearm (◇) is averaged for all patients and uptake in the hottest three tumor lesions is averaged per patient. Patient 1 (■), patient 2 (▲), patient 3 (▼).

Earlier studies with everolimus in mixed islet cell tumors reported mainly stable disease (60-80%) and partial responses (4-27%).[2,3] In insulinoma patients treated with everolimus two experienced stable disease and two a partial response.[4] The small effect on tumor size in our patients reflects these results. Also other treatment options for malignant insulinoma often have a limited effect on tumor size.[8-11] Regretfully these studies do not describe the swiftness of hypoglycemia control.

Despite the limited effect on tumor size, rapid glucose normalization was observed in our insulinoma patients when everolimus was initiated. First this will be due to the observed decreased (pro)insulin secretion, although (pro)insulin levels remained elevated. Therefore, besides the lower (pro)insulin levels, an additional factor must be responsible for the glucose normalization. We saw an avid ^{18}F-FDG-uptake before treatment in tumor lesions and muscles in our patients. This increased muscle uptake was also seen in euglycemic hyperinsulinemic clamping studies, in which insulin administration resulted in increased muscular uptake.[12] In our patients everolimus induced a significant reduction in ^{18}F-FDG-tumor uptake. This was also observed in lesions of patients with non-small cell lung cancer lesions treated with everolimus.[13] However in our insulinoma patients there was in addition a striking reduction in ^{18}F-FDG-muscle uptake. This points to a general metabolic effect of everolimus. We consider downregulation of glucose transporter 1 (GLUT1) in tumor as well as normal tissues by everolimus[14] the second reason for glucose normalization. GLUT1 regulates the cellular uptake of glucose in insulin-stimulated tissues.[15] In vitro prolonged mTOR-inhibitor treatment leads to Akt-inhibition by reduced mTOR complex 2 (mTORC2)-formation.[16] As a consequence of the declined Akt-phosphorylation, transcription and translation of GLUT1 to the plasma membrane is reduced as shown in vitro for adipocytes, fibroblasts and in xenograft tumor models.[14,17] In a xenograft pancreatic cancer model GLUT1-reduction during mTOR-inhibition coincided with a reduction in ^{18}F-FDG-uptake in

the xenograft.[17] GLUT1-reduction leads to a lower glucose transport into the cells and rising plasma glucose levels resulting in peripheral insulin resistance.[18-20] This phenomenon is also described in cancer patients and transplant patients on mTOR-inhibitors.[2,20-22] Nine percent of the neuroendocrine patients experienced plasma glucose levels above 13.9 mmol/L[2], in renal transplant patients this was 5.9%.[23] This difference reflects the higher everolimus doses administered to the cancer patients. However even in renal transplant patients treated with the mTOR-inhibitor sirolimus the oral glucose tolerance test showed already a 30% increase in incidence of impaired glucose tolerance.[20]

In conclusion, the effect of everolimus on glycemic control in metastatic insulinoma patients is not only the consequence of a decrease of (pro)insulin levels and anatomical anti-tumor effects but also due to peripheral glucose resistance pointing to on and off targets effects of everolimus.

REFERENCES

1. Missiaglia E, Dalai I, Barbi S, et al. Pancreatic endocrine tumors: Expression profiling evidences a role for AKT-mTOR pathway. J Clin Oncol 2010;28:245-255
2. Yao J, Phan A, Chang D, et al. Efficacy of RAD001 (everolimus) and octreotide LAR in advanced low- to intermediate-grade neuroendocrine tumors: results of a phase II study. J Clin Oncol 2008;26:4311-4318
3. Yao J, Lombard-Bohas C, Baudin E, et al. Daily oral everolimus activity in patients with metastatic pancreatic neuroendocrine tumors after failure of cytotoxic chemotherapy: A phase II trial. J Clin Oncol 2010;28:69-76
4. Kulke MH, Bergsland EK, Yao JC. Glycemic control in patients with insulinoma treated with everolimus. N Engl J Med 2009;360:195-197
5. Ruige JB, Dekker JM, Nijpels G, et al. Hyperproinsulinaemia in impaired glucose tolerance is associated with a delayed insulin response to glucose. Diabetologia 1999;42:177-180
6. Eisenhauer EA, Therasse P, Bogaerts J, et al. New response evaluation criteria in solid tumours: Revised RECIST guideline (version 1.1). Eur J Cancer 2009;45:228-247
7. Thie JA. Understanding the standardized uptake value, its methods, and implications for usage. J Nucl Med 2004;45:1431-1434
8. Moertel CG, Lefkopoulo M, Lipsitz S, et al. Streptozocin-doxorubicin, streptozocin-fluorouracil or chlorozotocin in the treatment of advanced islet-cell carcinoma. N Engl J Med 1992;326:519-523
9. Eriksson B, Oberg K. An update of the medical treatment of malignant endocrine pancreatic tumors. Acta Oncol 1993;32:203-208
10. Kwekkeboom DJ, de Herder WW, Kam BL, et al. Treatment with the radiolabeled somatostatin analog [177Lu-DOTA0,Tyr3]octreotate: toxicity, efficacy, and survival. J Clin Oncol 2008;26:2124-2130
11. Kulke M, Lenz H, Meropol N, et al. Activity of sunitinib in patients with advanced neuroendocrine tumors. J Clin Oncol 2008;26:3403-3410
12. Roy F, Beaulieu S, Boucher L, et al. Impact of intravenous insulin on 18F-FDG PET in diabetic cancer patients. J Nucl Med 2009;50:178-183

13. Nogova L, Boellaard R, Kobe C, et al. Downregulation of 18F-FDG uptake in PET as an early pharmacodynamic effect in treatment of non-small cell lung cancer with the mTOR inhibitor everolimus. J Nucl Med 2009;50:1815-1819
14. Taha C, Liu Z, Jin J, et al. Opposite translational control of GLUT1 and GLUT4 glucose transporter mRNAs in response to insulin. J Biol Chem 1999;274:33085-33091
15. Sargeant RJ, Paquet MR. Effect of insulin on the rates of synthesis and degradation of GLUT1 and GLUT4 glucose transporters in 3T3-L1 adipocytes. Biochem J 1993;290:913-919
16. Sarbassov DD, Guertin DA, Ali SM, et al. Phosphorylation and regulation of Akt/PKB by the rictor-mTOR complex. Science 2005;307:1098-1101
17. Ma W, Jacene H, Song D, et al. [18F]Fluorodeoxyglucose positron emission tomography correlates with Akt pathway activity but is not predictive of clinical outcome during mTOR inhibitor therapy. J Clin Oncol 2009;27:2697-2704
18. Di Paolo S, Teutonico A, Leogrande D, et al. Chronic inhibition of mammalian target of rapamycin signaling downregulates insulin receptor substrates 1 and 2 and AKT activation: a crossroad between cancer and diabetes? J Am Soc Nephrol 2006;17:2236-2244
19. Fraenkel M, Ketzinel-Gilad M, Ariav Y, et al. mTOR inhibition by rapamycin prevents beta cell adaptation to hyperglycemia and exacerbates the metabolic state in type 2 diabetes. Diabetes 2008;57:945-957
20. Teutonico A, Schena P, Di Paolo S. Glucose metabolism in renal transplant recipients: effect of calcineurin inhibitor withdrawal and conversion to sirolimus. J Am Soc Nephrol 2005;16:3128-3135
21. Motzer R, Escudier B, Oudard S, et al. Efficacy of everolimus in advanced renal cell carcinoma: a double-blind, randomised, placebo-controlled phase III trial. Lancet 2008;372:449-456
22. Yee K, Zeng Z, Konopleva M, et al. Phase I/II study of the mammalian target of rapamycin inhibitor everolimus (RAD001) in patients with relapsed or refractory hematologic malignancies. Clin Cancer Res 2006;12:5165-5173
23. Araki M, Flechner S, Ismail H, et al. Posttransplant diabetes mellitus in kidney transplant recipients receiving calcineurin or mTOR inhibitor drugs. Transplantation 2006;81:335-341

Chapter 8

Deficiencies in fat-soluble vitamins in long-term somatostatin analogue users

Helle-Brit Fiebrich[1], Gerrit van den Berg[2], Ido P. Kema[3], Thera P. Links[2], Jan H. Kleibeuker[4], André van Beek[2], Annemiek M.E. Walenkamp[1], Wim J. Sluiter[3], Elisabeth G.E. de Vries[1]

Departments of [1]Medical Oncology, [2]Endocrinology, [3]Laboratory Medicine, [4]Gastroenterology, University Medical Center Groningen and University of Groningen, Groningen, The Netherlands

Submitted

ABSTRACT

Background & Aims

Somatostatin analogues are administered to control amine and peptide hypersecretion in acromegaly and carcinoid patients. Somatostatin analogues reduce bowel uptake of fat, frequently resulting in steatorrhea. Increased fat in the stools can lead to loss of fat-soluble vitamins. The effect of long-term somatostatin analogue use on vitamin levels is unknown. Therefore we investigated the frequency and severity of fat-soluble vitamin deficiencies in long-term somatostatin analogue users.

Methods

All patients with acromegaly or carcinoid tumors using somatostatin analogues for ≥ 18 months visiting the UMCG, between December 2008 and April 2009 were eligible. Clinical and laboratory parameters, length and dose of treatment, vitamin or pancreatic enzyme suppletion, stool frequency and previous intestinal resection were collected.

Results

54 patients were included (19 with acromegaly, 35 with carcinoid disease). Twelve patients experienced steatorrhea, two carcinoid patients complained of night blindness. Forty-two (78%) were deficient for one or more vitamins, 32% (n = 17) for multiple. Deficiencies for vitamin A, D, E, K1 and E in erythrocytes occurred in respectively 6%, 28%, 15%, 63% and 58% of the patients. Elevated parathyroid hormone was seen in 14 patients, lengthened prothrombin time in three.

Frequency and severity of vitamin D, E and K1 deficiencies were similar in both patients groups. Treatment duration did not influence vitamin levels. Length of intestinal resection and age correlated negatively with vitamin A levels.

Conclusions

Deficiencies of fat-soluble vitamins are frequent during long-term somatostatin analogue treatment. Therefore, fat-soluble vitamins should be monitored and deficiencies supplemented in these patients.

Chapter 8

INTRODUCTION

Long-term somatostatin analogue therapy is important to control symptoms of hypersecretion of biologically active amines and peptides in diseases such as acromegaly or metastatic carcinoid tumors. Other indications for long-term use include certain pancreatic islet cell tumors and the dumping syndrome. Side effects of somatostatin analogue treatment are usually acceptable and often passing. The most common adverse effects are diarrhea, abdominal discomfort and nausea. Gallstones, usually asymptomatic, occur in 10–50% of the treated patients.[1-3] Steatorrhea is an adverse effect experienced by up to 29% of patients on somatostatin analogue treatment.[4] When patients with acromegaly or a carcinoid tumor cannot be cured by complete surgical tumor resection, they often require long-term somatostin analogue treatment for symptom control.

Two somatostatin analogues are currently available for clinical use. Octreotide is registered since 1989, and lanreotide in the Netherlands since 1999. With the passing of time, numerous patients have now received a significantly long-term treatment with these drugs. Given the fat loss in the stool following somatostatin treatment, this will go together with loss of fat-soluble vitamins A, D, E and K1 in the stool. A likely risk factor is the duration of somatostatin analogue treatment. Studies performed thusfar have investigated patients after a relative short treatment period and may therefore well underestimate the frequency of vitamin deficiencies during long-term somatostatin analogue treatment. The only evidence pointing towards an increased risk of a deficiency of fat-soluble vitamins in patients receiving long-term somatostatin analogue treatment comes from a study in acromegaly patients. In this study 103 patients were treated for 3-30 months with a mean duration 24 months. They reported a slight but significant fall of carotene, although values remained in the normal range. In addition, one patient in their study developed a prolonged prothrombin

time (PT), which resolved after vitamin K suppletion.[5] Others observed no changes in serum carotene, vitamin D, or vitamin K in eight acromegaly patients who were on octreotide for four months.[6]

The frequent resection of a part of the small intestine, as performed in midgut carcinoid patients, could be an additional reason for malabsorption. The severity of the malabsorption after an intestinal resection depends on the total of digestive surface area and the portion of small intestine remaining.[7] Carcinoid patients, that have undergone a partial small bowel resection, may therefore be at greater risk to develop vitamin deficiency than carcinoid or acromegaly patients without a bowel resection.

No previous study has systematically investigated long-term somatostatin users and has done so for levels of the complete set of fat-soluble vitamins. Therefore, the extent and severity of fat-soluble vitamin deficiency in patients with acromegaly or a carcinoid tumor are unknown. This study aims to determine the frequency and severity of fat-soluble vitamin deficiency in these patients with a treatment duration of at least 18 months.

MATERIALS AND METHODS

Patients

Patients eligible for this cross-sectional study visited the UMCG between December 2008 and April 2009 for acromegaly or a metastasized midgut carcinoid tumor and were treated with a somatostatin analogue for more than 18 months. Patient inclusion was limited to the winter months in order to rule out seasonal influences on vitamin levels (especially vitamin D) as an explanation for variation of vitamin levels between patients. Patients younger than 18 years and those unable to give informed consent were excluded. Patient charts were checked for diagnosis, reports of previous intestinal resection and length of resection, dose and length of

treatment with somatostatin analogues and possible signs and symptoms of a deficiency of fat-soluble vitamins. In addition, patients were asked if they took vitamin supplements, whether they experienced steatorrhea (defined as loose, greasy stools that are difficult to flush), had special eating habits and if they had complaints that could be due to a vitamin deficiency, such as night blindness or an increased propensity for bleeding.
The study was approved by the local medical ethics committee and all patients gave written informed consent. The study was registered at the Nederlands (Dutch) trial register (registry), trial code 1730.

Biochemical Analysis

To estimate the extent of side effects of somatostatin analogues on the uptake of fat-soluble vitamins we determined plasma concentrations of the fat-soluble vitamins A (retinol), D, E, K1 as described earlier.[8-11] Vitamin E was also measured in the membrane of erythrocytes with an HPLC method, as vitamin E levels in erythrocytes provide a better measure of long-term vitamin E status than plasma levels.[12,13] After liquid/liquid extraction with hexane, using tocol and retinol acetate as internal standards, a 35 µL sample was injected on a Waters Symmetry C18 column (Waters Corporation, Milford, MA) and analysed, using a ASI-100 autosampler (Dionex, Sunneyvale, CA), a P680 HPLC pump (Dionex, Sunneyvale, CA) and a Thermo-Finnigan PDA (photodiode array) detector (Thermo Fisher Scientific Inc., Waltham, MA). ATLAS Chromatography Data System (Thermo Fisher Scientific Inc., Waltham, MA) was used for recording and calculating the results. Lower limits of normal in plasma were 0.8 µmol/L for vitamin A, 50 nmol/L for vitamin D[14], 19.2 µmol/L for vitamin E and 0.8 nmol/L for vitamin K1. Lower limits of normal for vitamin E in erythrocytes was 4.58 µmol per 10^{13} erythrocytes. Reference interval verification, performed in 25 samples of healthy individuals using the EP Evaluator software package release 8 (Data Innovations Inc., South

Burlington, VT), confirmed that the values used in our center for vitamin A and E were correct.[15]

To measure effects of a possible fat-soluble vitamin deficiency, vitamin-dependent parameters were included. For vitamin D parathyroid hormone (PTH) was measured, while for vitamin K1, PT and activated partial thromboplastin time (aPTT) were evaluated.

Statistical Analysis

As control values for healthy individuals served the normal values and the 95% confidence interval as used by our laboratory. In a sample size of 19 acromegaly patients we can demonstrate a significant difference between vitamin levels if 3 abnormal values are measured (15%). In 35 carcinoid patients it is possible to show a significant difference between vitamin levels if 4 abnormal values are measured (12%).

The chi-square test was used to test for differences between patients and normal values and the Mann-Whitney U test to test for differences between groups of carcinoid and acromegaly patients. In a linear univariate regression analysis age, sex, length of treatment, treatment dose, type of somatostatin analogue, presence of steatorrhea, pancreatic enzyme suppletion, diagnosis and bowel resection were tested for associations with plasma vitamin levels. For the analysis, bowel resection was divided into four categories based on the risk of developing malabsorption: no resection, less than 100 cm of bowel resected, between 100 and 200cm resected and more than 200 cm resected.[16] Factors with a P level < 0.15 were tested in a multivariate regression analysis, using the reverse stepwise method. Significance level was 0.05, two-sided. Statistical tests were performed using the SPSS package version 16.0.

Chapter 8

RESULTS

Patient Characteristics

A total of 56 patients were asked to participate, one carcinoid patient and one acromegaly patient declined participation. The remaining 54 patients were analyzed, 19 patients with acromegaly and 35 with a carcinoid tumor. Characteristics of these patients are shown in Table 1.

Median length of somatostatin analogue treatment was 48 months (range 18-155), and did not differ between acromegaly and carcinoid patients ($P = 0.18$). Median dose of somatostatin analogue was 30 mg per 4 weeks for octreotide and 75 mg per 4 weeks for lanreotide. Median doses were the same for both patient groups. Of the carcinoid patients 25 had undergone a bowel resection in the past; in 23 less than 100 cm of bowel was resected, in one between 100 and 200 cm and in one more than 200 cm.

Symptoms

Two carcinoid patients experienced night blindness, which coincided with vitamin A deficiency. One patient was already referred to an ophthalmologist. Electroretinography demonstrated abnormalities typical for vitamin A deficiency in both patients. Oral suppletion of vitamin A resulted in a quick resolution of their symptoms. Twelve patients (n = 4 acromegaly patients and n = 8 carcinoid patients) complained about steatorrhea. Twelve carcinoid patients experienced increased stool frequency (range 1-10 times daily), but most had normal stools. An additional five carcinoid patients received suppletion of pancreatic enzymes for steatorrhea. Despite this suppletion all five patients had abnormal vitamin levels. Four patients (one acromegaly patient and three carcinoid patients) took non-prescribed vitamin supplements (which included vitamins A, D and E), but three of these patients did show

Table 1. Patient characteristics

	Total group	Acromegaly	Carcinoid tumor	*P* value
Number of patients	54	19	35	
Sex, male/female (N = 54)	27/27	11/8	16/19	0.40
Age in years, median (range)	60 (31-83)	56 (31-79)	62 (50-83)	0.003
Octreotide/lanreotide (N = 54)	46/8	10/9	34/1	0.000
Dose, median (range)				
Octreotide, mg / 4 weeks		25 (10-30)	30 (4.5-110)	
Lanreotide, mg / 4 weeks		90 (30-120)	60 (60)	
Length of somatostatin analogue treatment, median (range)	48 (18-222)	57 (18-222)	47 (19-155)	0.18
Complaints suggestive of steatorrhea (N = 54)	12	4	8	0.88
Complaints suggestive of vitamin deficiency (N = 54)	2	0	2	0.46

deficiencies for one (n = 2) or two (n = 1) of the fat-soluble vitamins. None of the patients had symptoms of increased bleeding tendency.

Overall vitamin-deficiencies

Abnormally low plasma levels for one or more fat-soluble vitamins were detected in 78% (n = 42). A deficiency of multiple vitamins was present in 32% (n = 17); in 26% (n = 14) of two, in 4% (n = 2) of three and in 2% (n = 1) of all fat-soluble vitamins. The three patients with a deficiency of three or four vitamins were all carcinoid patients. When vitamin E levels in erythrocytes, which reflects long-term vitamin E status, were considered for vitamin E status instead of plasma vitamin E levels more patients (n = 51, 91%) had a deficiency.

The most frequently deficient vitamin overall was vitamin K1 (n = 34, 63%). Low plasma levels of vitamin A were detected in 6%, of vitamin D in 28%, of vitamin E in 15% and low levels of vitamin E in erythrocytes in 58% of patients. The number of patients with a deficiency for vitamin D, E and K1 in plasma and for vitamin E in erythrocytes was significantly higher compared to what can be expected based on the normal values of our laboratory ($P < 0.001$). This was not the case for vitamin A ($P = 0.15$).

Subgroup Analysis

In the group of acromegaly patients 74% (n = 14) had abnormally low plasma levels for at least one vitamin and 47% for two vitamins. Based on vitamin E levels in erythrocytes, 89% had abnormally low levels for at least one vitamin. In this group all patients had normal levels of vitamin A. Vitamin D levels below 50 nmol/L were found in four acromegaly patients (21%). Lowered vitamin E plasma levels were present in three patients (16%), while vitamin K1 was deficient in 10 patients (53%). Vitamin E levels in erythrocytes were lowered in 14 (74%).

Of the carcinoid patients 80% (n = 28) had abnormally low plasma levels of at least one fat-soluble vitamin, while 32% had more than one deficiency. When vitamin E levels in erythrocytes were considered for vitamin E status, 91% had abnormally low levels for at least one vitamin. Vitamin A deficiency was detected in three patients (9%). Vitamin D levels below 50 nmol/L were found in 11 patients (31%). Low vitamin E plasma levels were found in five patients (14%), while vitamin K1 was deficient in 24 patients (69%). Vitamin E in erythrocytes was low in 15 (43%). Vitamin plasma levels for both patient groups are shown in Figure 1. Frequency or severity of deficiencies for vitamin D, E and K1 did not differ significantly between patients with acromegaly or a carcinoid tumor, while vitamin A deficiency was only seen in carcinoid patients.

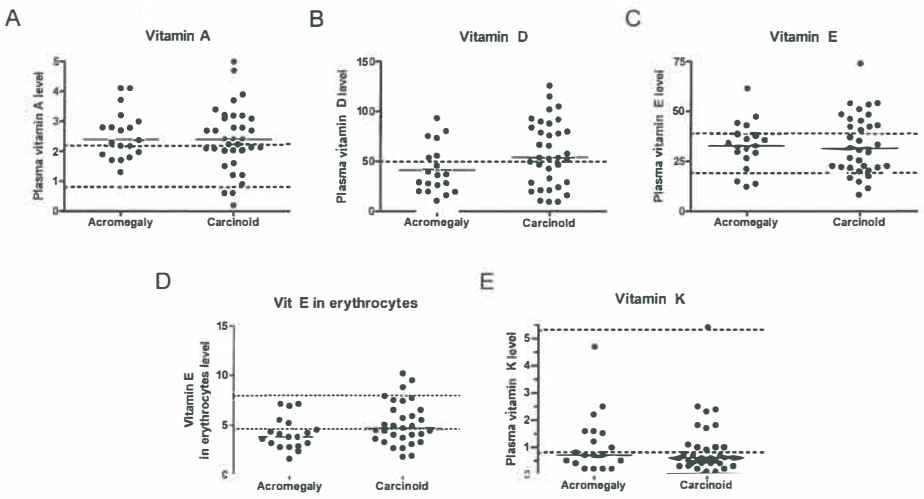

Figure 1. Scatter plots showing the range of plasma levels (unless otherwise noted) of the different fat-soluble vitamins per patient. **Panel A.** Vitamin A, **Panel B.** Vitamin D, **Panel C.** Vitamin E, **Panel D.** Vitamin E in erythrocytes **Panel E.** Vitamin K. Horizontal bars represent the median value, dotted lines the lower and upper limits of normal.

Vitamin-dependent parameters

In 60% of patients (n = 9) with vitamin D levels below 50 nmol/L PTH was elevated; these included 3 acromegaly patients and 6 patients with a carcinoid tumor. Four (12%) out of 34 patients with low vitamin K1 level, all with a carcinoid tumor, showed a prolonged PT, one patient also had a prolonged aPTT. This last patient was also on a vitamin K antagonist, which explains the prolonged PT and aPTT.

Multivariate regression analysis

Neither duration of treatment nor dose of either somatostatin analogue was associated with the plasma level of the various fat-soluble vitamins or vitamin E in erythrocyte levels. Increased stool frequency was not associated with lower vitamin levels in plasma or erythrocytes. Resection of a longer portion of small bowel showed an association with lower plasma vitamin A levels. In addition, higher vitamin A levels were negatively associated with older age. Plasma levels of vitamin D, E, K or levels of vitamin E in erythrocytes were not associated with any of the investigated factors.

DISCUSSION

This study shows that 78% of acromegaly and patients with metastasized midgut carcinoids who received a somatostatin analogue for longer than 18 months have deficiencies of one or more fat-soluble vitamins.

This high level of vitamin deficiency was until now unknown. Two earlier studies addressing vitamin levels in patients treated with a somatostatin analogue[5, 6] found a lowering of carotene, but values remained

in the normal range. The major difference of our study versus these studies is a median treatment duration which was much longer.

Our study indicates that over the coming years vitamin deficiencies will be seen more frequently in the increasingly growing group of long-term somatostatin analogue users. Acromegaly patients precluded from surgical cure can receive long-term somatostatin analogue treatment.[17] In addition, the life expectancy of patients with a metastasized carcinoid tumor has improved clearly during the last decades.[18] Consequently, patients receive somatostatin analogues for extended periods.

The most impressive symptom we observed was night blindness in two patients which showed a quick resolution of their complaints after vitamin A suppletion. Vitamin K1 was the most frequently observed deficient vitamin in our study. This deficiency resulted only in few patients in prolonged clotting times. However the plasma values indicate that these patients should be closely followed, in case of surgery vitamin K1 should be supplemented to prevent bleeding.

In our study bowel resection also influenced plasma levels of vitamin A, but interestingly not to plasma levels of the other fat-soluble vitamins. Patients with a less than 200 cm residual bowel after resection run the highest risk to develop vitamin deficiencies. Both the guidelines of the British Society of Gastroenterology and of the American Gastroenterology Association Institute mention that fat-soluble vitamins may need to be supplemented if less than 200 cm of short bowel remains after resection, but do not suggest a specific screening regimen.[16, 19] Early studies in small numbers of patients who had undergone resection of varying lengths of intestine showed that resection of more than 100 cm of the terminal ileum leads to insufficient intra-intestinal bile salt concentrations, which might in turn lead to fat and fat-soluble vitamin malabsorption.[20, 21] However, for patients with a resection of more than 100 cm no regular monitoring of these vitamins is recommended by any of the existing guidelines. In our

study in only two carcinoid patients this was the case. In most carcinoid patients only short segments of the small bowel have been resected.

Current guidelines of various national and international consensus groups for the treatment of acromegaly or carcinoid tumors do not recommend the monitoring of fecal fat excretion in patients treated with a somatostatin analogue.[1,17, 22-26] Furthermore, only the guidelines by the European Neuroendocrine Tumor Society (ENETS) and of the Nordic neuroendocrine tumor group mention that pancreatic enzyme replacement can be given to alleviate steatorrhea.[22, 25] Deficiencies of fat-soluble vitamins may be less frequent in patients, who take pancreatic enzyme suppletion to improve fat uptake and uptake of fat-soluble vitamins and consequently steatorrhea. In our population five patients took such medication. These five patients did however still show deficiencies of the fat-soluble vitamins.

Carcinoid patients may have another risk factor for the development of deficiencies of fat-soluble vitamins, as they frequently experience diarrhea as part of the carcinoid syndrome. Transit times in the small bowel and the colon are 2-6 times faster in carcinoid patients compared to healthy controls.[27] A shorter transit time reduces the time available for the absorption of water and nutrients. Consequently, less fat is absorbed with shorter transit time.[28] In that case fat-soluble vitamins will also be absorbed less. In our study no association between increased stool frequency and vitamin deficiency was found.

We determined plasma vitamin E as well as vitamin E levels in erythrocytes. Plasma vitamin E half-life is subject to extensive interindividual variation because of the many factors that influence the turnover of the various lipoproteins.[29] Vitamin E in erythrocytes, on the other hand, has a longer half life than vitamin E in plasma and therefore better reflects long-term vitamin E status.[12, 13] Vitamin E in erythrocytes is located in the cell membrane where it is essential to prevent free radical damage to tissues and specifically to unsaturated lipids.[30] Vitamin E levels in erythrocytes were deficient in 58% patients illustrating a clear effect on

long-term vitamin E status in these patients while plasma vitamin E levels was only lowered in 15%, likely due to recent dietary intake.

Decreased vitamin levels can also be the consequence of insufficient dietary intake. We did not perform a detailed dietary history, but none of our patients reported an abnormal eating behavior. The four patients who reported to take non-prescribed vitamin supplements did still have vitamin deficiencies. Apparently, over-the-counter available vitamin supplements do not contain doses high enough to prevent fat-soluble vitamin deficiencies in these patients.

In conclusion, deficiencies of fat-soluble vitamins in patients receiving long-term somatostatin analogue treatment are more frequent than previously known. Considering the possible consequences, we recommend routine assessment of fat-soluble vitamin status in these patients especially in patients with an intestinal resection, and in case of signs or symptoms.

REFERENCES

1. Oberg K, Kvols L, Caplin M, et al. Consensus report on the use of somatostatin analogs for the management of neuroendocrine tumors of the gastroenteropancreatic system. Ann Oncol 2004;15:966-973
2. Trendle MC, Moertel CG, Kvols LK. Incidence and morbidity of cholelithiasis in patients receiving chronic octreotide for metastatic carcinoid and malignant islet cell tumors. Cancer 1997;79:830-834
3. Melmed S. Acromegaly pathogenesis and treatment. J Clin Invest 2009;119:3189-3202
4. Shah T, Caplin M. Endocrine tumours of the gastrointestinal tract. Biotherapy for metastatic endocrine tumours. Best Pract Res Clin Gastroenterol 2005;19:617-636
5. Newman CB, Melmed S, Snyder PJ, et al. Safety and efficacy of long-term octreotide therapy of acromegaly: results of a multicenter trial in 103 patients--a clinical research center study. J Clin Endocrinol Metab 1995;80:2768-2775
6. Ho PJ, Boyajy LD, Greenstein E, et al. Effect of chronic octreotide treatment on intestinal absorption in patients with acromegaly. Dig Dis Sci 1993;38:309-315
7. Kastin DA, Buchman AL. Malnutrition and gastrointestinal disease. Curr Opin Clin Nutr Metab Care 2002;5:699-706
8. Haard PMM, Engel R, Bruyn ALJM. Quantitation of trans-vitamin K1 in small serum samples by off-line multidimensional liquid chromatography. Clinica Chimica Acta 1986;157:221-230
9. Zaman Z, Fielden P, Frost PG. Simultaneous determination of vitamins A and E and carotenoids in plasma by reversed-phase HPLC in elderly and younger subjects. Clin Chem 1993;39:2229-2234
10. Bui MH. Simple determination of retinol, alpha-tocopherol and carotenoids (lutein, all-trans-lycopene, alpha- and beta-carotenes) in human plasma by isocratic liquid chromatography. J Chromatogr B Biomed Appl 1994;654:129-133

11. Chen T, Turner A, Holick M. Methods for the determination of the circulating concentration of 25-hydroxyvitamin D. J Nutr Biochem 1990;1:315-319
12. Jeanes Y, Hall W, Lodge J. Comparative H-labelled a-tocopherol biokinetics in plasma, lipoproteins, erythrocytes, platelets and lymphocytes in normolipidaemic males. British Journal of Nutrition 2005;94:92-99
13. Lehmann J, Rao DD, Canary JJ, et al. Vitamin E and relationships among tocopherols in human plasma, platelets, lymphocytes, and red blood cells. Am J Clin Nutr 1988;47:470-474
14. Holick M. Vitamin D Deficiency. N Engl J Med 2007;357:266-281
15. Horowitz GL, Altaie S, Boyd JC, et al. Defining, establishing and verifying reference intervals in the clinical laboratory. Wayne, USA: Clinical and laboratory standards institute, 2008.
16. Nightingale J, Woodward JM, on behalf of the Small Bowel and Nutrition Committee of the British Society of Gastroenterology. Guidelines for management of patients with a short bowel. Gut 2006;55:iv1-12
17. Melmed S, Colao A, Barkan A, et al. Guidelines for acromegaly management: an update. J Clin Endocrinol Metab 2009;94:1509-1517
18. Yao J, Hassan M, Phan A, et al. One hundred years after "carcinoid": Epidemiology of and prognostic factors for neuroendocrine tumors in 35,825 cases in the United States. J Clin Oncol 2008;26:3063-3072
19. American Gastroenterological Association medical position statement: Short bowel syndrome and intestinal transplantation. Gastroenterology 2003;124:1105-1110
20. Booth CC, Alldis D, Read AE. Studies on the site of fat absorption: 2 Fat balances after resection of varying amounts of the small intestine in man. Gut 1961;2:168-174
21. Aldini R, Roda A, Festi D, et al. Bile acid malabsorption and bile acid diarrhea in intestinal resection. Dig Dis Sci 1982;27:495-502
22. Oberg K, Astrup L, Eriksson B, et al. Guidelines for the management of gastroenteropancreatic neuroendocrine tumours (including bronchopulmonary and thymic neoplasms). Acta Oncol 2004;43:617-625
23. Ramage JK, Davies AHG, Ardill J, et al. on behalf of UKNETwork for neuroendocrine tumours. Guidelines for the management of

gastroenteropancreatic neuroendocrine (including carcinoid) tumours. Gut 2005;54:iv1-16

24. Maroun J, Kocha W, Kvols L, et al. Guidelines for the diagnosis and management of carcinoid tumours. Part 1: The gastrointestinal tract. A statement from a Canadian National Carcinoid Expert Group. Curr Oncol 2006;13:67-76
25. Eriksson B, Kloppel G, Krenning E, et al. Consensus guidelines for the management of patients with digestive neuroendocrine tumors--well-differentiated jejunal-ileal tumor/carcinoma. Neuroendocrinology 2008;87:8-19
26. Cook DM, Ezzat S, Katznelson L, et al. AACE medical guidelines for clinical practice for the diagnosis and treatment of acromegaly. Endocr Pract 2004;10:213-225
27. Ohe M, Camilleri M, Kvols L, et al. Motor dysfunction of the small bowel and colon in patients with the carcinoid syndrome and diarrhea. N Engl J Med 1993;329:1073-1078
28. Neal DE, Williams NS, Barker MC, et al. The effect of resection of the distal ileum on gastric emptying, small bowel transit and absorption after proctocolectomy. Br J Surg 1984;71:666-670
29. Morrissey PA, Sheehy PJA. Optimal nutrition: vitamin E. Proc Nutr Soc 1999;58:459-468
30. Wang X, Quinn P. Vitamin E and its function in membranes. Progr Lipid Res 1999;38:309-336

Chapter 9

Summary and Future perspectives

SUMMARY

Neuroendocrine tumors are a heterogeneous group of rare tumors, which arise from cells of the (neuro)endocrine system. These cells are located throughout the body and are capable of secreting biologically active amines, peptides and hormones. They can be divided into cell types that form localized glands (for example the adrenal medulla and the paraganglia) and cells that are dispersed throughout the entire body in other organs: the diffuse neuroendocrine system. Tumors originating from the chromaffin cells of the adrenal medulla are classified as pheochromocytoma, while tumors of the sympathetic and parasympathetic paraganglia are called paraganglioma. Neuroendocrine tumors that arise from the diffuse neuroendocrine system are mainly localized in the intestine, pancreas and lung, although they can originate in other organs as well. Intestinal neuroendocrine tumors are most commonly found in the small intestine, followed by the rectum and appendix. Neuroendocrine tumors that arise from the pancreas are called islet cell tumors.

The World Health Organisation (WHO) categorizes neuroendocrine tumors based on histological features. The main categories defined by this classification system are well differentiated neuroendocrine tumors, well-differentiated neuroendocrine tumors of uncertain behavior, well-differentiated neuroendocrine carcinoma and poorly differentiated neuroendocrine carcinomas. In this thesis the term carcinoid tumor is used to describe the well-differentiated neuroendocrine tumor of the gastrointestinal tract.

For tumor localization anatomical imaging, including computer tomography (CT), magnetic resonance imaging (MRI) or endoscopic ultrasound, in combination with nuclear functional imaging is performed, such as somatostatin receptor scintigraphy (SRS) using ^{111}In-octreotide (for carcinoids and islet cell tumors) or scintigraphy with ^{123}I-labeled meta-

iodobenzylguanidine (for pheochromocytomas). Positron emission tomography (PET) using 6-[F-18]fluoro-L-dihydroxyphenylalanine (^{18}F-DOPA) or ^{11}C-5-hydroxytryptophan (^{11}C-5-HTP) are based on the intrinsic property of neuroendocrine tumors to take up, decarboxylate, and store amine precursors. They have shown a superior performance compared to conventional imaging methods in patients with neuroendocrine tumors. Despite this, a clear overview of the relative performance of all currently available imaging methods, especially for islet cell tumors is missing. Indications to image vary, direct head to head comparisons are rare and most studies are performed in small patient numbers.

Surgical excision is the only curative treatment option, but it can also be used in a palliative setting to prevent local problems and decrease hormone production. Also in case of metastatic disease median survival for well-differentiated neuroendocrine tumors is relatively long. Not only new imaging modalities but also new therapeutic options are currently being developed. New targeted drugs have shown promising results in patients with neuroendocrine tumors.

The aim of this thesis was to address the diagnosis and management of patients with neuroendocrine tumors, focusing on carcinoid tumors, islet cell tumors and pheochromocytoma.

In **chapter 2** we present an overview of the literature on the anatomical and functional nuclear medicine techniques for the detection of islet cell tumors. A search was performed in the PubMed Medline and Embase databases of all English publications on imaging of islet cell tumors between 1995 and December 2009. When more than 5 studies were available for an imaging technique, only studies with more than 10 patients for that imaging technique were considered. Three indications can be distinguished for imaging of these tumors namely 1) tumor localization and staging of a patient with symptomatic pancreatic hormone hypersecretion, 2) a chance finding of a neuroendocrine tumor or its

metastases and the subsequent search for a primary (pancreatic) tumor, and 3) screening in asymptomatic VHL and MEN1-mutation carriers. Results of the clinical application of the different imaging methods are described per imaging indication and per tumor type. With Forest plots, the sensitivity of the different imaging techniques is presented. For the applicability of each imaging technique a level of evidence was assigned, based on the system of the Oxford Centre of Evidence Based Medicine. The level of evidence for all imaging indications and modalities was remarkably weak (2b at best). No separate sensitivities could be extracted for patients with a chance tumor finding, as these patients were always reported together with symptomatic patients. Moreover, the number of patients in most studies was very small. For tumor detection in patients with symptoms or a chance finding of neuroendocrine tumor anatomical imaging with ultrasound, CT and MRI has moderate sensitivities, although technical developments allow improvements. Endoscopic ultrasound and new metabolic PET imaging techniques achieve better results. Only a few studies have investigated the performance of imaging modalities for screening of mutation carriers. The best results are obtained with EUS, while CT and SRS showed moderate detection rates. US, MRI and PET have not been investigated.

The aim of the study described in **chapter 3** was to evaluate the sensitivity of ^{18}F-DOPA PET in patients with proven catecholamine excess. Most studies until now included patients on the (suspected) presence of a pheochromocytoma or paraganglioma. In this study we address the issue from the even more basic clinical relevant question namely patients presenting with catecholamine excess. Currently, standard imaging in these patients consists of CT or MRI, usually in combination with ^{123}I-MIBG scintigraphy. After the localization of the primary tumor, ruling out metastatic disease before initial surgery is important, since the detection of metastases affects treatment. Based on initial results in smaller studies ^{18}F-

DOPA PET has emerged as an imaging technique with the potential to improve tumor detection and thus staging. In this study ^{18}F-DOPA PET was therefore compared to conventional imaging with CT or MRI and ^{123}I-MIBG scintigraphy.

A total of 48 patients were studied. Analysis was performed on a patient and lesion-based level. Results of cytological, histological findings, all imaging tests, follow-up and biochemical data served as a composite reference standard. Metanephrines and 3-methoxytyramine were determined in plasma and urine. In addition, uptake of ^{18}F-DOPA was measured with PET to determine the whole-body metabolic tumor burden and correlated with biochemical tumor markers.

^{18}F-DOPA PET showed tumor lesions in 43 patients, ^{123}I-MIBG in 31 and CT/MRI in 32. The final diagnosis was pheochromocytoma in 40, adrenal hyperplasia in two, paraganglioma in two, ganglioneuroma in one and unknown in three. Patient-based sensitivity for ^{18}F-DOPA PET, ^{123}I-MIBG and CT/MRI was 90, 65 and 67%, respectively ($P < 0.01$ for ^{18}F-DOPA PET versus both ^{123}I-MIBG and versus CT/MRI, and $P = 1.0$ ^{123}I-MIBG versus CT/MRI). Lesion-based sensitivities were 73, 48 and 44%, respectively ($P < 0.001$ for both ^{18}F-DOPA PET versus ^{123}I-MIBG and versus CT/MRI, $P = 0.51$ ^{123}I-MIBG vs. CT/MRI). The combination of ^{18}F-DOPA PET and CT/MRI was superior to ^{123}I-MIBG and CT/MRI (93 vs. 76%, $P < 0.001$). Whole-body metabolic tumor burden measured with ^{18}F-DOPA PET correlated with plasma free normetanephrine ($r = 0.82$), and urinary normetanephrine ($r = 0.84$), and metanephrine ($r = 0.57$).

From the results of this study it was concluded that ^{18}F-DOPA PET is superior to both ^{123}I-MIBG scintigraphy and CT/MRI for the localization of tumors in patients presenting with catecholamine excess. Additional information provided by ^{18}F-DOPA PET resulted in improved staging and influenced treatment decisions in 14 patients (29%). The combination of ^{18}F-DOPA PET and CT/MRI was most informative in the diagnostic work-up.

This combination has the additional advantage that CT and MRI provide anatomical localization for the lesions visualized by ^{18}F-DOPA PET.

In **chapter 4** we studied the value of ^{11}C-5-HTP PET to detect previously unknown cardiac metastases in patients with a metastasized islet cell tumor. We were alerted that cardiac metastases might be more frequent than previously reported by the chance discovery by a patient with an islet cell tumor that showed cardiac metastases on ^{11}C-5-HTP PET.

^{11}C-5-HTP PET is currently is the most sensitive imaging technique to visualize islet cell tumors. We therefore decided to re-analyze all patients with metastasized islet cell tumors who underwent as part of clinical trials an ^{11}C-5-HTP PET scan with regard to myocardial metastases.

From a database of all ^{11}C-5-HTP PET scans performed in the University Medical Center Groningen all patients with a metastasized islet cell tumor that had received a ^{11}C-5-HTP PET scan were selected. A group of 26 patients was available for analysis. Five patients (19%) had one or more lesion suspect for cardiac metastases on ^{11}C-5-HTP PET. No patient showed clinical signs or symptoms of cardiac involvement. In one patient the cardiac lesion was also discernible on CT after fusion with the ^{11}C-5-HTP PET scan. Unfortunately, the available chest-CT scans, not designed to detect cardiac metastases since data acquisition was not synchronized to the cardiac cycle, in general provided suboptimal information. Three of five patients with metastases showed ECG changes and 12 of 14 patients without cardiac metastases.

From this study we concluded that cardiac metastases of islet cell tumours are likely more frequent than reported in the literature until now. Increased awareness is necessary when evaluating patients with islet cell tumors for metastatic disease. If cardiac metastases are found serial ECG recordings during follow-up and the relation with changes might identify patients at risk for sudden cardiac death and allows timely initiation of treatment. The discovery of cardiac metastases may well have impact on the prognosis of

an individual patient. In these patients cardiac metastases can best be identified with ^{11}C-5-HTP PET.

This issue is further addressed in **chapter 4a**, by describing a patient in whom two previously unknown cardiac metastases of a carcinoid tumor were found on ^{18}F-DOPA PET, but missed on SRS and echocardiography. The ECG was normal, apart from a sinus bradycardia during metoprolol for hypertension. ECG-gated cardiac MRI confirmed the presence of cardiac metastases. This is another prove for raised awareness for cardiac metastases in a patient with a neuroendocrine, in this case with a carcinoid tumor.

In **chapter 5** we studied second primary malignancies in patients with carcinoid tumors, which are known to occur in up to 46% of these patients. These second primary malignancies can deserve full treatment, distinguishing a second primary malignancy from carcinoid lesions is important. Data were analyzed of 105 carcinoid patients seen at the Department of Medical Oncology for treatment and follow-up. We identified three patients who presented with a new second primary malignancy in whom differentiation between carcinoid lesions and the second primary malignancies was guided by functional imaging of the catecholamine pathway with ^{18}F-DOPA PET and ^{18}F-FDG PET as radiotracer for the glucose metabolism. All three patients had metastatic carcinoid disease and localized adenocarcinoma or planocellular carcinoma based on the PET scans. For their carcinomas they all received curative treatment.

This study showed that the difference in uptake between ^{18}F-FDG and ^{18}F-DOPA in tumor lesions can be used to distinguish between second primary malignancies and metastases from the carcinoid tumor, without the need for invasive diagnostics. This can clearly have therapeutic consequences, allowing curative treatment for non-metastasised second primary malignancies, even in case of metastatic carcinoid disease.

Carcinoid tumors can produce and secrete a variety of biochemical markers, including serotonin and in up to 48% of patients also catecholamines. If metastatic carcinoid tumors show production of biochemical tumor markers in plasma or urine, then the measurement of these markers is used in the diagnosis and follow-up of these tumors. PET imaging opens ways to analyze a whole-body metabolic tumor burden, defined as uptake intensity x tumor volume, as a new quantitative measure of the overall tumor load. ^{18}F-DOPA-tumor uptake is mediated by endocrine metabolic activity, just as the levels of tumor markers. In **chapter 6** we therefore whether total ^{18}F-DOPA -tumor uptake on PET, defined as the whole-body metabolic tumor burden is a measure of the tumor load per patient, as measured with tumor markers.

Data of 76 patients with a carcinoid tumor who underwent ^{18}F-DOPA PET as well as a careful collection of relevant biochemical tumor markers in two previously published ^{18}F-DOPA PET studies of our institute were analyzed. The inclusion criteria for these studies were patients with a strong suspicion of a carcinoid tumor, based on clinical and biochemical findings, and patients with histopathologically proven carcinoid tumor, with a clinical indication for (re)staging. All patients had to have at least one abnormal lesion on conventional imaging. As tumor markers served 24-hour urinary serotonin, urine and plasma 5-hydroxindole acetic acid (5HIAA); catecholamines (nor)epinephrine, dopamine and their metabolites, measured in urine and plasma, and serum chromogranin A. The whole-body metabolic tumor burden correlated with urinary and plasma and markers of both the serotonin and catecholamine pathway. ^{18}F-DOPA PET tumor uptake varied greatly between carcinoid lesions within individual patients, up to 29-fold differences between individual lesions were observed. In addition, there was also great inter-patient variance. The latter was caused by varying numbers of lesions between patients, but also by varying uptake intensities.

In conclusion, total tumor load per patient defined as whole-body metabolic tumor burden measured with ^{18}F-DOPA PET correlates with metabolic tumor activity in carcinoid patients. It also gives a whole-body presentation of the specific sites where endocrine production is occurring. In future, whole-body metabolic burden may come to serve as alternative assessment parameter to evaluate disease extent and biochemical activity in carcinoid patients.

Chapter 7 describes three patients with a metastasized insulinoma who were treated with the mammalian target of rapamycin (mTOR) inhibitor everolimus. A recent report described achievement of stunningly rapid control of hypoglycemias in four insulinoma patients upon everolimus treatment (Kulke et al. N Engl J Med 2009, 360, 195-197). The precise explanation for these findings is still unknown. We performed laboratory analyses and ^{18}F-FDG PET imaging to identify the kinetics of everolimus-effects on control of hypoglycemias and understand underlying mechanisms. Everolimus normalized plasma glucose levels in all three patients within 14 days which coincided with a lower glucose uptake in tumor and muscles on ^{18}F-FDG PET and decrease in (pro)insulin levels. This effect of everolimus on tumor as well as normal tissues is caused by decline in (pro)insulin excretion together with increased peripheral insulin resistance and explains the rapid control of hypoglycemias observed. In this study we demonstrated how imaging can help to understand and visualize the mechanism behind drug actions.

In **Chapter 8** we evaluated the frequency and severity of fat-soluble vitamin deficiencies in acromegaly and carcinoid patients, two groups that frequently receive long-term treatment with a somatostatin analogue. Somatostatin analogues negatively influence fat uptake in the bowel, frequently resulting in steatorrhea. Together with fat, potentially fat-soluble vitamins can be lost in the stool. In current standard practice vitamin status is not routinely assessed in these patients. The effect of long-

term use of somatostatin analogues on fat-soluble vitamin levels is unknown. Therefore we investigated the frequency and severity of fat-soluble vitamin deficiencies in long-term users.

We evaluated symptoms of vitamin deficiency and measured levels of all four fat-soluble vitamins together with vitamin-dependent parameters in 19 patients with acromegaly and 35 carcinoid patients that were treated with a somatostatin analogue for longer than 18 months in a single centre cross-sectional study. Twelve patients experienced steatorrhea, two carcinoid patients had signs of night blindness. Forty-two patients (78%) had too low levels of one or more fat-soluble vitamins, 17 patients (32%) for multiple vitamins. Vitamin K1 was with 63% most frequently deficient, vitamin A in 6%, D in 28%, E in 15% and vitamin E in erythrocytes in 58%. Frequency or severity of vitamin deficiencies did not differ between patients with acromegaly or carcinoid for vitamin D, E and K1. Duration of somatostatin analogue treatment did not influence vitamin levels. Length of intestinal resection and age were negatively correlated with vitamin A levels. Elevated parathyroid hormone was seen in 14 patients, lengthened prothrombin time in three.

From these data we concluded that deficiencies of fat-soluble vitamins, including vitamin K1 and vitamin A, are more frequent in patients receiving long-term somatostatin analogue treatment than previously reported. Therefore, fat-soluble vitamin status should be monitored and deficiencies supplemented, especially in patients with a previous intestinal resection.

FUTURE PERSPECTIVES

In this thesis we have addressed several aspects in the diagnosis and management of patients with neuroendocrine tumors. Neuroendocrine tumors are considered a rare disease according to the European definition

of rare diseases (i.e. a disease that affects less than 1 person per 2,000). We have shown how metabolic PET imaging can improve tumor localization in patients with catecholamine-producing tumors and detection of (unusual) metastases in patients with islet cell tumors. The specific ability of neuroendocrine tumors to take up and decarboxylate amine precursors, used by ^{18}F-DOPA PET imaging, can help to non-invasively distinguish carcinoid metastases from second primary malignancies. Furthermore, this ability makes that tumor load on ^{18}F-DOPA PET correlates with 5-HIAA, serotonin and the catecholamines in urinary measurements in carcinoid patients. All together, these results encourage further research to investigate the role metabolic PET imaging with ^{18}F-DOPA and ^{11}C-HTP can play in the diagnosis and management of patients with neuroendocrine tumors. In this chapter interesting future applications for which PET imaging with ^{18}F-DOPA and ^{11}C-HTP could be used will be briefly explored.

^{18}F-DOPA PET imaging for response assessment

Currently, there is some debate about the optimal tumor marker for follow-up and management of patients with a carcinoid tumor Serum chromogranin A has been suggested as replacement of urinary 5-HIAA, as the collection of the latter can be unreliable and is inconvenient for the patient. Chromogranin A was shown to correlate with tumor load in patients with neuroendocrine tumors. Unlike 5-HIAA it does not does not reflect the metabolic tumor activity, as we have demonstrated in chapter 6. CT shows mainly stable disease in patients with neuroendocrine tumors, while biochemical response rates are much higher. These CT based response rates should be viewed with some caution when trying to predict treatment outcome of agents that induce mainly growth suppression but little actual tumor shrinkage in these indolent tumors. Lack of progression may be associated with a longer survival. Currently, functional information

of PET is already incorporated into staging and follow-up as surrogate response marker in Non-Hodgkin lymphoma. In the revised RECIST guidelines (^{18}F-FDG) PET now serves to complement CT scanning in the assessment of progressive disease (especially for the detection of 'new' disease). It can also be used to establish a complete response in a manner similar to a biopsy in cases where a residual radiographic abnormality is thought to represent fibrosis or scarring In view of this the whole-body metabolic tumor burden may prove an interesting surrogate marker in carcinoid patients, since it has demonstrated a good correlation with the metabolic activity of the carcinoid tumor, as shown in chapter 6. The additional advantage is that it is a one-stop diagnostic modality where excellent tumor localization and information about the metabolic tumor activity are both obtained with one scan. The value of the whole-body metabolic tumor burden on ^{18}F-DOPA PET should therefore be investigated as marker for the evaluation of treatment. ^{18}F-DOPA PET scans performed before and after treatment, in addition to biochemical analyses are needed to elucidate the usefulness of this technique as a possible response marker.

^{18}F-DOPA and ^{11}C-5-HTP PET imaging of cardiac metastases

In recent years a number of case reports have appeared indicating that cardiac metastases from neuroendocrine tumors probably occur more frequently than reported in the past. PET scanning with ^{18}F-DOPA and ^{11}C-5-HTP PET has superior sensitivity compared to conventional imaging techniques in the detection of neuroendocrine tumors, due to its good spatial resolution and low cardiac background uptake. This offers the possibility to better detect cardiac metastases than in the past, as we have shown in chapter 4 and 4a. Detection of patients with cardiac metastases allows for closer monitoring of these patients, to prevent potentially dangerous arrhythmic episodes. A combination of better imaging techniques and raised awareness in all doctors involved is necessary to

change our understanding of the incidence of cardiac metastases from neuroendocrine tumors. No prospective studies have yet been performed to look at the incidence of cardiac metastases detected with ^{18}F-DOPA PET and/or ^{11}C-5-HTP PET. Future studies should prospectively investigate the value of metabolic PET tracers for the detection of cardiac metastases of neuroendocrine tumors, especially in patients with unexplained new ECG-abnormalities.

Expanding metabolic PET imaging to other tumors

^{18}F-DOPA PET has now been tried for the imaging of most neuroendocrine tumors, with great success. Theoretically, ^{18}F-DOPA PET should also be able to perform well in patients with neuroblastoma. These tumors arise from the sympathetic nervous system and are characterized by the fact that they can take up, store and secrete catecholamines. Currently, ^{123}I-MIBG scintigraphy is recommended as the functional nuclear imaging technique of first choice for the staging of neuroblastomas. The excellent spatial resolution and good tumor-to-background ratio of PET, may give ^{18}F-DOPA PET a better sensitivity in these tumors than ^{123}I-MIBG scintigraphy, as it did in pheochromocytomas. ^{123}I-MIBG scintigraphy can miss small lesions, especially in the liver and the brain, and also a considerable number of bone marrow relapses. In addition, up to 10% of neuroblastomas lack MIBG avidity. No studies have yet been performed to investigate the value of ^{18}F-DOPA PET in neuroblastomas which is of interest to see whether it can improve initial localization and the timely detection of recurrences.

Other PET tracers in neuroendocrine tumors

Next to metabolic PET imaging, also other properties of neuroendocrine tumors can be imaged. This can include somatostatin

receptors, as used with for example ^{68}Ga-DOTA TOC en ^{68}Ga-DOTA NOC. Another possible imaging target could be angiogenesis. Neuroendocrine tumors are highly vascularized, a result of profound angiogenesis. One of the best studied pro-angiogenic growth factors is the vascular endothelial growth factor (VEGF). In nude mice implanted with the human neuroendocrine tumor cell line BON-1 interferon-treatment induced reduction in VEGF expression, which was associated with reduction in microvessel density and tumor growth. Also, tumor VEGF expression patterns in 50 cases of resected human carcinoid tumors were found to correlate with metastases and decrease progression-free survival duration. These studies indicate that VEGF inhibition may be a useful therapeutic strategy in neuroendocrine tumors. Indeed, antiangiogenic drugs including sunitinib (which blocks the VEGF receptor), bevacizumab (a monoclonal antibody against VEGF) and the mTOR inhibitor everolimus have shown antitumor activity in neuroendocrine tumors. mTOR inhibitors block VEGF expression, angiogenesis and vascular permeability, but also achieve a direct antitumor effect. It is currently not possible to predict which individual patient will benefit from treatment with a mTOR inhibitor. A predictive biomarker for efficacy of mTOR inhibitors is urgently needed and would be helpful, as it may facilitate the development of combination therapies, of individual dose titration, may reduce costs and spare the patients unnecessary side effects. The aforementioned studies suggest that serial non-invasive VEGF quantification in tumor lesions may be an excellent predictive biomarker for efficacy of mTOR inhibitors. It would be interesting to investigate whether all neuroendocrine tumors produce VEGF and whether they differ in their response to inhibition of VEGF by mTOR inhibitors. A non-invasive way to achieve this is by using in vivo VEGF imaging with Zirconium-89 (^{89}Zr) bevacizumab PET, which binds to all VEGF-A splice variants.

Patient management in centers of reference

Finally, given the rarity of neuroendocrine tumors relevant knowledge and expertise are scarce. Misdiagnosis, non-diagnosis and lack of knowledge about treatment options are the main hurdles to improving life quality. Given the increasing options for diagnosis and treatment of patients with neuroendocrine tumors they should be referred to centres with specific expertise in this field. Concentrating management of these patients in centres with technical resources, a multidisciplinary team when necessary and clinical research expertise is important to ensure an optimal approach and facilitate meaningful research. In addition, creating large enough cohorts that are followed for a long time will enable us to gain insight in late adverse treatment effects of these rare tumors.

Chapter 10

Nederlandse samenvatting

Neuroendocriene tumoren zijn een heterogene groep, zeldzaam voorkomende tumoren. De incidentie van deze tumoren is ongeveer 10 tot 20 nieuwe gevallen per miljoen mensen per jaar. Deze neuroendocrine tumoren ontstaan uit cellen van het neuroendocriene systeem. Deze cellen bevinden zich in het hele lichaam en kunnen hormonen produceren. Ze worden onderverdeeld in cellen die gelokaliseerd zijn in klieren (bijv. in het bijniermerg en de paraganglia) en cellen die verspreid zijn in andere organen door het hele lichaam: het diffuse neuroendocriene systeem. Tumoren die uitgaan van de chromaffine-houdende cellen van het bijniermerg worden geclassificeerd als feochromocytomen, terwijl tumoren uitgaand van de sympathische en parasympathische paraganglia paragangliomen genoemd worden. Neuroendocriene tumoren van het diffuse neuroendocriene systeem bevinden zich voornamelijk in de darmen, de pancreas en de longen. Ze kunnen echter ook in andere organen ontstaan. Intestinale neuroendocriene tumoren bevinden zich meestal in de dunne darm, gevolgd door het rectum en de appendix. Neuroendocriene tumoren in de pancreas worden eilandjesceltumoren genoemd.

Het classificatiesysteem van de wereldgezondheidsorganisatie (WHO) deelt neuroendocriene tumoren in op basis van histologische eigenschappen. De hoofdcategorieën, op basis van dit classificatiesysteem, zijn goed gedifferentieerde neuroendocriene tumoren, goed gedifferentieerde neuroendocriene tumoren met onzeker gedrag, goed gedifferentieerde neuroendocriene carcinomen en slecht gedifferentieerde neuroendocriene carcinomen. In dit proefschrift wordt de naam carcinoïd gebruikt voor goed gedifferentieerde intestinale neuroendocriene tumoren.

Om de primaire tumor te lokaliseren bij een patiënt die verdacht wordt van een neuroendocriene tumor wordt anatomische beeldvorming, zoals computer tomografie (CT), magnetic resonance imaging (MRI) of endoscopische echografie. Functionele nucleaire beeldvorming wordt eveneens toegepast bij het opsporen van de primaire tumor en wordt

gebruikt om eventuele uitzaaiingen opsporen die buiten het bereik van de gekozen anatomische beeldvorming liggen. Voorbeelden van nucleaire technieken zijn somatostatinereceptorscintigrafie (SRS) met ^{111}In-octreotide (voor carcinoïdtumoren en eilandjesceltumoren) of scintigrafie met ^{123}I-gelabeled meta-iodobenzylguanidine (voor feochromocytomen). Positronemissietomografie (PET) met de catecholamine-voorloper 6-[F-18]fluoro-L-dihydroxyphenylalanine (^{18}F-DOPA) of de serotonine-voorloper ^{11}C-5-hydroxytryptophan (^{11}C-5-HTP) is gebaseerd op het feit dat neuroendocriene tumoren deze specifieke amine-voorlopers kunnen opnemen, decarboxyleren en opslaan. Deze technieken zijn veel gevoeliger dan conventionele beeldvormende technieken bij patiënten met neuroendocriene tumoren. Er is nog geen goed overzicht van de relatieve waarde van alle op dit moment beschikbare beeldvormende technieken, in het bijzondere voor eilandjesceltumoren. Dit wordt mede veroorzaakt door het feit dat dit zeldzame tumoren zijn en veel nieuwe technieken nog maar kortdurend en beperkt beschikbaar zijn. Daar komt bij dat in de gepubliceerde onderzoeken de indicaties voor het inzetten van beeldvorming variëren, directe één-op-één vergelijkingen zijn zeldzaam en de meeste studies zijn gedaan met kleine patiëntenaantallen.

Chirurgische resectie is de enige curatieve behandelingsoptie. Chirurgie kan echter ook toegepast worden in de palliatieve fase om lokale problemen te voorkomen of om de hormoonproductie te verminderen. Zelfs in geval van gemetastaseerde ziekte is de mediane overleving van goed gedifferentieerde neuroendocriene tumoren relatief lang.

Het doel van dit proefschrift is om het diagnosticeren en de behandeling van patiënten met neuroendocriene tumoren te onderzoeken, in het bijzondere van carcinoïdtumoren, eilandjesceltumoren en feochromocytomen.

In **hoofdstuk 2** geven we een overzicht van de literatuur op het gebied van anatomische en functionele nucleaire technieken voor het lokaliseren van eilandjesceltumoren. De PubMed, Medline en Embase

databases zijn doorzocht naar alle Engelstalige publicaties over beeldvorming van in de pancreas gelokaliseerde eilandjesceltumoren tussen 1995 en januari 2010. Indien meer dan vijf studies beschikbaar waren over een bepaalde beeldvormende techniek, zijn alleen de studies met meer dan 10 patiënten in de analyse meegenomen. Wij hebben drie indicaties onderscheiden voor het toepassen van beeldvorming, namelijk 1) tumor lokalisatie en stadiëring van een patiënt met symptomatische hormoonhypersecretie, 2) een toevallig ontdekte neuroendocriene tumor of metastasen daarvan en de daaropvolgende opsporing van een primair (pancreas)tumor en 3) screening van asymptomatische VHL en MEN1-mutatiedragers. Resultaten van de klinische toepassing van de verschillende beeldvormende technieken werden per indicatie en per tumortype besproken. Met Forest plots werd de sensitiviteit van de verschillende beeldvormende technieken weergegeven. Voor de toepassing van elke beeldvormende techniek werd een 'level of evidence' toegekend. De 'level of evidence' voor alle indicaties en beeldvormende technieken was opmerkelijk laag (maximaal 2b). Voor patiënten met een bij toeval ontdekte neuroendocriene tumor kon er geen aparte sensitiviteit berekend worden, aangezien de patiënten in studies altijd samen geanalyseerd werden met symptomatische patiënten. De patiëntenaantallen in de meeste studies waren klein. Bij symptomatische patiënten en patiënten met een bij toeval gevonden tumor heeft anatomische beeldvorming door middel van echografie, CT, MRI een matige sensitiviteit, hoewel technische ontwikkelingen de sensitiviteit zouden kunnen verbeteren. Endoscopische echografie en nieuwe metabole PET technieken laten betere resultaten zien. Slechts weinig studies hebben de waarde van beeldvormende technieken voor screening van mutatiedragers onderzocht. De beste resultaten zijn behaald met endoscopische echografie, terwijl CT en SRS een matige sensitiviteit laten zien. Echografie, MRI en PET zijn niet onderzocht in deze patiëntenpopulatie.

In **hoofdstuk 3** onderzoeken we de sensitiviteit van ^{18}F-DOPA PET bij patiënten met een verhoogde catecholamine productie. Tot op heden includeerden de meeste studies patiënten op basis van (de verdenking van) een feochromocytoom of paraganglioom. In deze studie bekijken we deze kwestie vanuit de klinische situatie, waarin de patiënten zich presenteren met een catecholamine overproductie. De standaard beeldvormende diagnostiek bij deze patiënten bestaan uit CT of MRI, meestal in combinatie met ^{123}I-MIBG scintigrafie. Als de lokalisatie van de primaire tumor bekend is, is het belangrijk om metastasen uit te sluiten, aangezien het vaststellen hiervan de behandeling sterk kan bepalen. Gebaseerd op de initiële resultaten van kleinere studies lijkt ^{18}F-DOPA PET de potentie te hebben om de tumor en eventuele metastasen beter te lokaliseren en dus ook stadiëring te kunnen verbeteren. In deze studie hebben we daarom ^{18}F-DOPA PET vergeleken met de conventionele beeldvormende technieken CT of MRI en ^{123}I-MIBG scintigrafie.

In totaal werden 48 patiënten geanalyseerd. De analyse werd uitgevoerd op patiënt- en tumorlaesie-niveau. Resultaten van de combinatie van cytologie, histologie, alle beeldvormende technieken, follow-up en biochemie dienden als samengestelde gouden standaard. Metanefrines en 3-methoxytyramine werden bepaald in plasma en urine. Opname van ^{18}F-DOPA in de laesies werd gemeten met PET om de 'totale lichaam metabole tumor last' te bepalen en deze te correleren aan biochemische tumormerkstoffen.

^{18}F-DOPA PET liet tumorhaarden zien in 43 patiënten, ^{123}I-MIBG in 31 en CT/MRI in 32 patiënten. Uiteindelijk werden de volgende diagnoses gesteld: feochromocytoom in 40, bijnierhyperplasie in twee, paraganglioom in twee, ganglioneuroom in één. De diagnose bleef onbekend in drie. Sensitiviteit op patiëntniveau voor ^{18}F-DOPA PET, ^{123}I-MIBG en CT/MRI was respectievelijk 90, 65 en 67% ($P < 0.01$ voor ^{18}F-DOPA PET versus zowel ^{123}I-MIBG als CT/MRI en $P = 1.0$ ^{123}I-MIBG versus CT/MRI). Sensitiviteit op laesieniveau was respectievelijk 73, 48 en 44% ($P < 0.01$ voor

^{18}F-DOPA PET versus zowel ^{123}I-MIBG als CT/MRI en P = 0.51 ^{123}I-MIBG versus CT/MRI). De combinatie van ^{18}F-DOPA PET en CT/MRI was superieur aan de combinatie van ^{123}I-MIBG en CT/MRI (93 versus 76%, P < 0.001). De 'totale lichaam metabole tumor last' gemeten met ^{18}F-DOPA PET correleerde met plasma vrije normetanefrine (r = 0.82), en urine normetanefrine (r = 0.84) en metanefrine (r = 0.57).

Uit de resultaten van deze studie concluderen we dat ^{18}F-DOPA PET beter in staat is tumoren te lokaliseren bij patiënten met een catecholamine overproductie dan ^{123}I-MIBG scintigrafie en CT/MRI. Additionele informatie verkregen met de ^{18}F-DOPA PET scan heeft een verbeterde stadiëring en een verandering van het behandelplan bij 14 patiënten (29%) tot gevolg. De combinatie van ^{18}F-DOPA PET en CT/MRI levert de meeste informatie op voor het diagnostische traject van deze patiënten. Deze combinatie heeft als extra voordeel dat CT en MRI anatomische lokalisatie leveren voor de laesies die gezien worden op ^{18}F-DOPA PET.

In **hoofdstuk 4** bestuderen we de waarde van ^{11}C-5-HTP PET om cardiale metastasen in patiënten met een gemetastaseerde eilandjesceltumor te ontdekken. Door bij toeval gevonden cardiale metastasen in een patiënt met een eilandjesceltumor werden we geattendeerd op het feit dat deze metastasen mogelijk frequenter voorkomen dan verondersteld. ^{11}C-5-HTP PET is op het moment de meest gevoelige beeldvormende techniek om eilandjesceltumoren zichtbaar te maken. Daarom besloten we alle ^{11}C-5-HTP PET scans van patiënten met een gemetastaseerde eilandjesceltumor opnieuw te analyseren, met speciale aandacht voor myocardiale metastasen.

Uit een database van alle ^{11}C-5-HTP PET scans die uitgevoerd zijn in het Universitair Medisch Centrum Groningen werden alle patiënten met een gemetastaseerde eilandjesceltumor geïdentificeerd die een ^{11}C-5-HTP PET scan ondergingen. Een groep van 26 patiënten was beschikbaar voor verdere analyse. Vijf patiënten (19%) hadden een of meer voor cardiale metastasen verdachte laesies op ^{11}C-5-HTP PET. Geen enkele patiënt had

klinische tekenen of klachten passend bij cardiale dysfunctie. Bij één patiënt was de cardiale laesie na fusie met ^{11}C-5-HTP PET ook zichtbaar op CT. Gezien het feit dat de beschikbare thorax-CT scans niet gemaakt waren met de intentie om cardiale metastasen aan te tonen en dus niet gesynchroniseerd waren met het hartritme, leverden deze over het algemeen suboptimale informatie. Drie van de vijf patiënten met cardiale metastasen lieten ECG-veranderingen zien, net als 12 van de 14 patiënten zonder cardiale metastasen bij wie een ECG beschikbaar was.
Uit deze studie concluderen we dat cardiale metastasen van eilandjesceltumoren waarschijnlijk vaker voorkomen dan tot nu toe in de literatuur beschreven wordt. Kennis en aandacht voor het voorkomen van cardiale metastasen is van belang bij de evaluatie van patiënten met een eilandjesceltumor om de uitgebreidheid van de gemetastaseerde ziekte vast te stellen.

In **hoofdstuk 4a** beschrijven we een patiënt met cardiale metastasen van een carcinoïdtumor. Bij deze patiënt werden twee van tevoren onbekende cardiale metastasen van een carcinoïdtumor ontdekt op de ^{18}F-DOPA PET scan, die niet gezien werden op SRS en met echocardiografie. Afgezien van een sinusbradycardie, onder metoprolol gebruik voor hypertensie, was het ECG normaal. Een ECG-gesynchroniseerde cardiale MRI bevestigde de aanwezigheid van cardiale metastasen. Deze patiënt illustreert dat cardiale metastasen ook voor kunnen komen bij patiënten met een carcinoïdtumor. Hiermee wordt nog eens extra benadrukt dat cardiale metastasen waarschijnlijk frequenter voorkomen bij patiënten met neuroendocriene tumoren en dat hier bewust aan gedacht moet worden.

In **hoofdstuk 5** bestuderen we tweede primaire niet-carcinoïde maligniteiten bij patiënten met een carcinoïdtumor. Deze worden gezien bij tot wel 46% van deze patiënten. Gezien de lange overleving van patiënten met een carcinoïdtumor kan behandeling van een tweede niet-carcinoïde primaire maligniteit gerechtvaardigd zijn. Daarom is het van belang om onderscheid te maken tussen een tweede primaire maligniteit en

metastasen van de carcinoïdtumor. Het verschil in opname tussen ^{18}F-DOPA, als tracer van de catecholamine pathway welke uitstekend opgenomen wordt door carcinoïdtumoren, en ^{18}F-FDG als tracer voor het glucose metabolisme, die door vele niet-carcinoïde maligniteiten goed opgenomen wordt, kan gebruikt worden bij het onderscheid tussen tweede primaire niet-carcinoïde maligniteiten en carcinoïd metastasen. De therapeutische consequenties van het in kaart brengen van de uitbreiding van de tweede primaire niet-carcinoïde maligniteit is om het nut van eventuele curatieve resectie bij een reeds gemetastaseerde carcinoïdtumor te bepalen.

Data van 105 patiënten met een carcinoïdtumor, die gezien werden op de Afdeling Medische Oncologie van het UMCG voor behandeling en follow-up, werden geanalyseerd om carcinoïdpatiënten te identificeren, die tijdens de onderzoeksperiode een primair adeno- of plaveiselcelcarcinoom ontwikkeld hadden en bij wie differentiatie tussen carcinoïdlaesies en adeno- of plaveiselcelcarcinoom essentieel was voor het al dan niet instellen van een curatieve behandeling van het carcinoom. We konden drie carcinoïdpatiënten identificeren bij wie deze differentiatie werd gefaciliteerd door functionele beeldvorming middels ^{18}F-DOPA PET en ^{18}F-FDG PET. Alle drie patiënten hadden een gemetastaseerde carcinoïdtumor en een gelokaliseerd adenocarcinoom of plaveiselcelcarcinoom op basis van hun PET scans. De niet-carcinoïde maligniteit kon curatief behandeld worden in alle patiënten.

Deze studie laat zien dat het verschil in opname tussen ^{18}F-DOPA en ^{18}F-FDG door tumor laesies inderdaad gebruikt kan worden om op niet-invasieve manier bepaalde tweede primaire maligniteiten en carcinoïd metastasen van elkaar te onderscheiden.

Carcinoïdtumoren kunnen een verscheidenheid aan biochemische tumormerkstoffen, zoals serotonine en catecholamines, produceren en secerneren. Deze kunnen gebruikt worden voor het diagnosticeren en de follow-up van de carcinoïdtumor. Met behulp van een PET scan kan op

een andere manier een 'totale lichaam metabole tumorlast' bepaald worden als een nieuwe kwantitatieve maat voor de totale hoeveelheid tumor. Deze wordt gedefinieerd als intensiteit van de opname x tumor volume. ^{18}F-DOPA tumoropname wordt bepaald door de endocriene metabole activiteit van de tumor, net als het niveau van de tumormerkstoffen. In **hoofdstuk 6** onderzoeken we of de totale ^{18}F-DOPA-opname op de PET scan, gedefinieerd als de 'totale lichaam metabole tumorlast' een maat is voor de hoeveelheid tumor, zoals deze bepaald wordt met biochemische tumormerkstoffen.

Gegevens van 76 patiënten met een carcinoïdtumor, die een ^{18}F-DOPA PET hadden gehad in twee eerder door ons instituut gepubliceerde ^{18}F-DOPA PET-studies en van wie eveneens biochemische tumormerkstoffen bekend waren werden geanalyseerd. Patiënten werden geïncludeerd in deze voorgaande studies als er een sterke verdenking bestond op een gemetastaseerde carcinoïdtumor, gebaseerd op kliniek en biochemie, of als ze een histologisch bewezen carcinoïdtumor hadden en er een klinische indicatie voor (her)stadiëring was. Alle patiënten moesten minimaal één abnormale laesie hebben op conventionele beeldvorming. Als tumormerkstoffen dienden 24-uurs urine serotonine, urine en plasma 5-hydroxyindool azijnzuur (5HIAA), de catecholamines (nor)adrenaline, dopamine en hun metabolieten gemeten in urine en plasma en serum chromogranine A. De 'totale lichaam metabole tumor last' correleerde met tumormerkstoffen uit zowel de serotonine als de catecholamine pathway gemeten in urine en plasma. ^{18}F-DOPA PET-opname liet tot wel 29-voudige verschillen zien tussen verschillende carcinoïdlaesies binnen een patiënt. Tevens was er sprake van een grote variatie tussen de patiënten. Dit laatste werd veroorzaakt door verschillende aantallen laesies, maar ook door verschillende opname-intensiteiten.

Uit deze analyse kan worden geconcludeerd dat de totale tumorlast gedefinieerd als 'totale lichaam metabole tumorlast' gemeten met ^{18}F-DOPA PET correleert met metabole tumor activiteit in de gemetastaseerde

carcinoïdpatiënt. Daarnaast geeft het in het gehele lichaam een overzicht over de plaatsen waar endocriene productie plaatsvindt. In toekomst zou de 'totale lichaam metabole tumor last' gebruikt kunnen worden als alternatieve parameter om uitgebreidheid en biochemische activiteit van carcinoïdtumoren te evalueren.

In **Hoofdstuk 7** beschrijven we drie patiënten met een gemetastaseerd insulinoom die behandeld werden met de mammalian target of rapamycin (mTOR) remmer everolimus. Een recent artikel heeft laten zien dat everolimus verbazingwekkend snelle controle van hypoglycemieën bewerkstelligde in vier patiënten met een insulinoom (Kulke et al. N Engl J Med 2009, 360, 195-197). Het precieze werkingsmechanisme is nog niet bekend. Om bij onze patiënten hierin meer inzicht te krijgen voerden we laboratoriumanalyses en ^{18}F-FDG PET uit om de kinetiek van de everolimus effecten op de glycemische controle en diens onderliggende mechanismen te onderzoeken. Everolimus normaliseerde de plasma glucosespiegels in alle drie patiënten binnen 14 dagen. Dit viel samen met een lagere glucoseopname in de tumor en spieren op ^{18}F-FDG PET en een daling van de (pro)insulinespiegels. Het effect van everolimus op zowel tumor als op normale weefsels werd veroorzaakt door gedaalde (pro)insuline uitscheiding in combinatie met perifere insulineresistentie en verklaarde de snelle glucosecontrole. In deze studie laten we zien hoe beeldvorming kan helpen om het werkingsmechanisme van geneesmiddelen te begrijpen en te visualiseren.

In **hoofdstuk 8** evalueren we de frequentie en de ernst van het gebrek aan vetoplosbare vitamines in acromegalie- en carcinoïdpatiënten. Beide patiëntengroepen worden vaak langdurig behandeld met een somatostatine-analoog. Somatostatine-analogen hebben een negatieve invloed op de vetopname in de darmen, waardoor er vaak steatorrhoe ontstaat. Samen met het vet kunnen mogelijk ook de vetoplosbare vitamines verloren gaan. De vetoplosbare vitamines worden niet routinematig gecontroleerd bij deze patiënten. Het effect van langdurige

behandeling met somatostatine-analogen op vetoplosbare vitaminespiegels is nog onbekend. Daarom onderzochten wij de frequentie en de ernst van het gebrek aan vetoplosbare vitamines.

In een cross-sectionele studie evalueerden we symptomen van een mogelijke deficiëntie van vetoplosbare vitamines bij 19 acromegalie-patiënten en 35 carcinoïdpatiënten die langer dan 18 maanden behandeld waren met een somatostatine-analoog. Tevens bepaalden we de spiegels van de vier vetoplosbare vitamines (A, D, E en K1) en vitamine-afhankelijke parameters (parathormoon voor vitamine D, prothrombine en geactiveerde partiële thromboplastine tijd voor vitamine K1). Twaalf patiënten hadden last van steatorrhoe, twee carcinoïdpatiënten klaagden over nachtblindheid. Tweeënveertig patiënten (78%) hadden te lage spiegels van één of meer vetoplosbare vitamines, 17 patiënten (32%) hadden een verlaagde spiegel van meerdere vitamines. Vitamine K1 was het meest frequent verlaagd (in 63%), vitamine A was verlaagd in 6%, D in 28%, E in 15% en vitamine E gemeten in erythrocyten in 58%. Frequentie en ernst van deficiënties in vitamine D, E en K1 waren niet verschillend tussen acromegalie- en carcinoïdpatiënten. De behandelduur met de somatostatine-analoog had geen invloed op de vitaminespiegels. Lengte van de darmresectie en leeftijd correleerden negatief met vitamine A spiegels. Een verhoogd parathormoon werd gezien in 14 patiënten en een verlengde prothrombine tijd in drie patiënten.

Uit deze gegevens concluderen wij dat een tekort aan vetoplosbare vitamines, waaronder vitamine K1 en vitamine A, vaker voorkomen in patiënten die behandeld worden met een somatostatine analoog dan voorheen gedacht. Daarom zouden de spiegels van deze vetoplosbare vitamines gecontroleerd en zo nodig gesuppleerd moeten worden, in ieder geval bij patiënten die in het verleden een darmresectie ondergingen.

Samenvattend, door middel van PET met ^{18}F-DOPA en ^{11}C-5-HTP is een betere detectie van neuroendocriene tumorlaesies mogelijk ten opzichte van conventionele beeldvorming en deze technieken zijn daardoor

medebepalend voor het beleid bij deze patiënten. Inzichten in het werkingsmechanisme en bijwerkingen van de behandeling van deze patiënten bieden nieuwe mogelijkheden voor het monitoren van de ingestelde behandeling.

Chapter 11

Color figures

Chapter 2

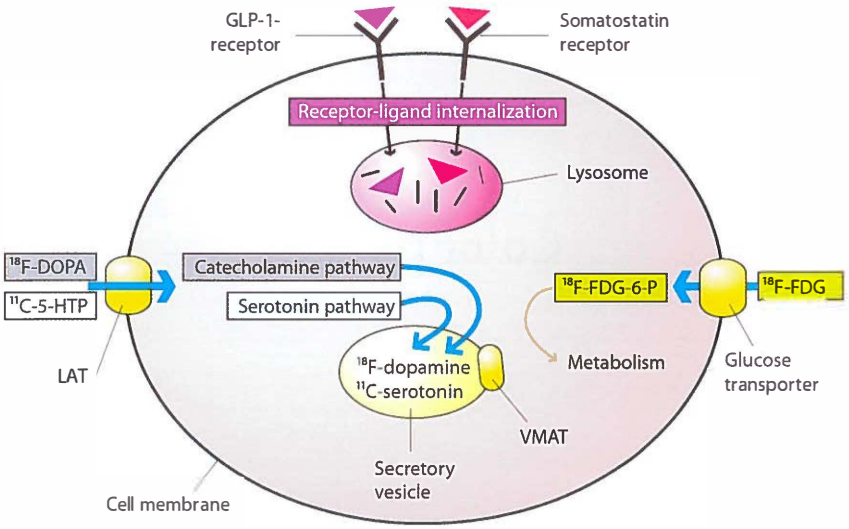

Figure 6. Schematic depiction of the different metabolic pathways by which neuroendocrine tumors can be visualized using nuclear medicine imaging techniques. This can be receptor based techniques and techniques which use the metabolic properties of these tumors. ^{11}C-5-HTTP: ^{11}C-5-hydroxytryptophan, ^{18}F-DOPA: ^{18}F-fluoro-dihydroxyphenylalanin, ^{18}F-FDG: ^{18}F-fluoro-2-deoxy-d-glucose, ^{18}F-FDG-6-P: ^{18}F-fluoro-2-deoxy-d-glucose-6-phosphate, GLP-1: glucagon-like peptide 1, LAT: large amino acid transporter, VMAT: vesicular monoamine transporter

Chapter 3

Figure 2. Imaging of a patient with a known metastatic pheochromocytoma. (A) ^{18}F-DOPA PET shows increased uptake in the left adrenal gland and three lesions in the spine (arrows). (B) Fusion image of ^{18}F-DOPA PET and CT shows uptake in the region of the left adrenal gland, without anatomical substrate. (C) CT image of the region of the left adrenal gland. ^{123}I-MIBG imaging was negative (not shown).

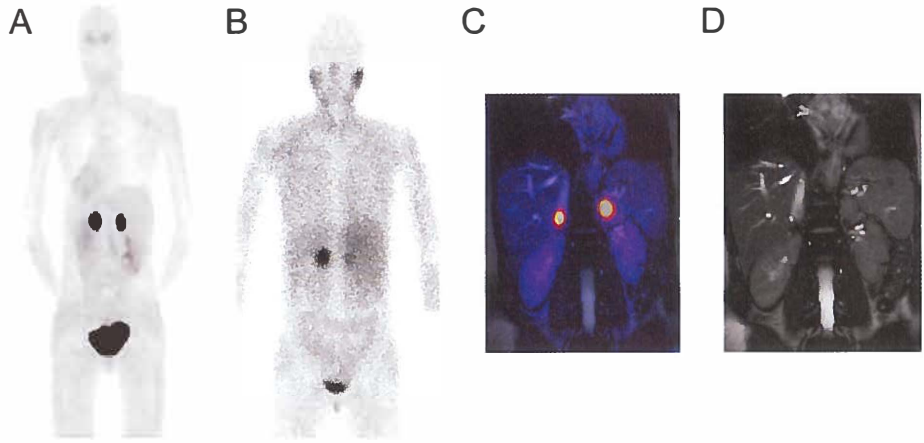

Figure 3. Patient with bilateral pheochromocytoma. (A) ^{18}F-DOPA PET shows increased uptake in both adrenal glands. (B) ^{123}I-MIBG imaging: asymmetric ^{123}I uptake in the adrenals: the left adrenal shows markedly increased uptake, whereas uptake in the right adrenal can easily be mistaken as physiological. (C) Fusion of ^{18}F-DOPA PET and MRI shows uptake in both adrenal glands. (D) MRI showing the left adrenal pheochromocytoma.

Chapter 4

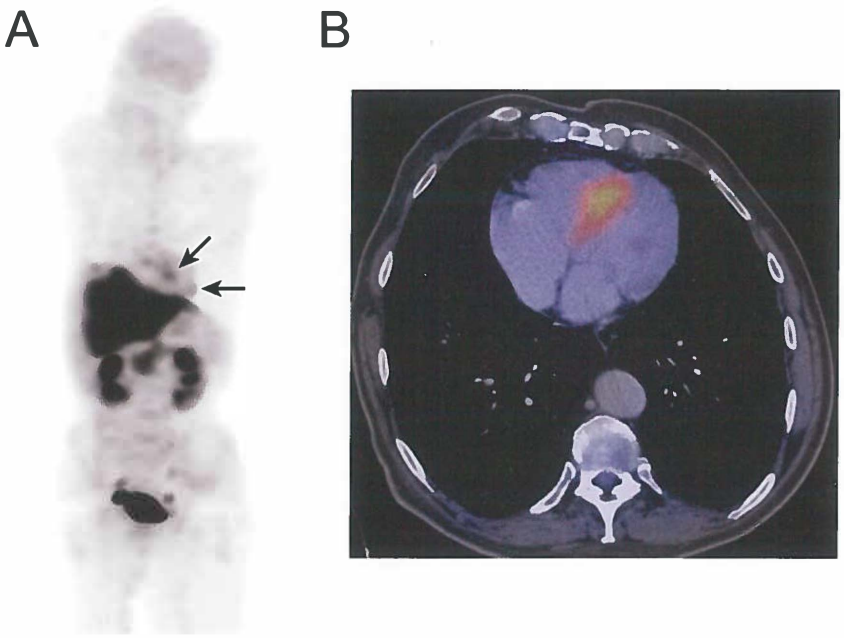

Figure 1. Patient 3 **A.** ^{11}C-5-HTP PET scan showing two cardiac metastases (arrows), both confirmed by CT scan, and extensive liver metastases. Diffuse physiological uptake in the pancreas and excretion via the kidneys, ureters and bladder. **B.** Fusion image of CT and ^{11}C-5-HTP PET showing one of the cardiac metastases.

Chapter 4a

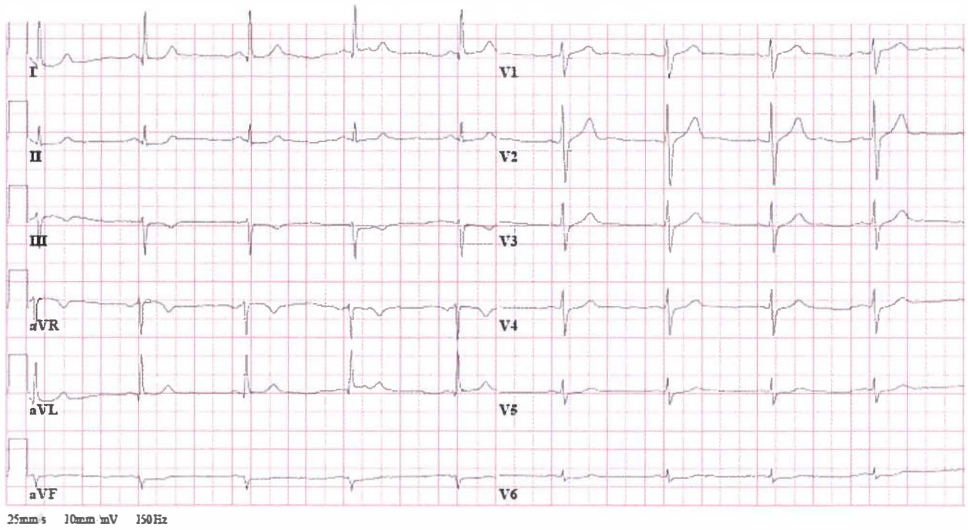

Figure 2. ECG showing sinus bradycardia.

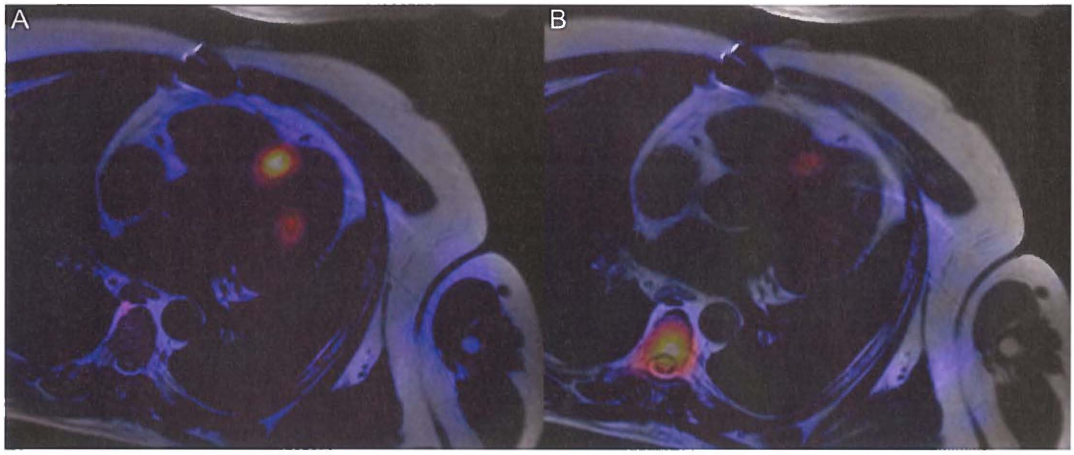

Figure 3. A, fusion of ^{18}F-DOPA PET and MRI confirms the presence of two lesions in the left ventricular myocardium. **B**, fusion of MRI and SRS shows only one myocardial lesion.

Chapter 7

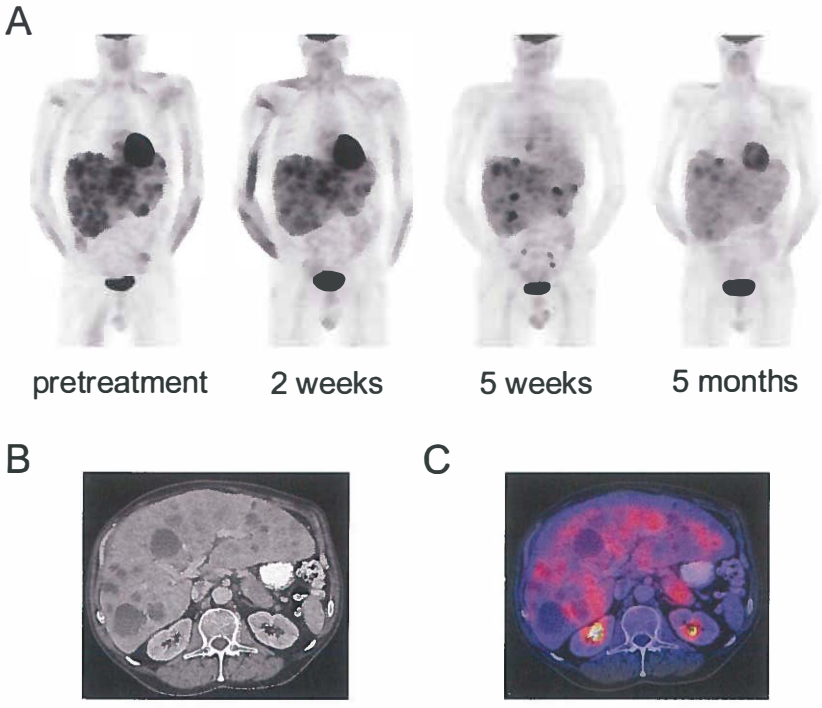

Figure 3. Patient 1. A. 18F-FDG-PET scans. Pathological uptake in the liver lesions and physiological uptake in the muscles and myocardium decreases during treatment with everolimus. B. Pre-treatment CT scan showing a pancreatic mass and multiple liver lesions. C. Fusion of the pre-treatment CT and 18F-FDG-PET confirming uptake in the pancreatic and liver lesions.

Chapter 12

Dankwoord

Onderzoek naar neuroendocriene tumoren wordt gedaan op het grensvlak van meerdere specialismen. Ik ben dan ook zeer blij dat ik tijdens mijn promotie van verschillende kanten hulp en begeleiding gehad hebt. Dit was altijd gezellig, soms frustrerend en leverde vele leerzame en vermakelijke discussies op.

Prof. dr. E.G.E. de Vries, Liesbeth, jouw scherpe blik en kritische opmerkingen hielpen menig probleem en onduidelijkheid oplossen. Het is ongelooflijk hoe snel je documenten van treffende opmerkingen kan voorzien, zodat ik vaak de volgende dag alweer verder kon werken.
Samen poli doen op vrijdag was een mooie afwisseling van het onderzoek doen. Ik ben blij dat ik op deze manier toch met een been in de kliniek heb kunnen blijven staan.

Prof. dr. T.P. Links, Thera, samen hebben we veel gefilosofeerd met een kopje thee op jouw kamer. Al pratende kwamen er zo vaak nieuwe inzichten om weer verder te kunnen. Ook als het even niet mee leek te zitten had je altijd opmonterende woorden.

Prof. dr. I.P. Kema, Ido, de biochemie was vaak het lastigste punt van mijn voornamelijk klinisch georiënteerde onderzoek. Dan was ik altijd blij als jij tijd had om met jouw kennis naar de data te kijken en zo nieuwe inzichten te verkrijgen. Vaak leverde dat trouwens net zoveel nieuwe (onderzoeks)vragen op als waarmee ik bij je kwam.

Dr. A.H. Brouwers, Adrienne, bij jou kon ik altijd laagdrempelig aankloppen voor kleine alledaagse vragen en praktische problemen. Op het eind even vanaf de achtergrond om tijd te hebben voor je eigen wonder.

Mijn kamergenoten, jullie waren er voor een kop latte met iets lekkers, als er weer een artikel geaccepteerd was, en om alle meevallers en tegenslagen mee te delen. Hartelijk dank voor alle gezelligheid!
Corina en Renske, mijn paranimfen. Jullie waren er vanaf het begin bij en samen hebben we dit pad bewandeld. Hopelijk staan jullie hier binnenkort ook!

Beste co-auteurs, hartelijk dank voor het bijdragen van jullie specifieke kennis om zo ons onderzoek steeds weer te kunnen verbeteren.
Speciale dank in dit kader aan prof. dr. R.A.J.O. Dierckx, dr. J.R. de Jong, en dr. K.P. Koopmans. Beste Rudi, hartelijke dank voor alle steun en alle mogelijkheden die ik gekregen heb om onderzoek te doen op de afdeling Nucleaire Geneeskunde en Moleculaire Beeldvorming (NGMB). Johan, dank je dat je altijd tijd had om moeilijke en 'suvve' concepten opnieuw uit te leggen. Klaas Pieter, dankzij jouw hulp hoefde ik aan het begin niet steeds het wiel opnieuw te ontdekken, dank je.

Dank aan de velen op de afdeling NGMB die me steeds weer geholpen hebben met (technische) vragen. Een speciale dank ook aan de medisch nucleair werkers voor het "terugzetten" van ontelbare scans.
Dear colleagues from the Department of Nuclear Medicicine and Molecular Imaging. It was always fun to talk to you over coffee during the coffee break, eat fish on the market or have a drink after work.

Thom, hartelijk dank voor het maken van de mooie plaatjes en de lay-out! Zonder jouw hulp zou dit proefschrift er een stuk minder mooi en kleurrijk uitzien.

Monique, hartelijk dank voor je redactie en voor de geestelijke en lichamelijke ontspanning en afleiding die onze vele gezellige (sport)avonden brachten. Ik zal ze gaan missen!

Jonathan, dank voor alle gezelligheid en vriendschap waar ik m.n. tijdens het begin van mijn promotie veel steun aan had. Het is altijd handig advies in te kunnen winnen bij een ervaringsdeskundige. Ondanks de afstand blijven we hopelijk goede vrienden!

Liebe Mams, Paps, und Jorge. Danke für eure Unterstützung und Liebe. Es war schön zu sehen, wie ihr mit Begeisterung und Stolz meine Fortschritte miterlebt habt und trotz eurer wenigen spezifischen Kenntnisse versucht habt meine wissenschaftliche Artikel zu verstehen. Ich habe euch lieb!

Lieve Eduard, hartelijk dank voor heel veel vitamine E. Op naar de gezamelijke toekomst!